NAVAL POSTGRADUATE SCHOOL
Monterey, California



THESIS

AUTOMATED PERFORMANCE
EVALUATION TECHNIQUE

by

Brian E. Skimmons

March 1992

Thesis Advisor: Donald V.Z. Wadsworth

Approved for public release; distribution is unlimited

REPORT DOCUMENTATION PAGE

Form Approved
OMB No 0704-0188

1a REPORT SECURITY CLASSIFICATION UNCLASSIFIED	1b RESTRICTIVE MARKINGS
2a SECURITY CLASSIFICATION AUTHORITY	3 DISTRIBUTION / AVAILABILITY OF REPORT Approved for public release; distribution is unlimited
2b DECLASSIFICATION / DOWNGRADING SCHEDULE	
4 PERFORMING ORGANIZATION REPORT NUMBER(S)	5 MONITORING ORGANIZATION REPORT NUMBER(S)
6a NAME OF PERFORMING ORGANIZATION Naval Postgraduate School 6b OFFICE SYMBOL (If applicable) EC	7a NAME OF MONITORING ORGANIZATION Naval Postgraduate School
6c ADDRESS (City, State, and ZIP Code) Monterey, CA 93943-5000	7b ADDRESS (City, State, and ZIP Code) Monterey, CA 93943-5000
8a NAME OF FUNDING / SPONSORING ORGANIZATION 8b OFFICE SYMBOL (If applicable)	9 PROCUREMENT INSTRUMENT IDENTIFICATION NUMBER
8c ADDRESS (City, State, and ZIP Code)	10 SOURCE OF FUNDING NUMBERS PROGRAM ELEMENT NO / PROJECT NO / TASK NO / WORK UNIT ACCESSION NO

11 TITLE (Include Security Classification)

AUTOMATED PERFORMANCE EVALUATION TECHNIQUE

12 PERSONAL AUTHOR(S)

SKIMMONS, Brian E.

13a TYPE OF REPORT	13b TIME COVERED	14 DATE OF REPORT (Year, Month, Day)	15 PAGE COUNT
Master's Thesis	FROM _____ TO _____	1992 March	153

16 SUPPLEMENTARY NOTATION The views expressed in this thesis are those of the author and do not reflect the official policy or position of the Department of Defense or the US Government.

17 COSATI CODES			18 SUBJECT TERMS (Continue on reverse if necessary and identify by block number)
FIELD	GROUP	SUB-GROUP	RFI Mitigation; CDAA Performance; RFDF Management

19 ABSTRACT (Continue on reverse if necessary and identify by block number)

The U.S. Navy operates a number of radio receiving and signal collection sites throughout the world. These sites have been modified and upgraded a number of times to incorporate new equipment technology and advanced receiving and data processing systems. In addition, the encroachment of other activities near the sites has increased the levels of radio and electrical noise to harmful levels. The impact of some site modifications and increased noise levels on the ability of the sites to receive and process data from signals-of-interest (SOIs) is a major concern.

A means to evaluate the positive (or negative) impact of site improvements, site upgrades, and site encroachment on the performance of a site has not been available in past years. To fill this void, a performance

20 DISTRIBUTION / AVAILABILITY OF ABSTRACT	21 ABSTRACT SECURITY CLASSIFICATION	
☒ UNCLASSIFIED/UNLIMITED ☐ SAME AS RPT ☐ DTIC USERS	UNCLASSIFIED	
22a NAME OF RESPONSIBLE INDIVIDUAL WADSWORTH, Donald V.Z.	22b TELEPHONE (Include Area Code) 408-646-2115	22c OFFICE SYMBOL EC/Wd

DD Form 1473, JUN 86 *Previous editions are obsolete*

S/N 0102-LF-014-6603

19. cont.
evaluation technique (PET) was developed by the staff and students of the Naval Postgraduate School. PET has gradually evolved into a useful analytic tool used during field surveys conducted by the Signal-to-Noise Enhancement Program (SNEP). SNEP teams visit selected sites to assess the impact of site modifications and man-made ratio noise on the reception of SOIs. The primary tool used to quantify the impact of factors affecting SOI reception is the PET curve.

This thesis describes the steps involved in the PET, the construction and interpretation of PET curves, and new techniques employing a computer to generate PET curves. Examples of curves produced by the new automated process are presented using data from a recent SNEP survey at the Sabana Seca CDAA site.

Approved for public release; distribution is unlimited

AUTOMATED PERFORMANCE EVALUATION TECHNIQUE

by

Brian E. Skimmons
Lieutenant, United States Navy
B.S., United States Naval Academy, 1986

Submitted in partial fulfillment of the
requirements for the degree of

MASTER OF SCIENCE IN ELECTRICAL ENGINEERING

from the

NAVAL POSTGRADUATE SCHOOL
March 1992

ABSTRACT

The U.S. Navy operates a number of radio receiving and signal collection sites throughout the world. These sites have been modified and upgraded a number of times to incorporate new equipment technology and advanced receiving and data processing systems. In addition, the encroachment of other activities near the sites has increased the levels of radio and electrical noise to harmful levels. The impact of some site modifications and increased noise levels on the ability of the sites to receive and process data from signals-of-interest (SOIs) is a major concern.

A means to evaluate the positive (or negative) impact of site improvements, site upgrades, and site encroachment on the performance of a site has not been available in past years. To fill this void, a performance evaluation technique (PET) was developed by the staff and students of the Naval Postgraduate School. PET has gradually evolved into a useful analytic tool used during field surveys conducted by the Signal-to-Noise Enhancement Program (SNEP). SNEP teams visit selected sites to assess the impact of site modifications and man-made radio noise on the reception of SOIs. The primary tool used to quantify the impact of factors affecting SOI reception is the PET curve.

This thesis describes the steps involved in the PET, the construction and interpretation of PET curves, and new techniques employing a computer to generate PET curves. Examples of curves produced by the new automated process are presented using data from a recent SNEP survey at the Sabana Seca CDAA site.

TABLE OF CONTENTS

I. INTRODUCTION 1

II. PURPOSE 3

III. THE PERFORMANCE EVALUATION TECHNIQUE 5

A. APPLICABLE SYSTEMS 6

B. REQUIRED MEASURING EQUIPMENT AND TEST CONFIGURATION 8

C. PRELIMINARY INFORMATION NEEDED FOR ANALYSIS 8

1. Specify the Receiver Site and Equipment 9

a. Ideal Equipment Capabilities 9

(1) Ideal Minimum and Reference Noise Floors 12

(2) Automatic Detection Figure 12

b. PROPHET Data 12

(1) Receive Antenna Type and Gain 13

(2) Location and Limitations 13

2. Specify the Source and Associated Parameters 13

a. Transmission Equipment 13

(1) Antenna Type 14

(2) Maximum Transmission Power 14

(3) Frequency Range 14

b. Environmental Factors 14

(1) Time of Day and Season 14

3. Maximum Signal Strength Expected 14

D. SITE MEASUREMENTS 15

1. Radio Frequency Distribution (RFD) System Loss 15

a. Cable Loss 16

b. ENLARGER Loss 16

c. Primary Multicouplers (PMC) 20

2. Excess Noise Floor 20

3. Internal Sources of Man-Made Noise 20

4. External Sources of Man-Made Noise 23

5. International Broadcast Service Interference 30

E. THE PET CURVE 30

1. Construction 32

a. SOI Amplitude Distribution 32

b. +12 dB Distribution 34

c. Percent SOIs Lost 34

d. Performance With RFD Loss Added 38

e. Performance With Excess Noise Floor Added 38

f. Performance With Internal or External Noise Added 43

2. Interpretation of PET Curve Results 43

3. Site Performance Evaluation 55

IV. AUTOMATED PERFORMANCE EVALUATION TECHNIQUE 58

A. GRAFTOOL, SCIENTIFIC ANALYSIS PROGRAM 58

B. FILE MANAGEMENT AND DATA INPUT 59

C. CREATING PET CURVES 60

1. Graph Creation Without Data 61

2. Signal Strength Data Entry 63

3. Combining Signal Data With PET Template 65

4. Site Performance Curve With RFD Loss 70

5. PET Curves With Excess Noise Floor 70

6. PET Curves With Internal and External Noise 72

D. EXTRACTING DATA FOR ANALYSIS AND PRESENTATION . . 72

E. PET OUTPUTS 73

V. USE OF THE AUTOMATED PET TO ASSESS SITE PERFORMANCE . . 75

A. DETERMINING THE RECEPTION CAPABILITY OF A TRANSMITTER AND SOIs 75

B. COST OF SITE MODIFICATIONS AND REPAIRS VERSUS SOI GAINS 76

C. GENERAL SITE SURVEY AND MAN-MADE NOISE ASSESSMENT 76

VI. AUTOMATED PET ANALYSIS OF SABANA SECA DATA 77

VII. CONCLUSIONS AND RECOMMENDATIONS 107

A. CONCLUSIONS 107

B. RECOMMENDATIONS 107

APPENDIX A. NOISE MEASUREMENT SYSTEMS 109

APPENDIX B. SNEP NOISE DEFINITION EQUIPMENT AND CONFIGURATION 110

APPENDIX C. PROPHET SIGNAL STRENGTH COMPUTATION 118

APPENDIX D. HF SIGNAL AMPLITUDE STATISTICS 122

LIST OF REFERENCES 141

BIBLIOGRAPHY 142

INITIAL DISTRIBUTION LIST 143

I. INTRODUCTION

The Naval Security Group Command (NSG) operates a worldwide network of Radio Frequency Direction Finding (RFDF) and signal collection facilities. These sites are tasked to perform many functions, but their primary mission is to provide support services to the operational fleet [Ref. 1:p. 1-1]. To measure the effectiveness of the sites to perform their assigned missions, a performance evaluation technique (PET) was developed over the past several years by the staff and students of the Naval Postgraduate School during participation in the NSG Signal-to-Noise Enhancement Program (SNEP)[Ref. 2:p. 4]. The technique has evolved into an effective means to measure a site's performance (the ability to receive weak signals-of-interest). The effects of site modifications and destructive man-made radio interference problems are now quantified into specific measures of performance.

There is an ongoing need to revise, update, and improve upon the PET because of advancements in site equipment, prediction models, and measuring equipment. The current manual evaluation process is limited in scope due to the large amount of time and detail required to complete a PET survey. The recent reduction in the defense budget has put a priority on site performance because the Navy cannot afford to continue to operate facilities that are unable to perform their mission. The high cost of repairs or upgrades may limit major site improvements at this time. Therefore, an improved and in-depth implementation of the performance technique is needed to assess the costs and

benefits of expensive site modifications, improvements, maintenance, and repairs. This is provided by the automated PET described in this thesis.

Along with the need to expand the engineering analysis portion of the evaluation technique, is the desire to make the results more helpful to system and site managers and other non-technical personnel associated with receiving site operations. An expanded and more comprehensive evaluation of performance provides the documentation needed to evaluate and support future site improvement programs. This thesis details the necessary steps to improve both the analysis and presentation of the performance evaluation results.

II. PURPOSE

The purpose of this thesis is to describe an automated performance evaluation technique which has greater accuracy and diagnostic value that the current manual method. This document can be used as a reference manual for applying PET to monitor and manage site performance. To achieve this, a synopsis of the procedures used in conducting a performance evaluation and creating the performance curves is presented in Chapter III. The construction, use of measured data, and interpretation of the performance curves is presented in detail.

Chapter IV describes the automation of the manual evaluation technique using a personal computer and standard analysis software. The use of data storage files under the automated technique allows the user to document the current state of site operations, transfer results from one file to another, propose improvements, assign costs to site changes, and analyze the impact of different parameters on performance. This is difficult and time consuming with the manual method. The current practice of manually formatting, transferring, and presenting results has limited the scope of the analysis process.

Chapter V lists the new types of analysis that are made possible using computer support. This section describes the current state of progress of the automated PET, but new ideas and improvements are still being devised.

This thesis reviews the current performance evaluation technique and describes significant improvements to the evaluation process. Data and operational examples for this document are derived from participation in SNEP team quick-look surveys conducted at Naval Security Group Activity (NSGA) Edzell, Scotland and NSGA Sabana Seca, Puerto Rico. Conversations with SNEP team members and training sessions with the SNEP teams were also a major source of information. Supporting documents for the theory of the performance technique are the Signal-to-Noise Enhancement Program (SNEP) Manual (Draft) [Ref. 2] and Doctoral Dissertation by LCDR Gus G. Lott [Ref. 3].

Chapter VI is the application of the automated PET using the data recently collected from a CDAA site. The chapter is a step-by-step description of the technique described in the previous chapters. The results of the analysis are provided in graphical form.

Appendices are provided to present detailed information about portions of the evaluation technique. Appendix A describes the relationship of the PET to the Automated Noise Measurement System (ANMS) and is provided for the interested reader. Appendix B lists the measurement procedures and equipment. Appendix C is a sample PROPHET signal-strength calculation. Appendix D is the supporting data from certain SOI amplitude distribution studies.

III. THE PERFORMANCE EVALUATION TECHNIQUE

The PET is a systematic approach to quantifying the operational performance of receiving systems located at a receiving or RFDF site. The PET was designed by the staff and students of the Naval Postgraduate School to evaluate the ability of receiving sites to intercept and process data from SOIs. The percentage of SOIs lost due to any site-related parameter is the performance measurement standard. SOIs are lost as a direct result of site operating deficiencies and noise interference. Specific causes of performance degradation have been identified by SNEP teams, the most prominent being:

- Excessive attenuation in the Radio Frequency Distribution system (RFD).
- High noise floor in the RFD.
- Entry of site-generated noise into the RFD.
- Saturation of the active elements in the RFD.
- Excessive interference and attenuation in coaxial cables and connectors due to improper installation and shielding.
- Excessive Radio Frequency Interference (RFI) from internal and external noise sources.

Upon completion of a SNEP team survey, a performance evaluation report is provided to the site Commander and Naval support activities. This report identifies all problems that adversely affect site performance and assesses their impact on the reception of SOIs.[Ref. 2:p. 4]

The current practice of manually compiling data from the SNEP survey, described in this chapter, is very tedious for lack of automated support. Chapter IV develops the procedures to automate the PET analysis using a personal computer to store, manipulate, and expand the results for easier evaluation and presentation.

The PET can be used to evaluate the performance of various receiving systems as addressed in Section A. A performance evaluation requires special test and signal-processing equipment and trained operators. Section B and Appendix B describe the details of the measurement equipment needed to obtain the data for the PET.

The PET curve is used to determine the percent of SOIs lost. A generic PET curve is shown in Figure 1. The creation of the curves requires the compilation of site parameters and the amplitude distribution of selected classes of SOIs. These are obtained from computations and site measurements. Section C outlines the preliminary computation and evaluation steps, Section D addresses site measurements, and Section E presents the curve construction and interpretation procedures.

A. APPLICABLE SYSTEMS

The PET analysis can be performed for any receiving system provided the SOI amplitude distribution can be reasonably measured or predicted. Measurements are taken throughout the system to define and identify noise or attenuation problems.

The primary example used in this thesis will be the Navy's High Frequency AN\FRD-10 direction finding equipment. This is a wide-aperture receiving system, using the Wullenweber antenna configuration, or Circularly Disposed Antenna Array

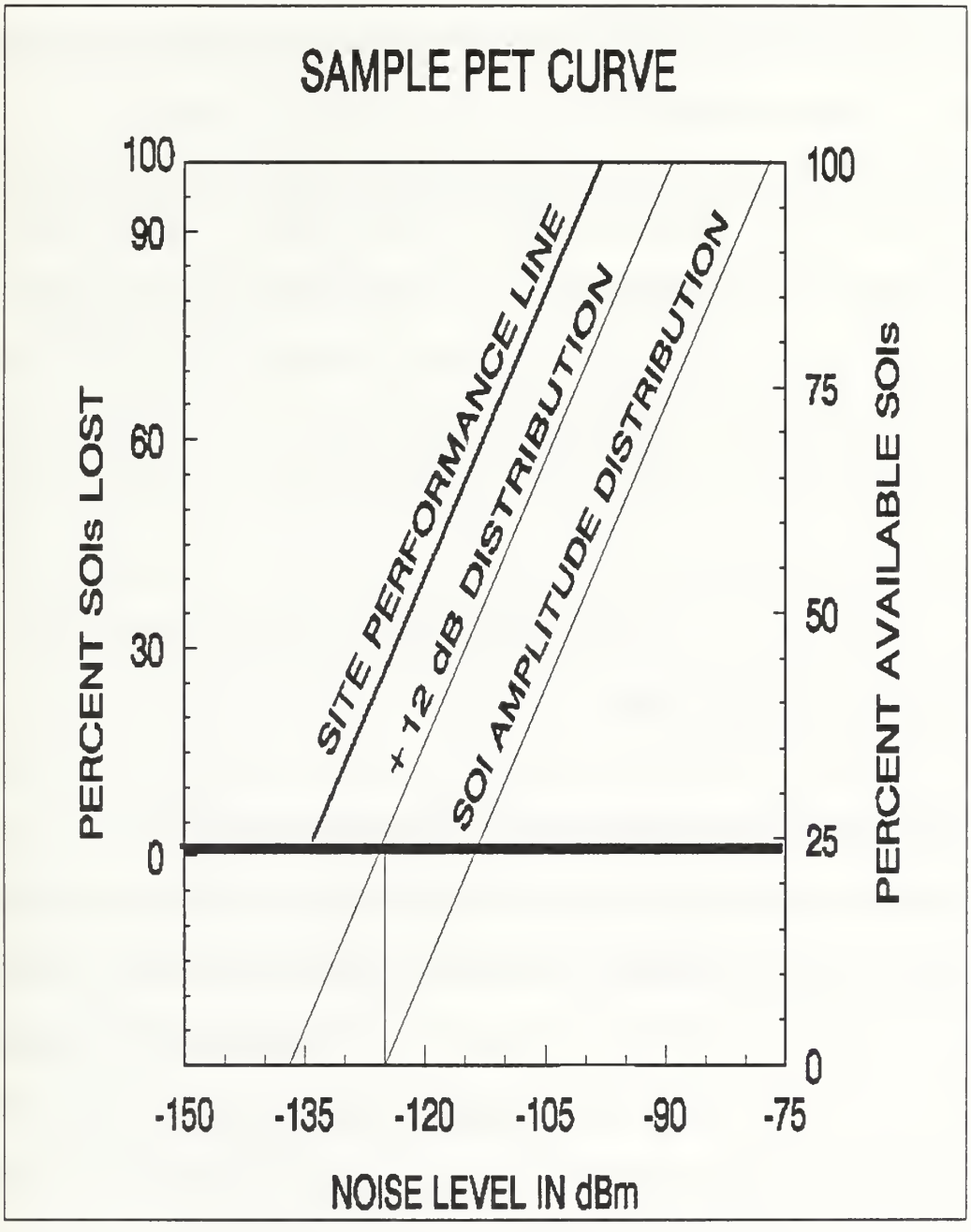


Figure 1. Sample PET Curve.

(CDAA).[Ref. 1:pp. 3-6, 6-15] A diagram of a typical Radio Frequency Distribution (RFD) path for this system is shown in Figure 2. Signal strength and noise measurements are made at various points in the RFD, and the data are recorded for analysis.

B. REQUIRED MEASURING EQUIPMENT AND TEST CONFIGURATION

Appendix B provides a description of the required test equipment, its setup and operation [Ref. 3:pp. 172-178]. A personal computer equipped with the Naval Ocean Systems Command (NOSC) PROPHET prediction program and 3-D Visions analysis program GRAFTOOL is needed to perform the automated PET. Although PROPHET was used to obtain the ionospheric predictions of SOI amplitudes used in this thesis, the user can substitute any other similar prediction program or measurement method to obtain data for the automated PET.

C. PRELIMINARY INFORMATION NEEDED FOR ANALYSIS

Preliminary study and preparation are required prior to a SNEP team's arrival at a site. The completion of the following information-gathering steps prior to a survey is necessary to minimize the survey time, determine that the preliminary data is realistic, and ensure the team has an idea of expected results. Once the preparation is finalized, the site measurements, data compilation, analysis and presentation remain to complete the SNEP survey. The steps and information are summarized:

- Specify the receiver site.
- Select the equipment for the PET analysis.

- Specify the receiving system operating parameters.
- Specify the ideal performance capabilities.
- Specify the sources of SOIs (range, bearing, frequency, time, season).
- Designate the equipment parameters used for SOI transmissions (EIRP, waveform).
- Specify the likely sources of maximum signal levels for the site and the operating parameters for these sources.
- Identify the appropriate parameters needed for the prediction of maximum signal strength expected.

Most of the preliminary data is used to establish a practical and meaningful PROPHET prediction scenario. The remaining information is used in the PET curves.[Ref. 2:pp. 4-15]

1. Specify the Receiver Site and Equipment

The receiving site and a receiving system must be identified. The CDAA System shown in Figure 2 is used as an example in this thesis. PROPHET is used to predict the maximum signal strength of SOIs and strongest signals expected at each site. The location of the signal strength measurement point within the RFD system is shown in Figure 3. Additionally, the ideal RFD operational parameters from Part a. are needed to complete the PET curves.

a. Ideal Equipment Capabilities

The receiving equipment has basic operating parameters. The ideal equipment capabilities, without the introduction of loss, will be used as the base values to determine the operating performance.

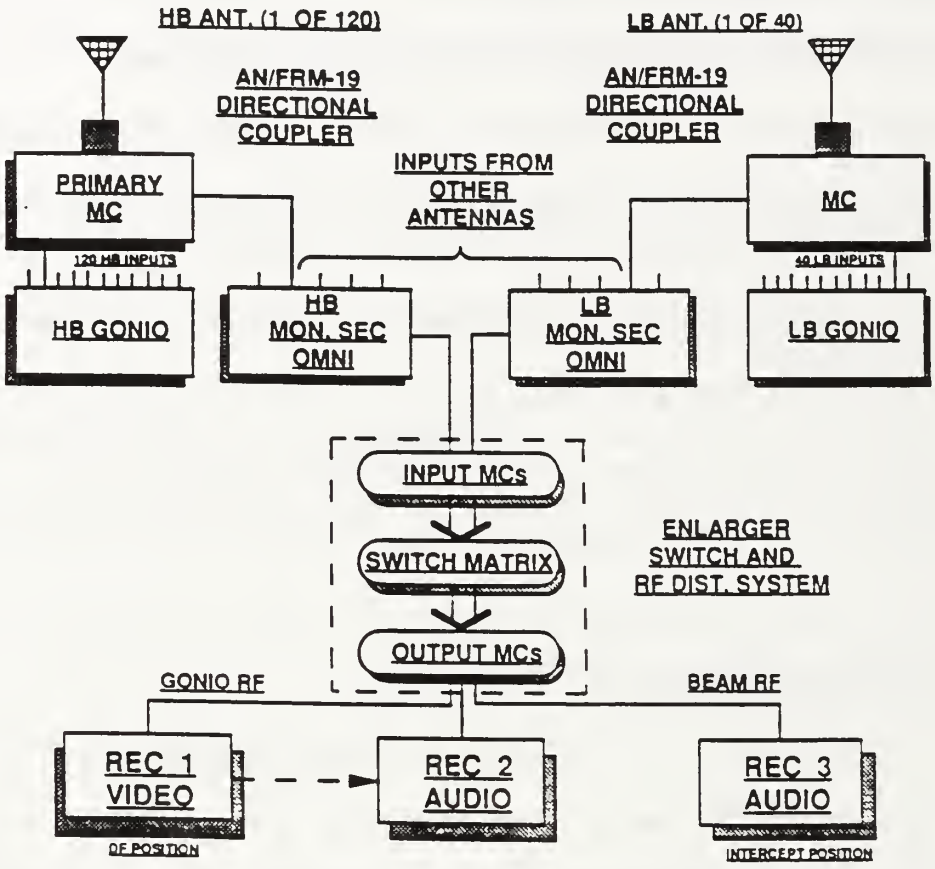


Figure 6-11

RF Signal Path of One Antenna Element to Various Receivers

OCTOBER 1989 6-15

Figure 2. RFD Diagram [Ref. 1:p. 6-15].

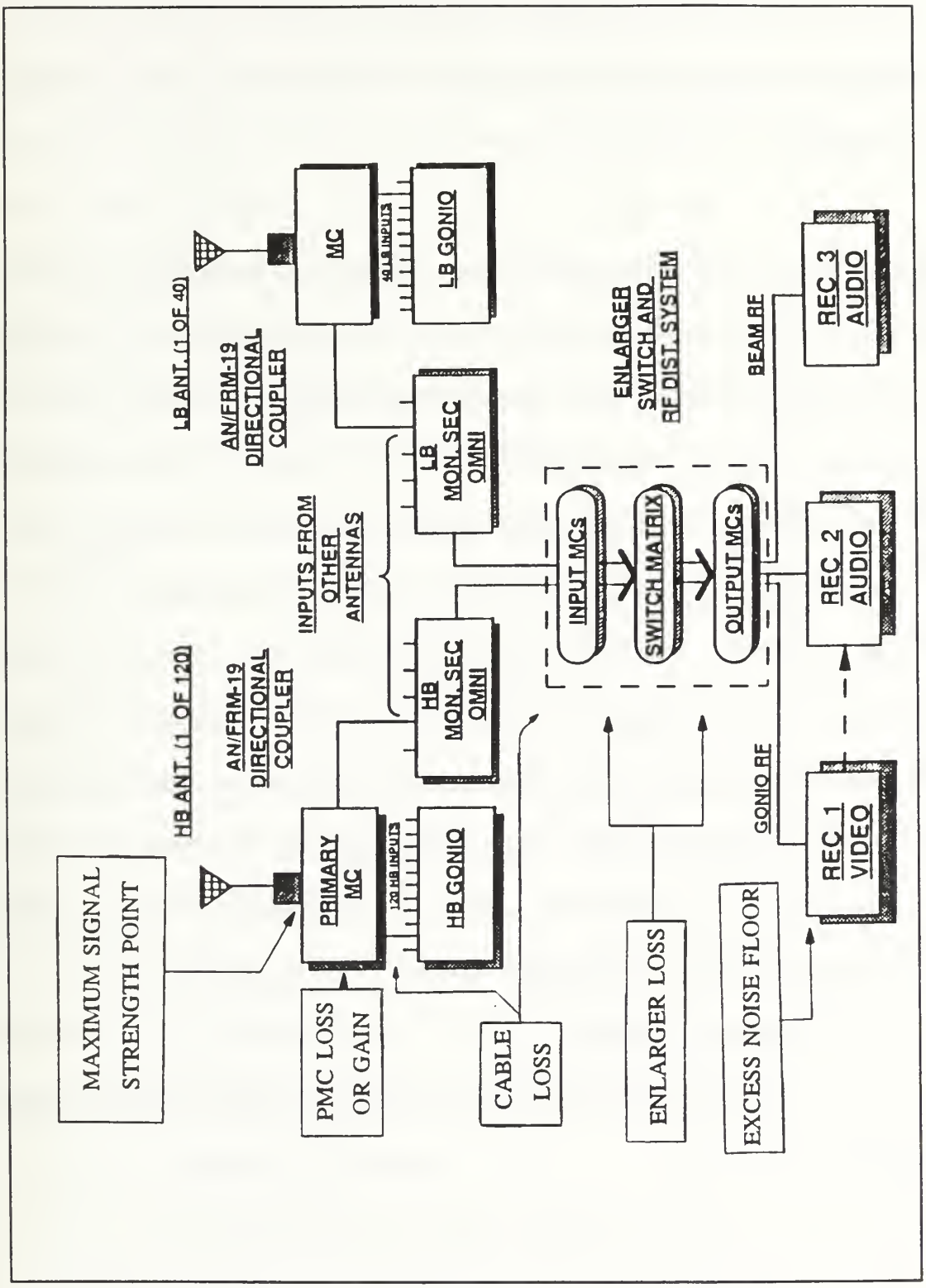


Figure 3. Signal Strength Measurement Points [Ref. 1:p. 6-15].

(1) Ideal Minimum and Reference Noise Floors. The "ideal minimum noise floor" is a calculated operating parameter. It is based on the well-known noise power expression

$$P = kTB \qquad (1)$$

where P is the power in watts, k is Boltzmann's constant, T is the absolute temperature in Kelvin, and B is the measured operating bandwidth in Hz. [Ref. 4:p. 385]. The minimum noise value for a 3 kHz bandwidth at an operating temperature of 290 K (27 Celsius or room temperature) is -144 dBm. Most receivers are not capable of operating at this level, and a practical minimum reference level of -125 dBm, for a 3 kHz gaussian shaped bandwidth, is used [Ref. 3:pp. 24-25]. Unless the equipment is capable of increased performance, the reference level should be used.

(2) Automatic Detection Figure. For the equipment to have a reasonable chance to detect a signal in the presence of noise, a signal strength about +12 dB above the noise floor is needed. If the detection system is able to work at a higher level of performance through enhanced software or operator interface, this excess signal level can be reduced to the appropriate level.

b. PROPHET Data

The following sections list the receiver parameters needed in the PROPHET set up [Ref. 5].

(1) Receive Antenna Type and Gain. The receiving site antenna type and gain will usually be listed within PROPHET. Some receiving systems use the Omni antenna port of a CDAA. If such a system is used for the PET analysis, the gain of an isotropic antenna is used.

(2) Location and Limitations. The geographic location (latitude and longitude coordinates) of the receiving site is required to determine the propagation path of the SOIs. Other known limitations of the system based on receiving direction or terrain features are needed in the final PROPHET calculations.

2. Specify the Source and Associated Parameters

A transmitting source must be identified as the origin of the signals-of-interest. Different performance evaluations will use different transmitters. The various types of evaluations will be discussed in the last chapter. Once the source is identified, its characteristics must be used to determine the amplitude distribution of the SOIs. The source can be a known transmitter used as a test station to determine how well a site can perform its mission.

The following list will complete the information required for PROPHET computations. The final desired result from PROPHET will be a prediction of the maximum signal strength of an SOI for the set up conditions chosen.

a. Transmission Equipment

The transmitting system will be defined by the following information.

(1) Antenna Type. The transmitting antenna must be known to determine its antenna pattern and the resulting gain. PROPHET can use a number of predefined antennas, and the user may define other antennas of interest.

(2) Maximum Transmission Power. The expected maximum average transmitting power is needed for calculating signal power. The unit of watts is required.

(3) Frequency Range. Since the systems to be analyzed are in high frequency (HF) sites, the frequency range is 2-30 MHz. If a specific target has a smaller operating range, this should be used in order to reduce the number of data points and provide a smaller analysis range.

b. Environmental Factors

Certain characteristics of the transmissions are influenced by the environment. The following parameters are used in the PROPHET set up.

(1) Time of Day and Season. HF propagation is affected by the time of day and the season of the year. For the PROPHET prediction runs, a full 24 hours will be used for signal-strength calculations. If the target transmitter operates only at certain times, the times of transmission will be used for performance evaluation.

3. Maximum Signal Strength Expected

The most important preliminary step required is the prediction of the maximum signal strength expected at the receiver site. All of the amplitude distributions used in the PET curves are based on this prediction. There are various methods used to determine the maximum signal strength; the approach used here is the PROPHET

prediction program. Appendix C provides a complete step-by-step example of the process. The value of the maximum signal strength expected is the desired result from PROPHET.

Measurements are made at the site to confirm the validity of the signal strength predictions. Transmitters of known power are monitored and their signal strengths are measured to compare with the predictions from PROPHET. These measurements must be made during ionospherically quiet periods in order to avoid propagation anomalies caused by ionospheric storms.

D. SITE MEASUREMENTS

Measurements of RFD loss, excess noise floor, and noise interference are an important part of the performance evaluation technique. While all of the previous data can be compiled and readied for use prior to arrival at the site, loss, noise floor, and noise interference measurements must be made on site. This section describes on-site measurements. The on-site measurements must be made in a careful, systematic way to assure valid performance results.

1. Radio Frequency Distribution (RFD) System Loss

The actual RFD path at a specific site may vary slightly from Figure 1, but the equipment and measurement locations will be essentially as shown. The RFD includes all components from the antenna termination plates to the receiver, including all cable runs, multicouplers, and the complete ENLARGER. For reference, all measuring points used in this thesis are based on the locations marked in Figure 3.

The total RFD loss is the sum of the individual component losses, and it is a function of frequency. Test signals are required over the entire 2-30 MHz range to establish the frequency dependence of the loss. A sample graph of total RFD loss versus frequency is shown in Figure 4.

A breakdown of the main components of the RFD loss follows.

a. Cable Loss

Coaxial cable loss is obtained by injecting test signals at known levels into the RFD at the antenna termination plates. Signal level measurements are then made at the end of each coaxial cable. The losses for each cable are summed at each test frequency. While not all cable runs in the RFD are precisely the same length, a run can be selected that is reasonably representative of all runs. Care must be exercised to ensure that the selected run does not contain sections of damaged cable or improperly installed connectors. A sample graph of cable loss versus frequency is shown in Figure 5.

b. ENLARGER Loss

ENLARGER loss is measured by injecting test signals of known strength and frequency into the diplexer associated with ENLARGER and measuring the level at the output ports of the system. The loss for ENLARGER is due solely to path loss experienced within the system [Ref. 6:p. 25]. A graph of ENLARGER loss versus frequency is shown in Figure 6. Internal noise measurements will be described in Part 2. of this chapter.

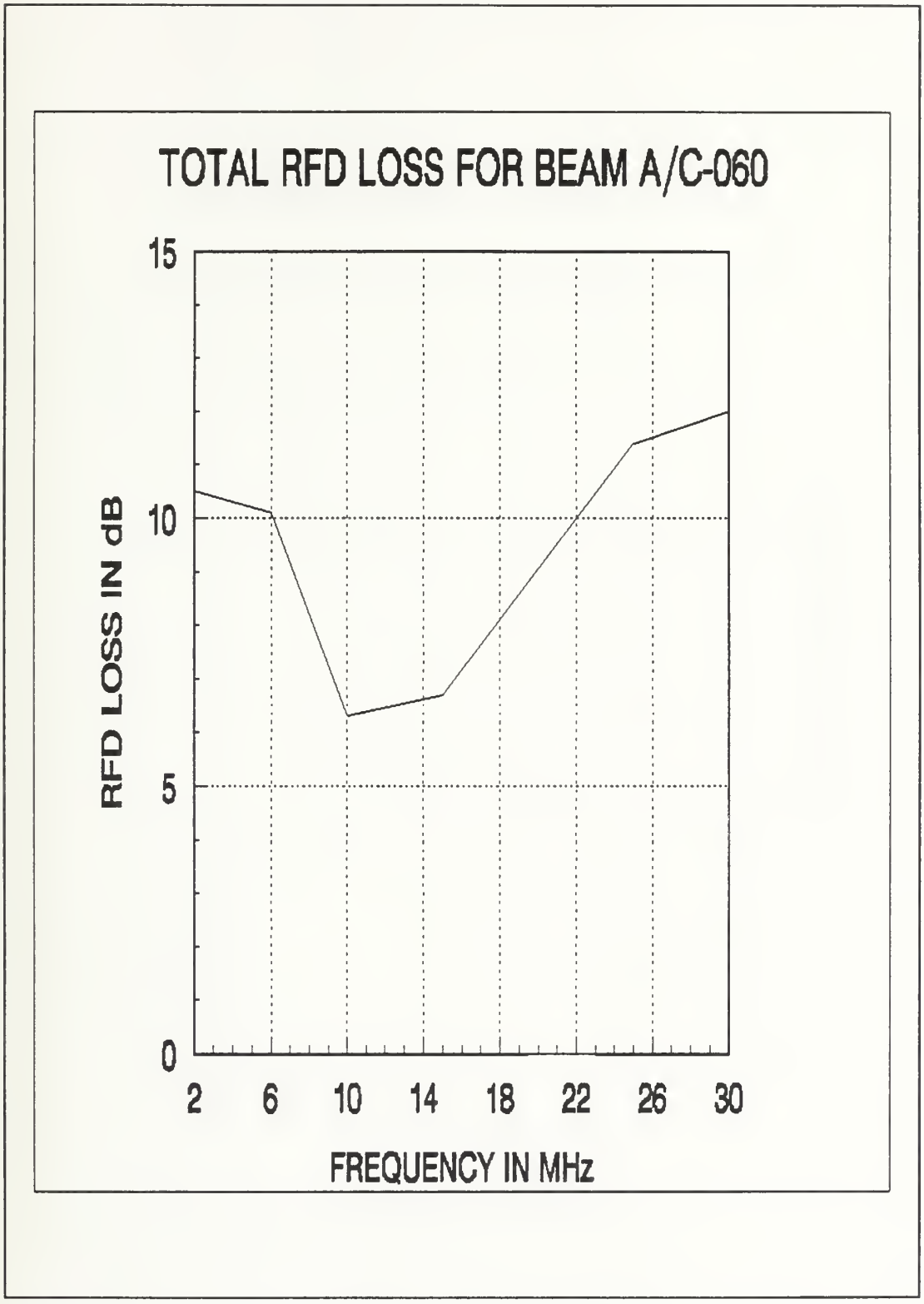


Figure 4. RFD Loss vs. Frequency.

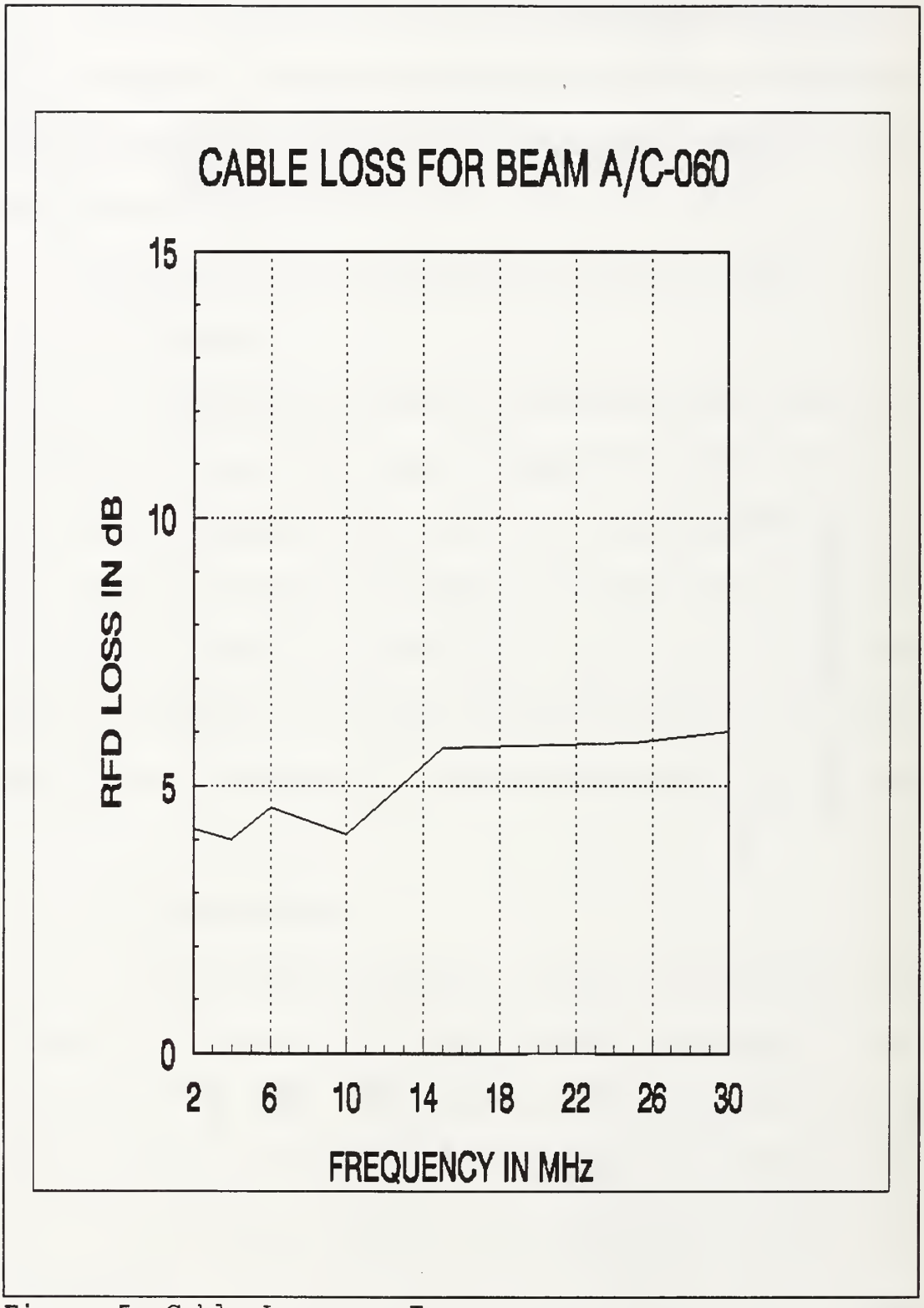


Figure 5. Cable Loss vs. Frequency.

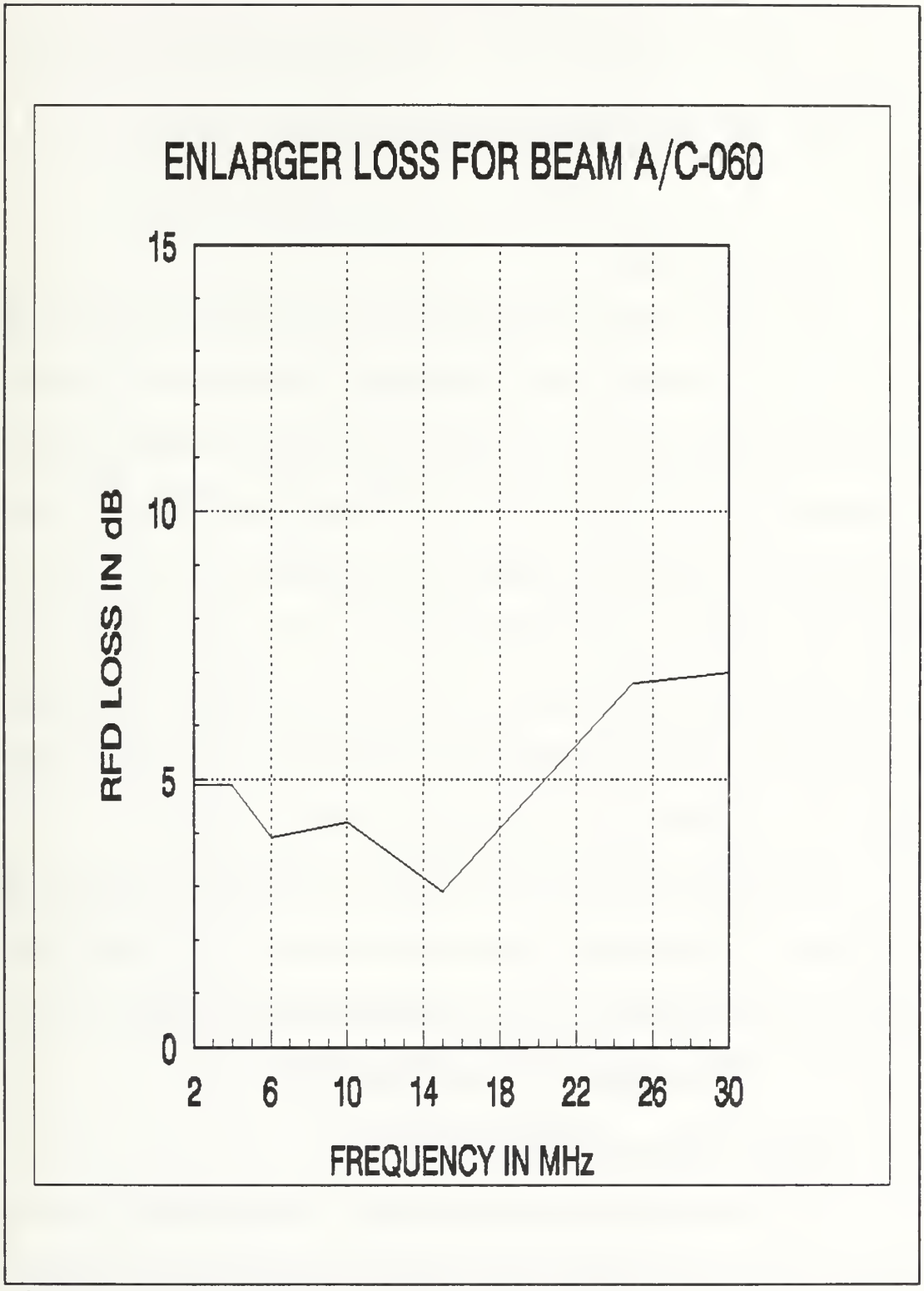


Figure 6. ENLARGER Loss vs. Frequency.

c. Primary Multicouplers (PMC)

Primary multicoupler loss or gain is measured by the same technique used to measure the ENLARGER loss. A graph of PMC loss and gain is shown in Figure 7.

2. Excess Noise Floor

Excess noise produced by components within the RFD system may increase the noise floor over that of the primary multicouplers. The reference noise floor limit for the receiving systems was set at -125 dBm for a 3 kHz gaussian-shaped bandwidth. This is approximately the noise floor of the type 1382 multicouplers used as the PMCs. It is also close to the noise floor of several receiving systems used in CDAA sites. If the RFD system produces noise levels in excess of the reference limit, then low-level signals will be undetectable because they are below the RFD noise floor. The difference between the reference floor limit and the RFD measurements is the excess noise floor. A graph of the excess noise floor versus frequency is shown in Figure 8.

The noise floor is measured (see Figure 3) with all inputs to the appropriate beam terminated. This eliminates all externally generated noise and avoids the problem of separating external from internal noise. The primary source of excessive noise in the RFD is the active elements within ENLARGER [Ref. 6:p. 25].

3. Internal Sources of Man-Made Noise

The introduction of inadequately and improperly shielded electronic equipment within the CDAA sites has resulted in an internal noise problem at most locations.

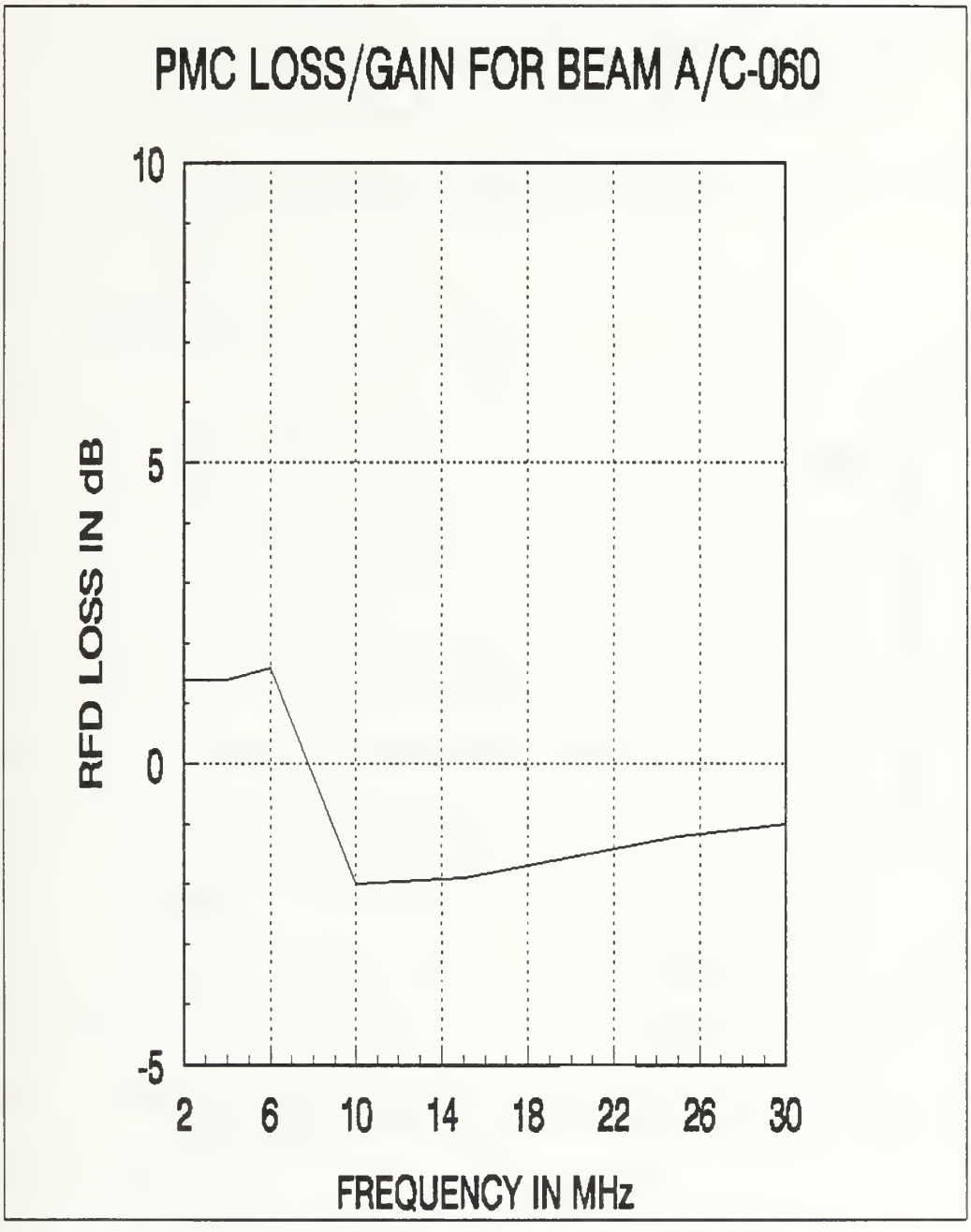


Figure 7. PMC Loss or Gain.

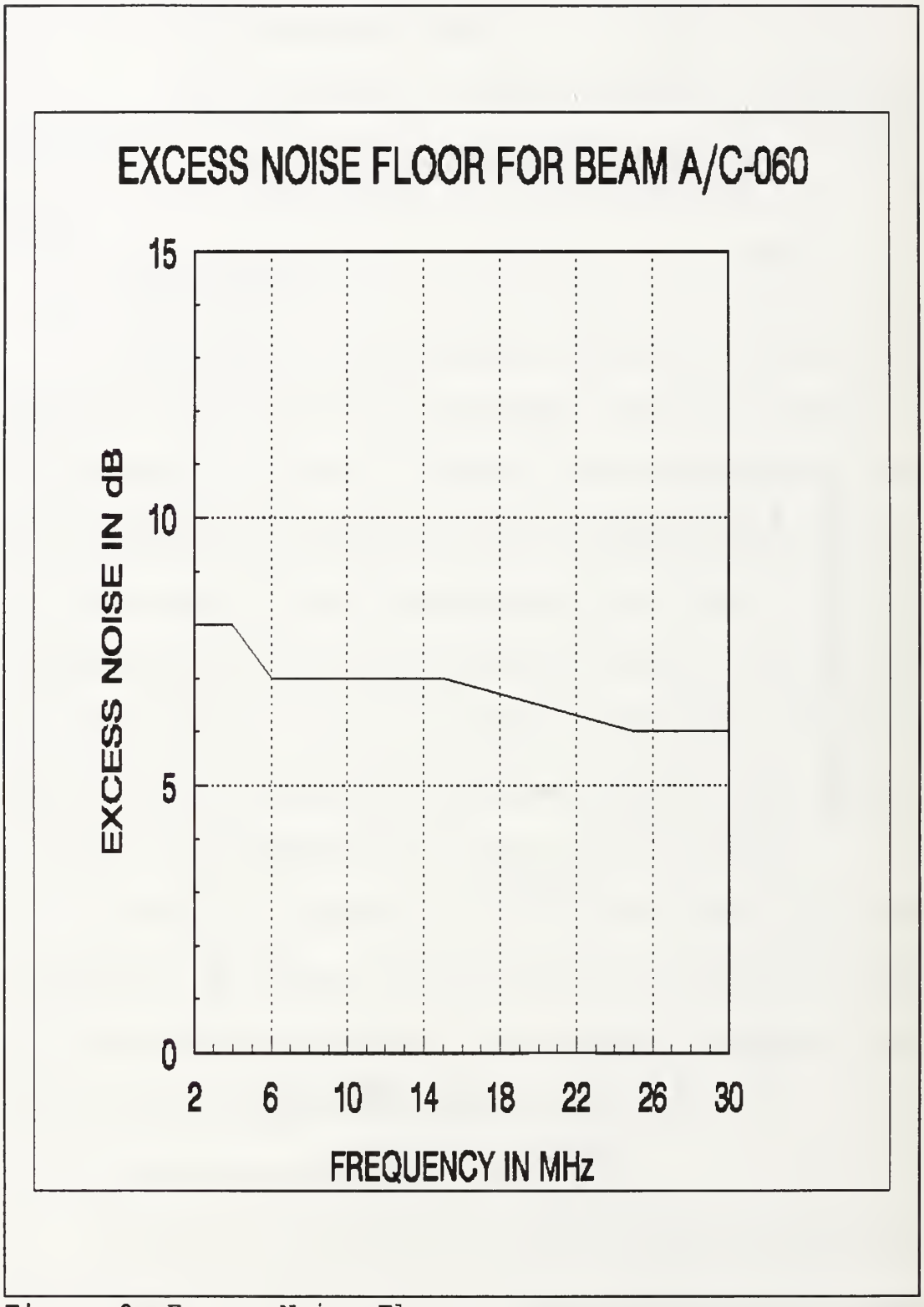


Figure 8. Excess Noise Floor.

Internal electronic devices such as mini-computers, workstations, PC's, LAN's, uninterruptible power supplies (UPS), frequency converters, digital telephone switches, and other digital equipment generate radio interference. The noise from such devices is conducted along power wires, ground buses, cable shields, air-conditioning ducts, and other conductors. It enters the RFD by a variety of paths and is in turn fed to the input terminals of receivers.

The measurement, identification, and location of specific internal noise sources is a long and tedious process. The most effective method of locating internal sources is to monitor the waveform (temporal and spectral structure) of each suspected internal noise source and then physically search for sources that can generate these structures. For example, by correlation with an on/off light switch, a faulty fluorescent light ballast close to an antenna cable bundle may be positively identified as the source of HF noise observed on the 3-axis display (see Appendix B). This process, often involving trial and error, may require many man-days of effort, especially if the source is intermittent. If the source is not physically located and eliminated, then its noise interference contributes to the noise floor used in the PET evaluation. Equipment currently used to identify and record the noise or interference source waveforms is described in Appendix B. The waveforms obtained with the 3-axis display for internal sources are often similar to those for external sources.

4. External Sources of Man-Made Noise

Sources of noise external to the site are an ever-increasing problem as the development of land in close proximity to the site is constantly taking place. Power-line

noise is the most prevalent of all external noise sources [Ref. 7:p. 17]. A photograph of the 3-axis display waveform (temporal and spectral structure) for power-line noise is shown in Figure 9. All signals within the 2.6 to 4.0 MHz band and having a smaller signal strength will be lost to the noise interference. The masking of the weaker signals by another case of power-line noise is shown in Figure 10. The temporal and spectral structure of ignition noise is shown in Figure 11. This source is external to the site. A view of the gross spectral structure of a specific kind of internal noise is shown in Figure 12. Figure 13 shows the distinctive fine temporal and spectral shape of the internal noise of Figure 12.

Out-of-band emanations from equipment in the Industrial, Scientific, and Medical (ISM) radio service causes large numbers of SOIs to be lost in some receiving systems [Ref. 8:pp. 76-79]. The intermittent nature of out-of-band ISM signals makes their identification difficult unless wide-band monitoring systems are available. Even when identification and location is possible, it may not be feasible to correct all ISM problems. This is especially true for distant ISM sources located in other countries. Such signals may traverse one or two ionospheric propagation hops before arriving at a receiving site.

The spectral and temporal characteristics of all man-made noise, from both internal and external sources, must be measured and recorded for use in the performance evaluation. The percentage of signals lost due to man-made sources is often significant.

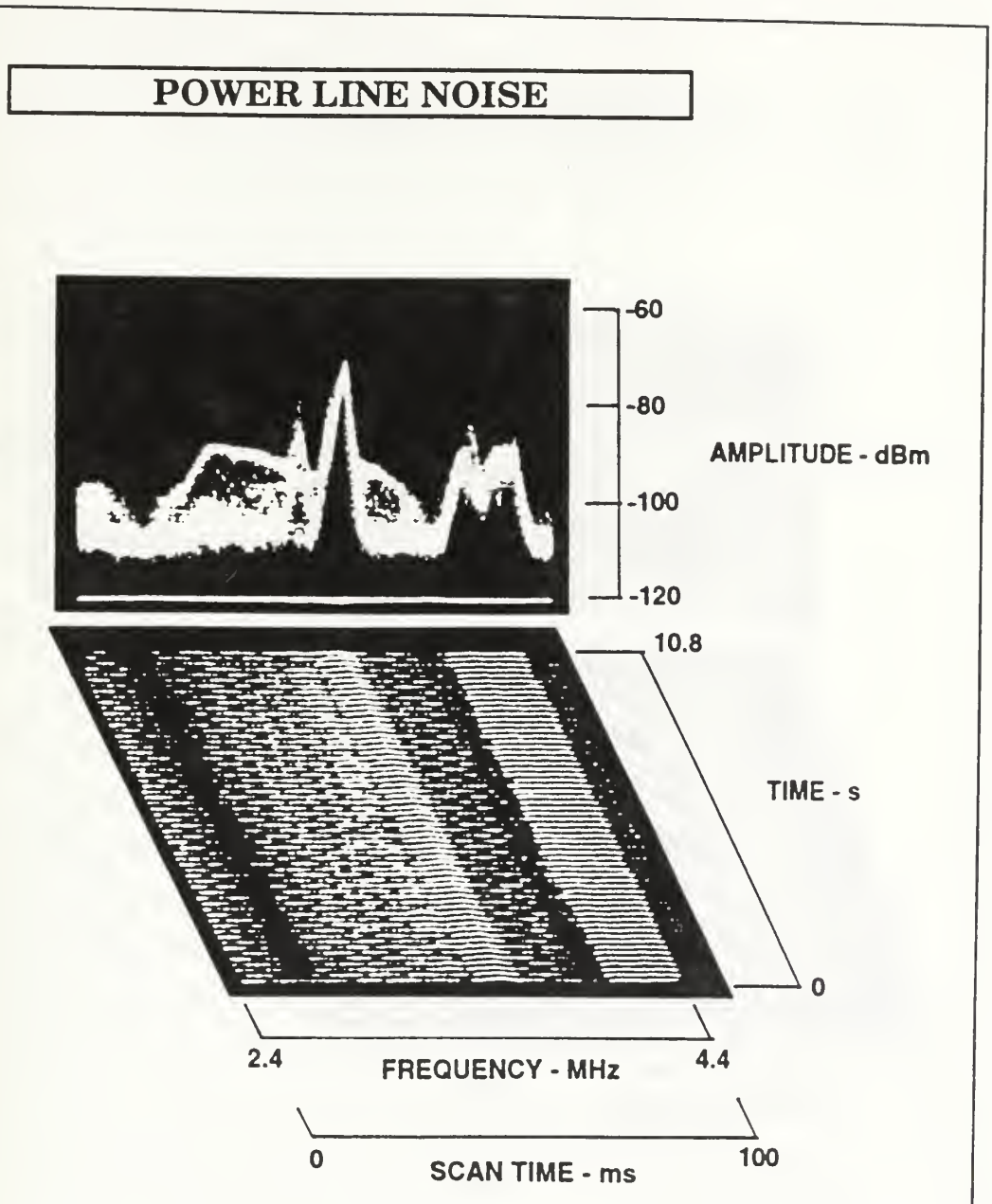


Figure 9. Power Line Noise.

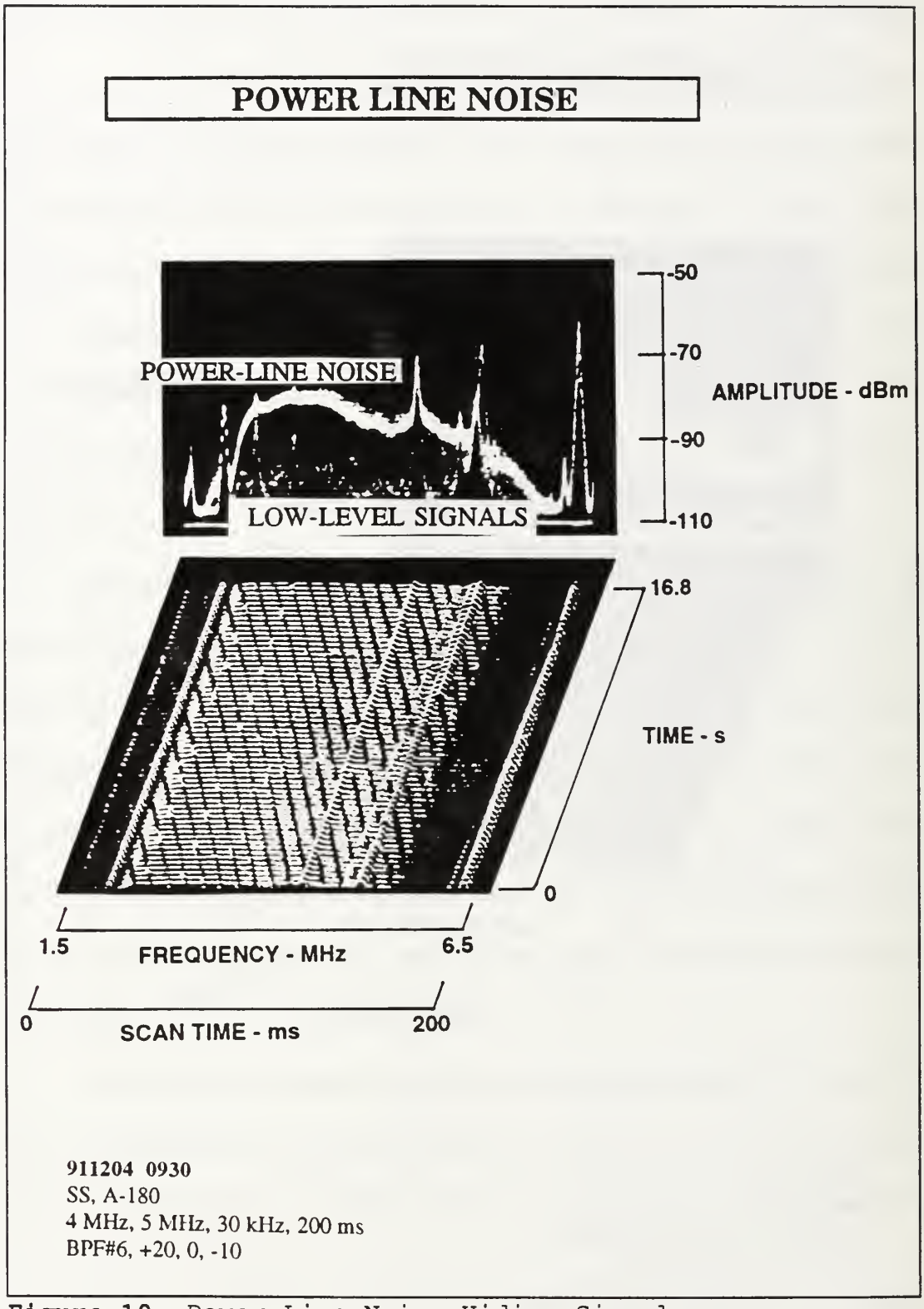


Figure 10. Power Line Noise Hiding Signals.

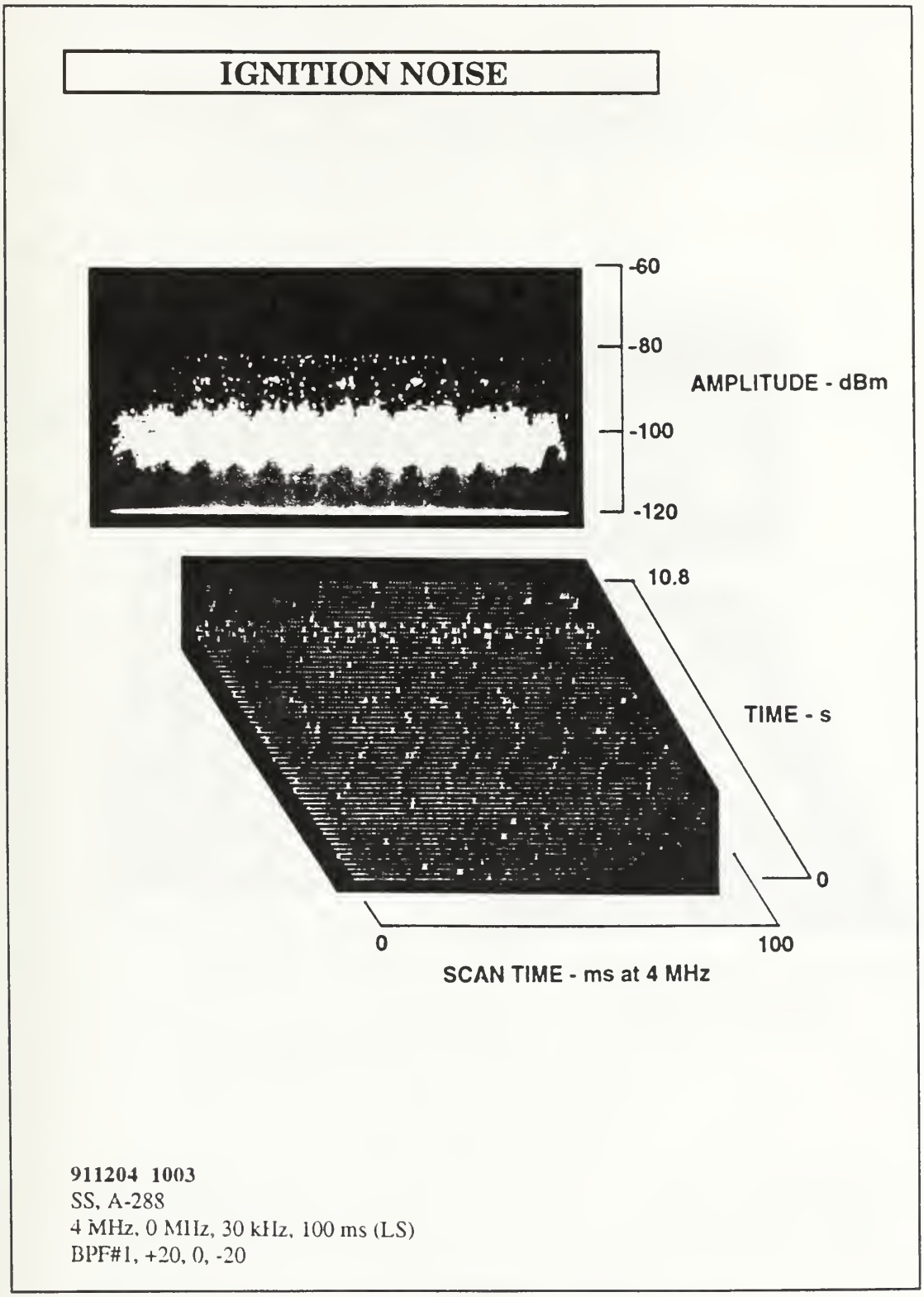


Figure 11. Ignition Noise.

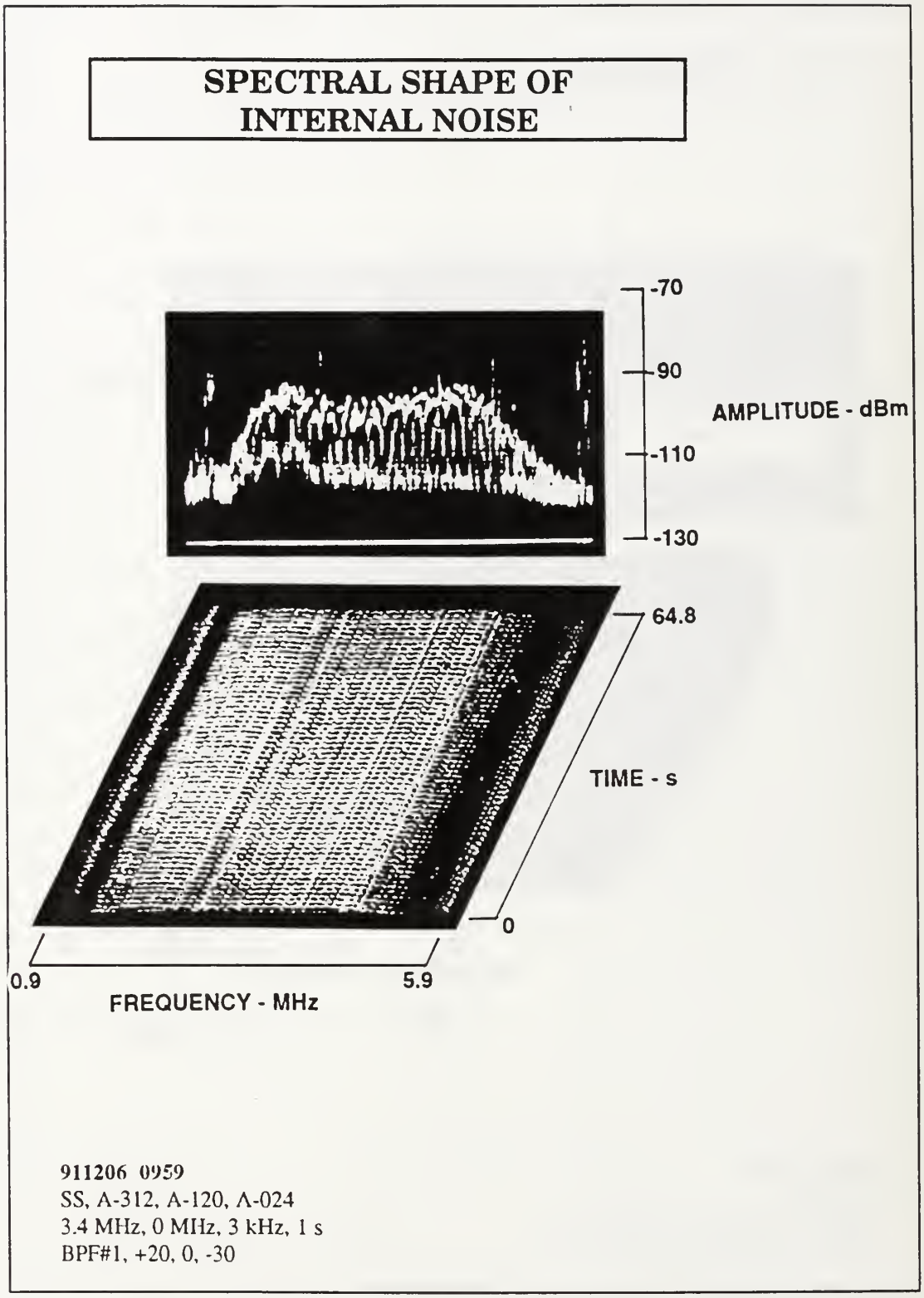


Figure 12. Internal Noise.

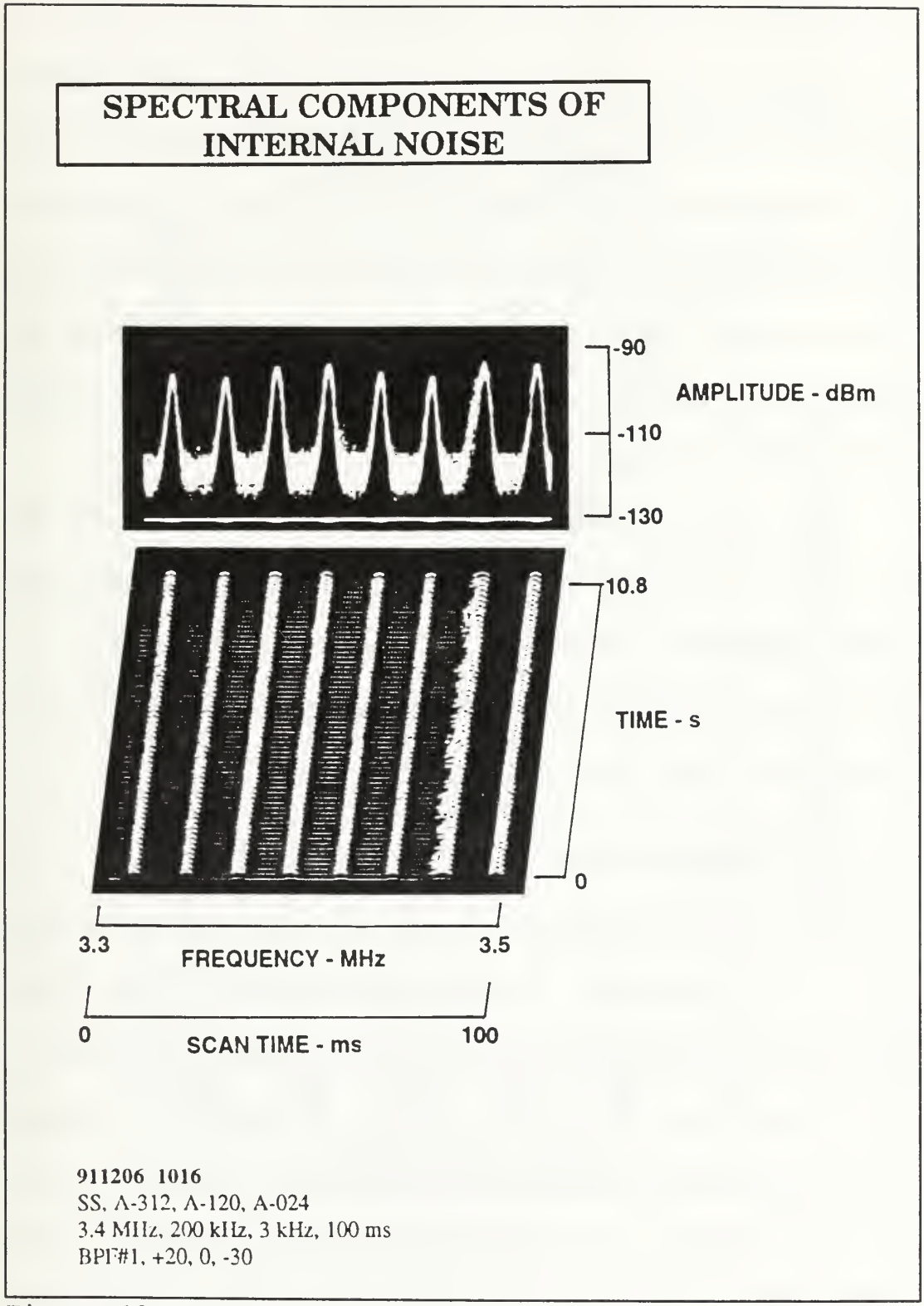


Figure 13. Internal Noise.

5. International Broadcast Service Interference

The HF band contains a number of sub-bands allocated to the International Broadcast Service. Transmitters in this service frequently employ power levels of 1 MW or higher and antennas with gains approaching 20 dB. These transmitters produce extremely strong signal levels at CDAA sites. The signals may be as high as 40 to 50 dB above the maximum levels of most SOIs. The mix of very strong signals from transmitters in the International Broadcast Band and low-level SOIs requires that RFD components have very high dynamic range (more than 100 dB).

RFD components with insufficient dynamic range to handle the large amplitude range of received signals will generate intermodulation (IM) products. These IM products also degrade the performance of CDAA or other receiving sites. The impact of IM products on site performance is not the primary topic of this thesis, and the adverse impact of this aspect of site operation is not covered.

E. THE PET CURVE

The PET curve has been developed to quantify and measure the effects of system degradation on the reception of SOIs. It combines the diverse factors of signal strength, noise floor, RFD loss, and man-made noise into a meaningful graphical relationship. By using the PET graph and varying the input parameters, the performance of a receiver system can be measured by determining the percent of SOIs lost. A complete PET curve sample is shown in Figure 14. The steps for the construction and interpretation of the curve are as follows.

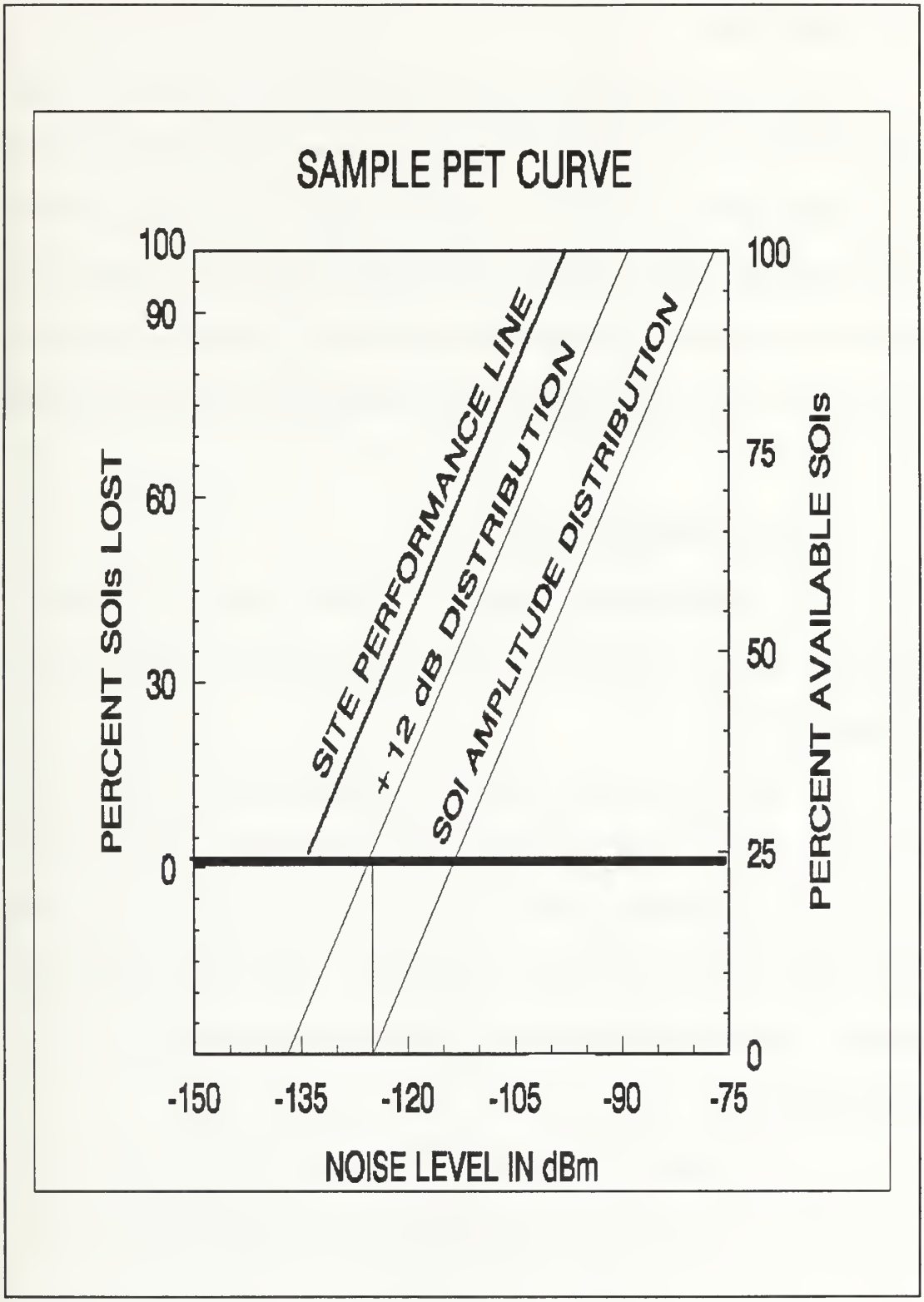


Figure 14. Sample PET Curve.

1. Construction

The PET curve construction process begins with a two dimensional x-y plot as shown in Figure 15. The x-axis represents the signal power in dBm of SOIs received by a site's antenna system. The y-axis is located to the right, vice the normal convention of location on the left. This will allow for the subsequent addition of a second y-axis. The y-axis scale represents the percent of available SOIs that exceed the received power level shown on the x-axis. The resulting curve is the amplitude distribution of a selected class SOIs.

a. SOI Amplitude Distribution

A straight-line approximation of the SOI Amplitude Distribution is sufficiently accurate for general PET use. The procedure for generating this approximation follows.

Enter a point on the x-axis at the noise floor level of -125 dBm and the y-axis value of 0 percent. This point is the left end of the distribution. The second point of the straight-line approximation is the x-axis value of the maximum signal strength expected, in dBm, and the y-axis value of 100 percent. Connect the two points with a straight line. This line will represent the straight-line approximation of the SOI Amplitude Distribution.

The amplitude distribution of SOIs is more accurately shown by a log-normal distribution. An illustration of the straight-line approximation superimposed over

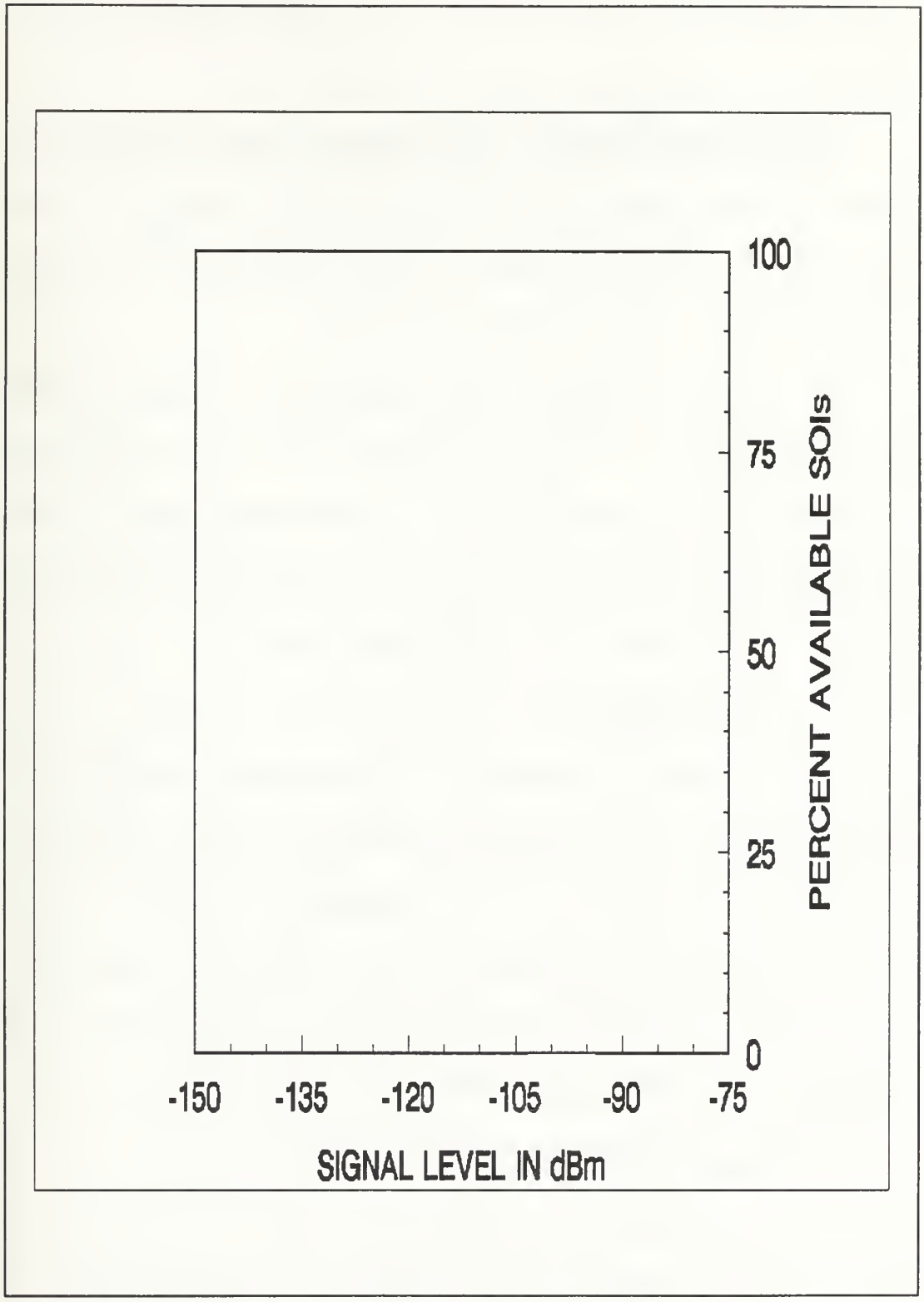


Figure 15. Start of PET Curve.

a log-normal distribution is shown in Figure 16. The primary differences are at the extreme ends of the distribution.

Appendix D presents data confirming the log-normal amplitude distribution of certain classes of SOIs [Ref. 3:pp. 28-45]. While the log-normal distribution can be used in the PET process, the minor error generated by the straight-line approximation does not greatly affect the final results.

To understand the use of the linear approximation of the SOI Amplitude Distribution, consider the following example. In Figure 17, enter the x-axis with a signal level of -95 dBm, the intersection of this level with the distribution line will yield a corresponding value of SOIs available on the y-axis. Sixty-four percent of the total SOIs are below this level and 36 percent of the total SOIs are above this level.

b. +12 dB Distribution

A +12 dB Distribution line is drawn parallel and to the left of the SOI Amplitude Distribution. This line represents the amplitude distribution of SOIs that are 12 dB above the receiver noise floor. This is approximately the signal-to-noise ratio required for the detection and processing of SOIs by conventional digital signal processing techniques. All procedures from this point on will be based on the +12 dB Distribution and the left y-axis. Figure 18 shows the +12 dB Distribution line.

c. Percent SOIs Lost

A second y-axis scale located on the left of the curve will be constructed using the following steps. Enter the x-axis at the reference noise floor limit, in this case

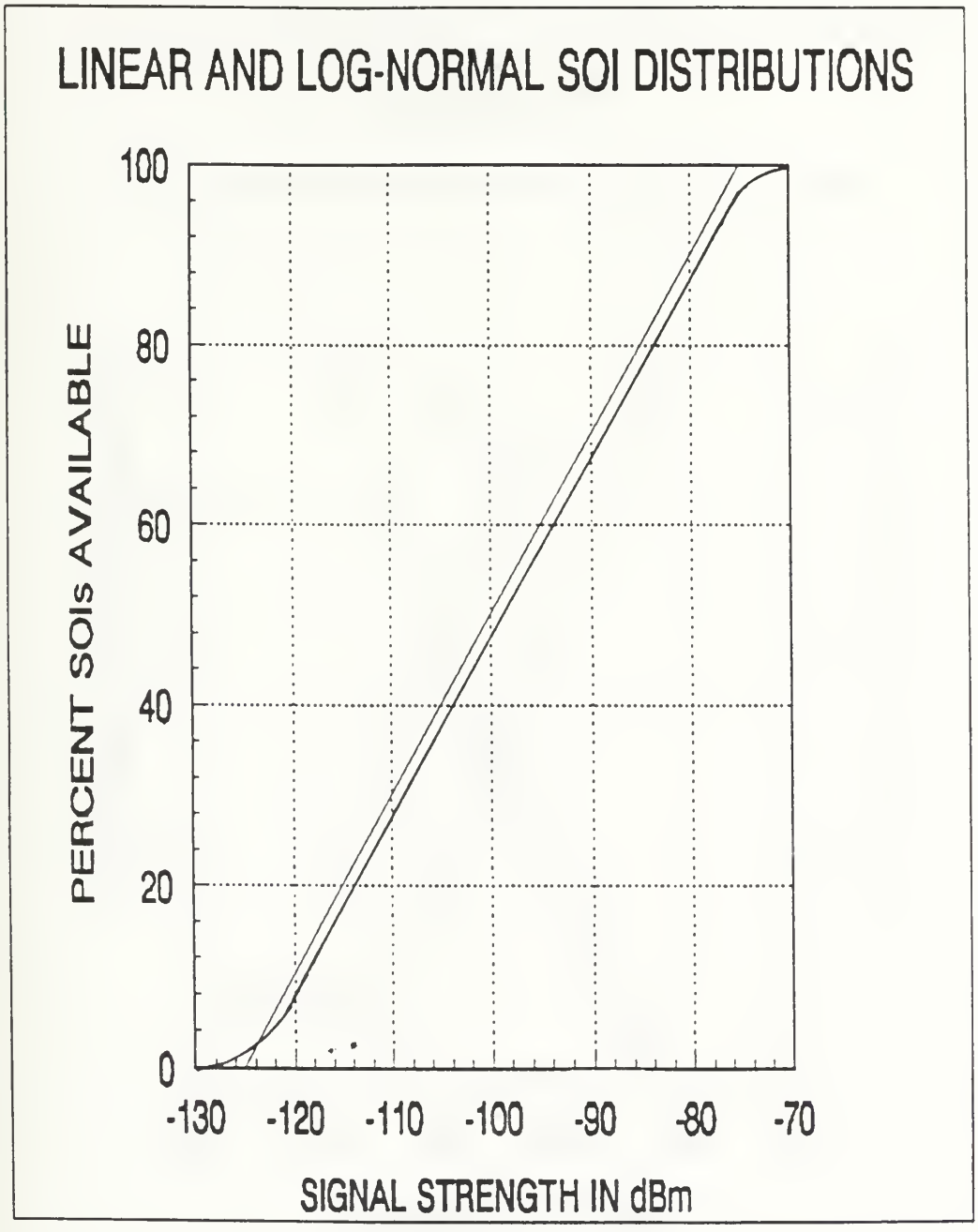


Figure 16. Linear and Log Normal Distributions.

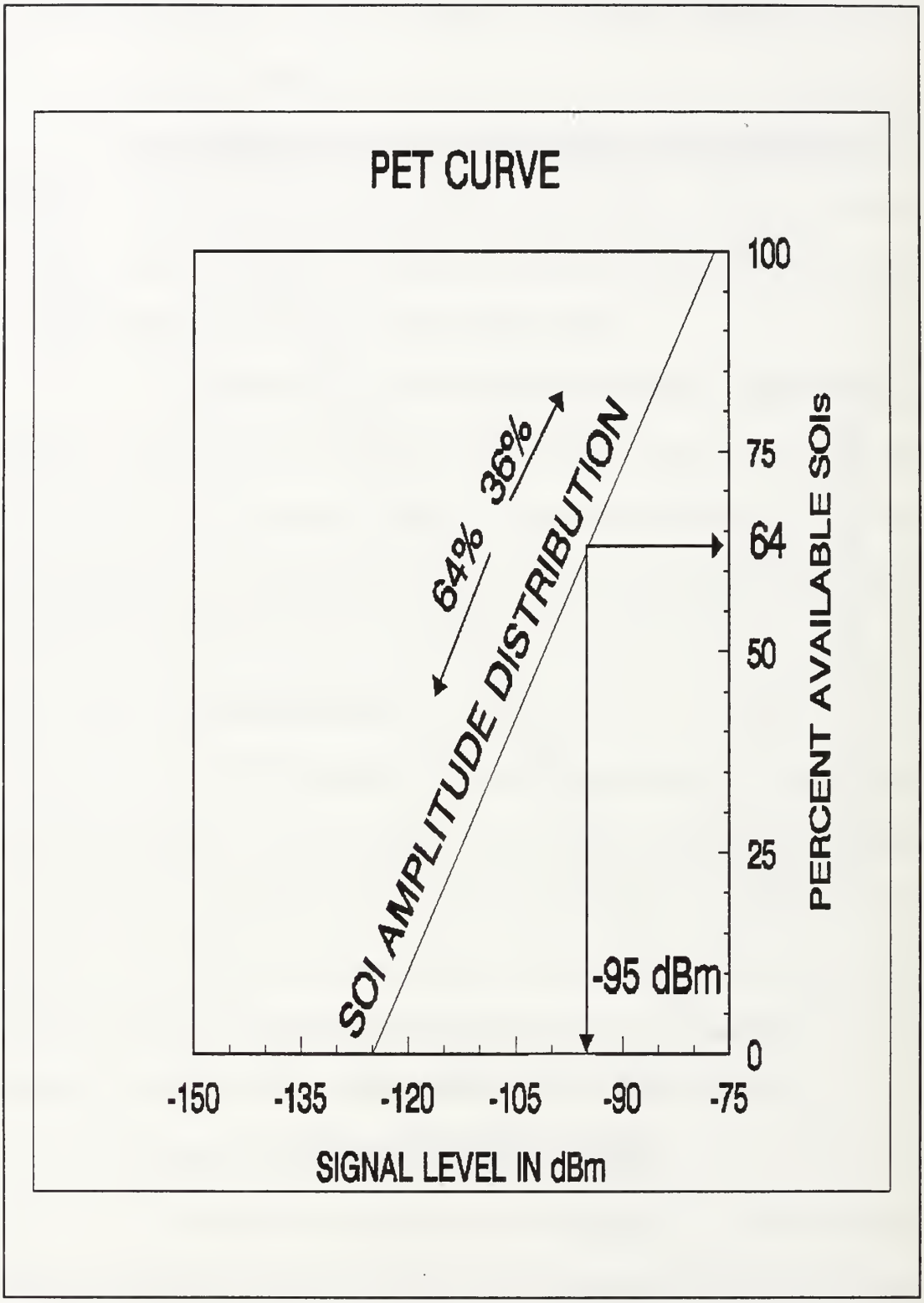


Figure 17. Amplitude Distribution Example.

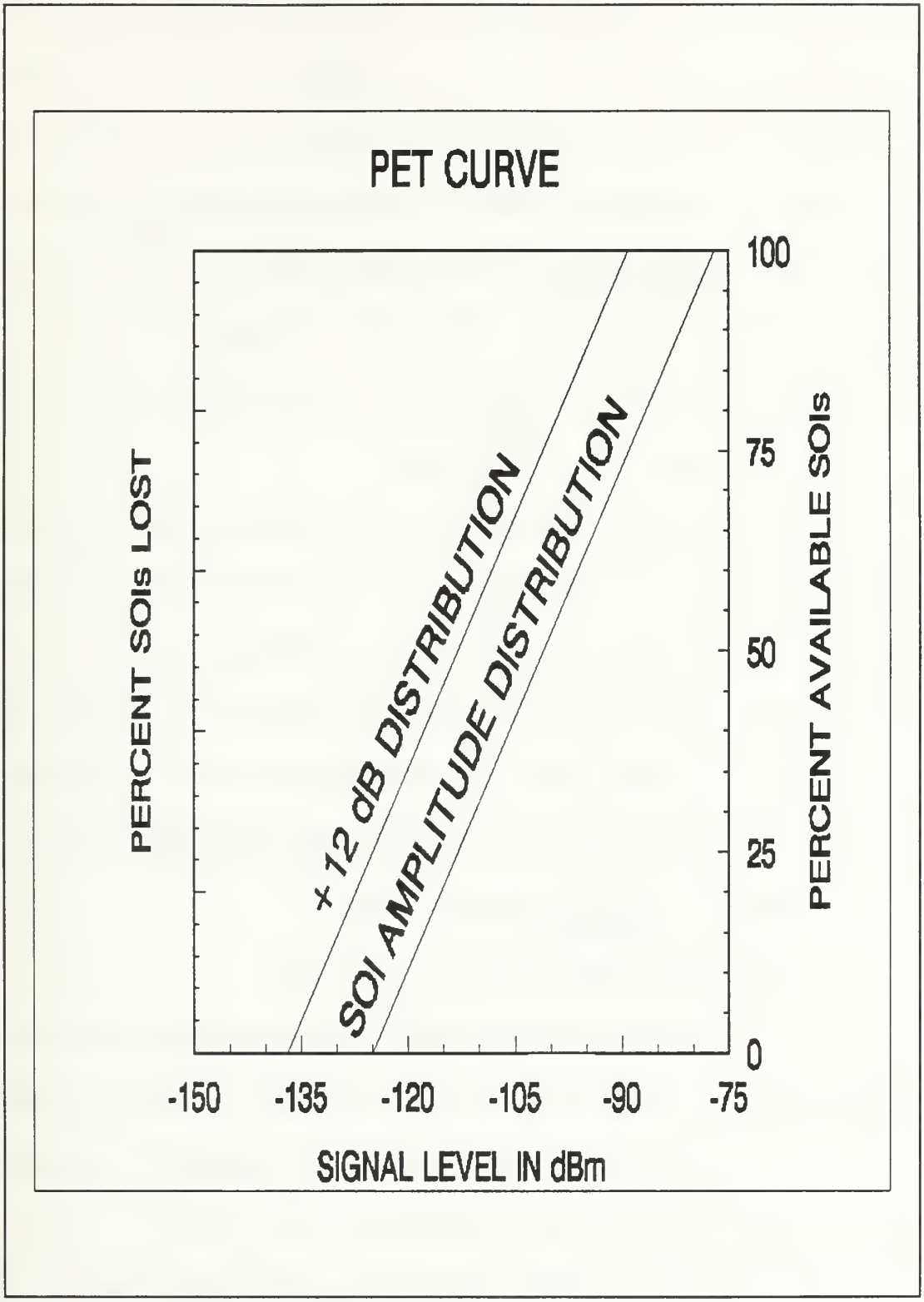


Figure 18. +12 dB Distribution.

-125 dBm. Proceed up to the +12 dB Distribution line. Where -125 dBm intersects the line, proceed left and mark the y-axis 0 as shown in Figure 19. This marks the base value of percent of SOIs lost. The top point of the y-axis will be 100, with the axis scaled accordingly. The graph now represents the optimum performance of a receiving system. The operating point where -125 dBm intersects with the +12 dB distribution corresponds to a 0 percent signals lost. With no RFD loss introduced into the curves, the +12 dB Distribution line, shown in Figure 20, is the Site Performance line.

d. Performance With RFD Loss Added

The curve from Figure 20 will now be revised to include the effect of the signal attenuation within the RFD. The sum of the attenuations of all components in the RFD at a particular frequency is added to the Site Performance line. This moves the line to the left as shown in Figure 21. The new performance line represents the optimum performance the site can attain with the RFD loss introduced. The intersection of the -125 dBm level with the Site Performance line produces the percent of SOIs lost due to signal attenuation in the RFD as shown in Figure 22.

e. Performance With Excess Noise Floor Added

The impact of an increase in system noise over the reference noise floor is illustrated as follows. Enter the actual noise floor of the RFD (-125 dBm plus excess noise level) into the x-axis for the corresponding frequency of operation. Signals that are above -125 dBm but still below the excess noise floor are now lost. The new operating point is the intersection of the excess noise floor with the Site Performance line

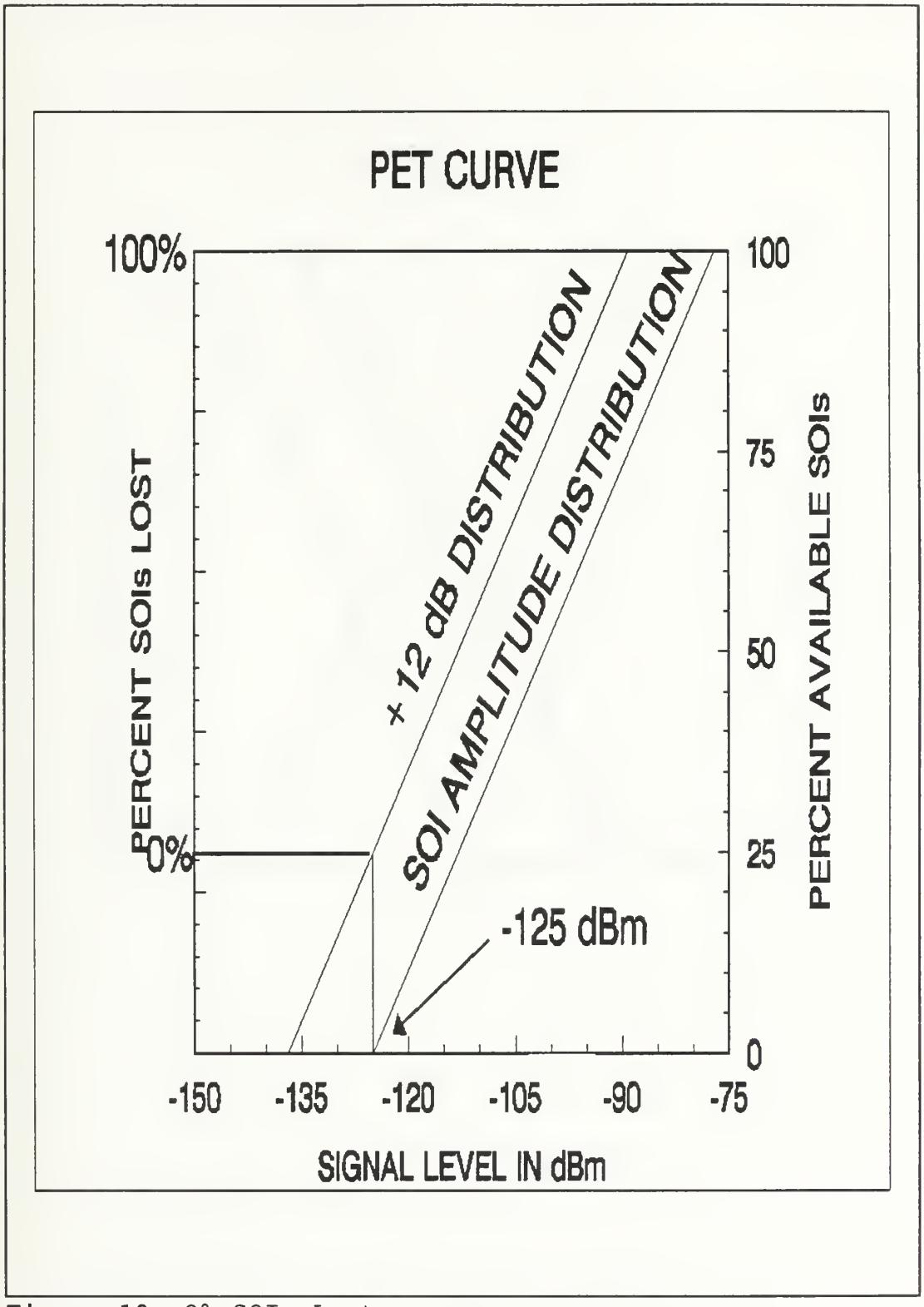


Figure 19. 0% SOIs Lost.

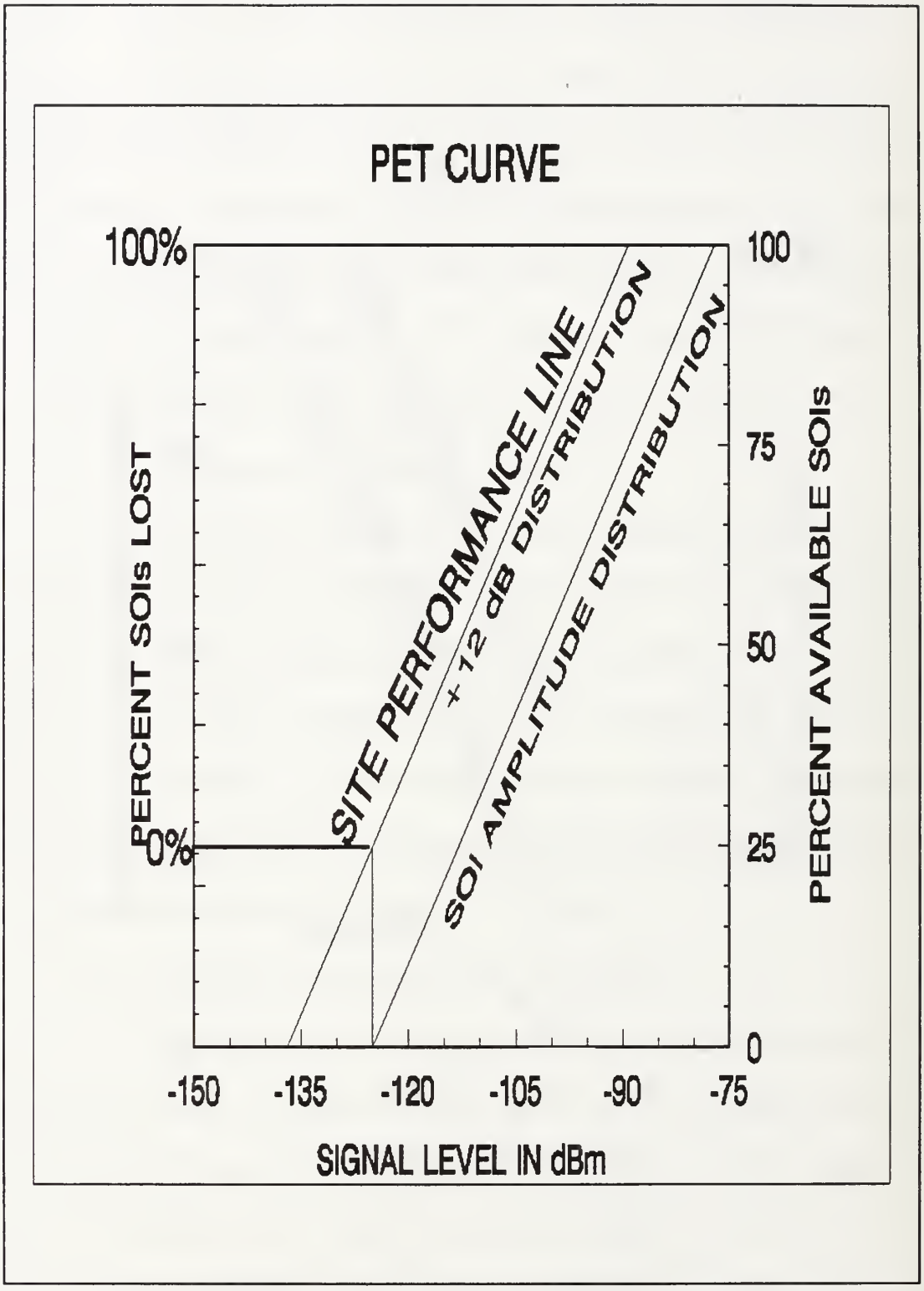


Figure 20. Site Performance Line.

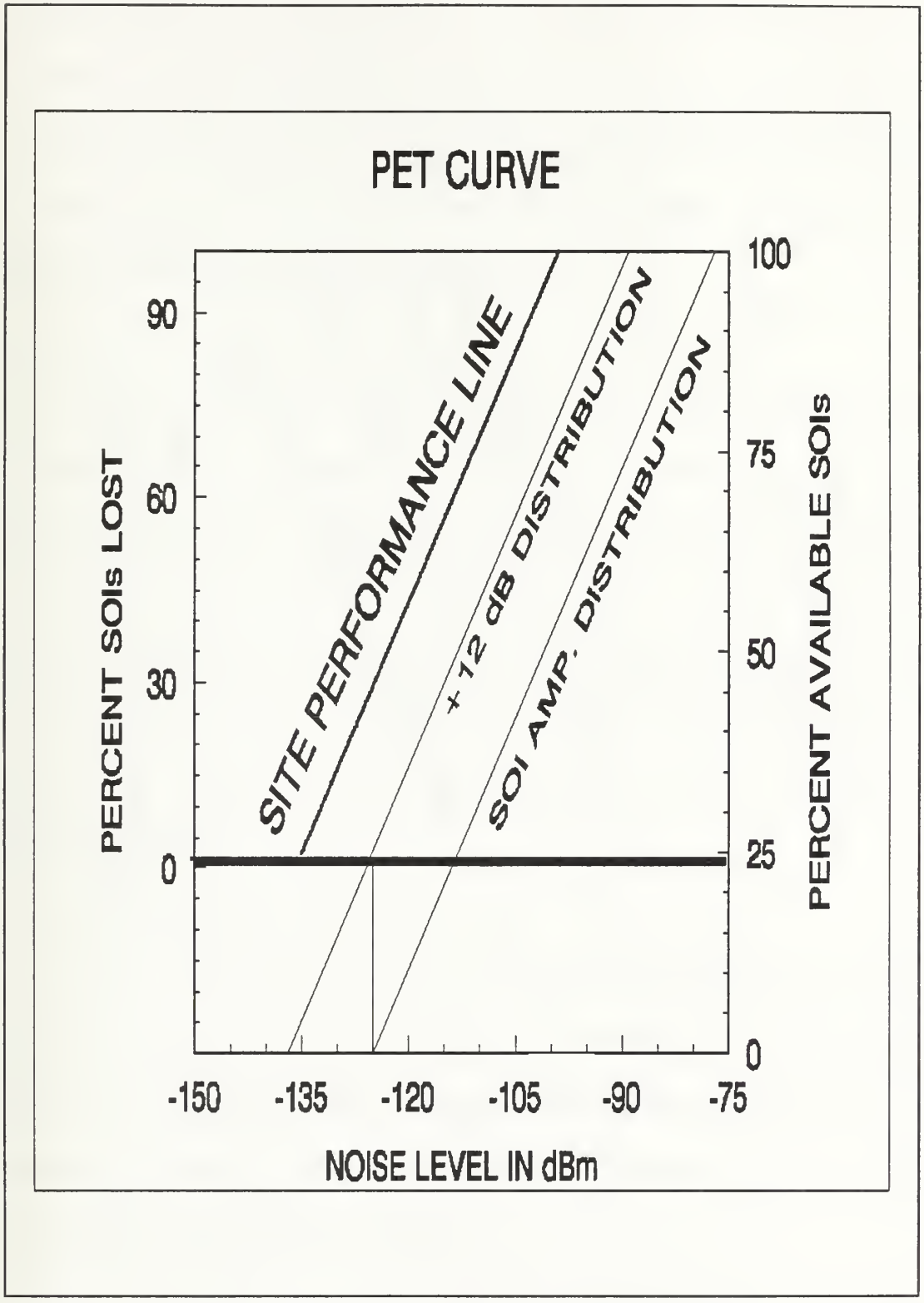


Figure 21. RFD Loss.

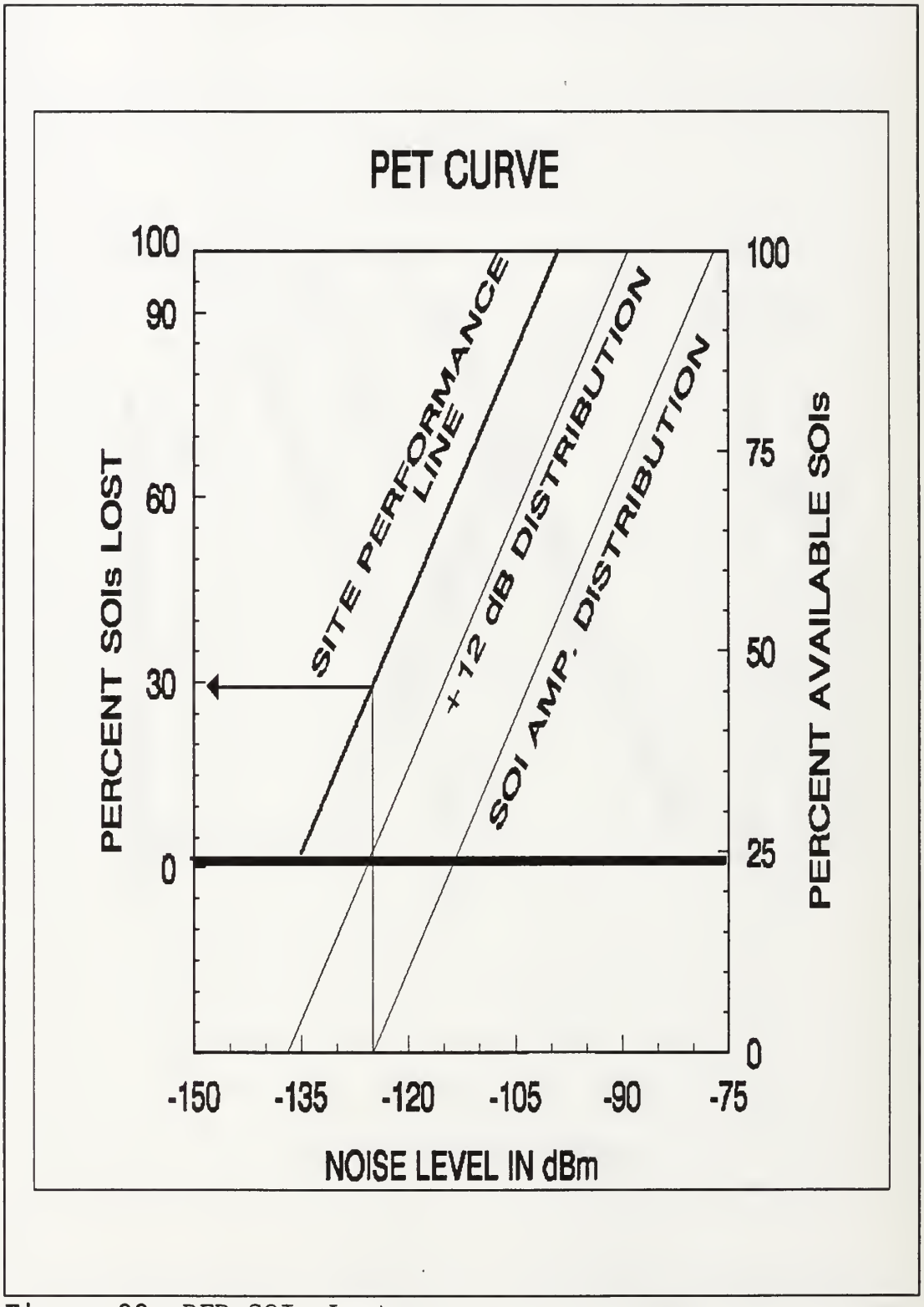


Figure 22. RFD SOIs Lost.

as shown in Figure 23. The intersection of the excess noise floor with the Site Performance line yields the percent of SOIs lost on the y-axis, due to both RFD attenuation and excess noise floor. Figure 24 shows percent of SOIs lost due solely to RFD attenuation and RFD noise floor at one particular frequency. Excess noise floor over the entire HF band is defined in Section III.D.2.

f. Performance With Internal or External Noise Added

The PET curve can be further modified to assess the impact of internal and external man-made noise that is received by the system. Enter the amplitude level of man-made noise into the x-axis for a selected frequency. The point at which this level intersects with the Site Performance line represents the new operating point for the presence of noise. Where this point intersects with the y-axis yields the percent of SOIs lost due to man-made noise, excess noise floor, and RFD loss. Figure 25 shows an example of the impact of an internal or external noise level of -107 dBm on the performance curve.

2. Interpretation of PET Curve Results

This section provides a more comprehensive description of the effects of RFD noise, excess noise floor, and noise levels on site performance. It provides additional examples of site degradation with the corresponding changes on percent SOIs lost. The optimum performance curve shown in Figure 20 and reproduced in Figure 26, will be the basis from which to start the examples.

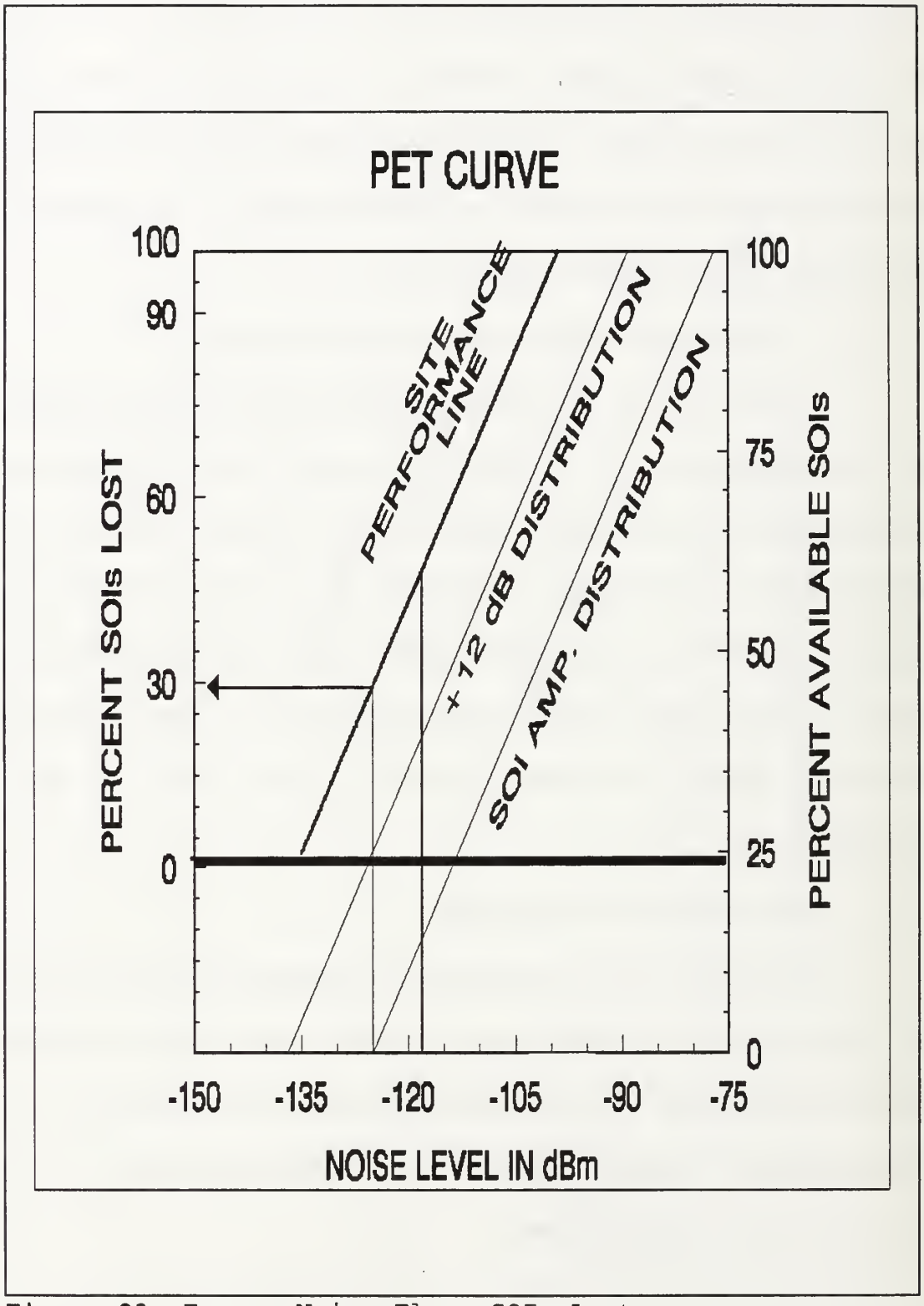


Figure 23. Excess Noise Floor SOIs Lost.

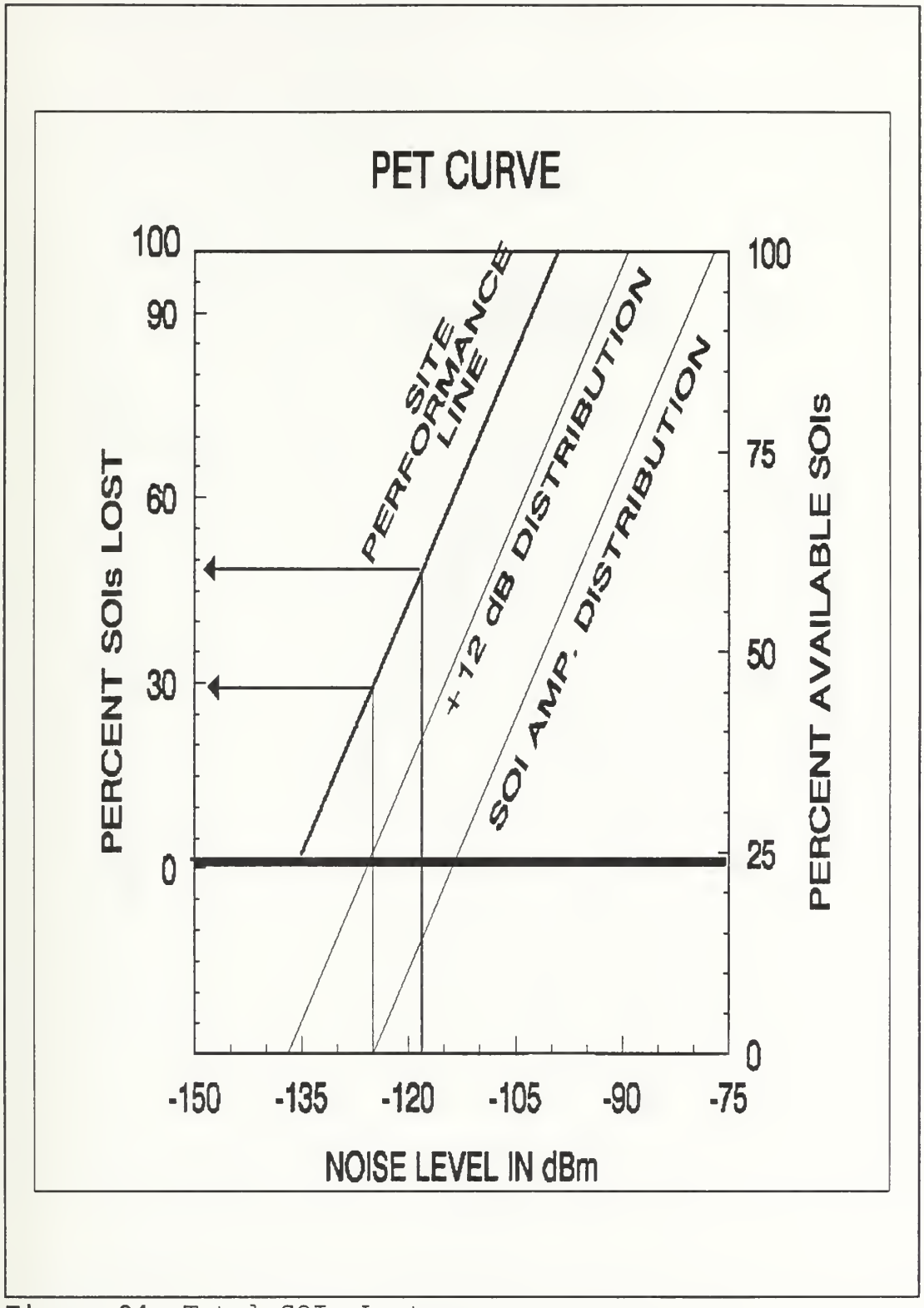


Figure 24. Total SOIs Lost.

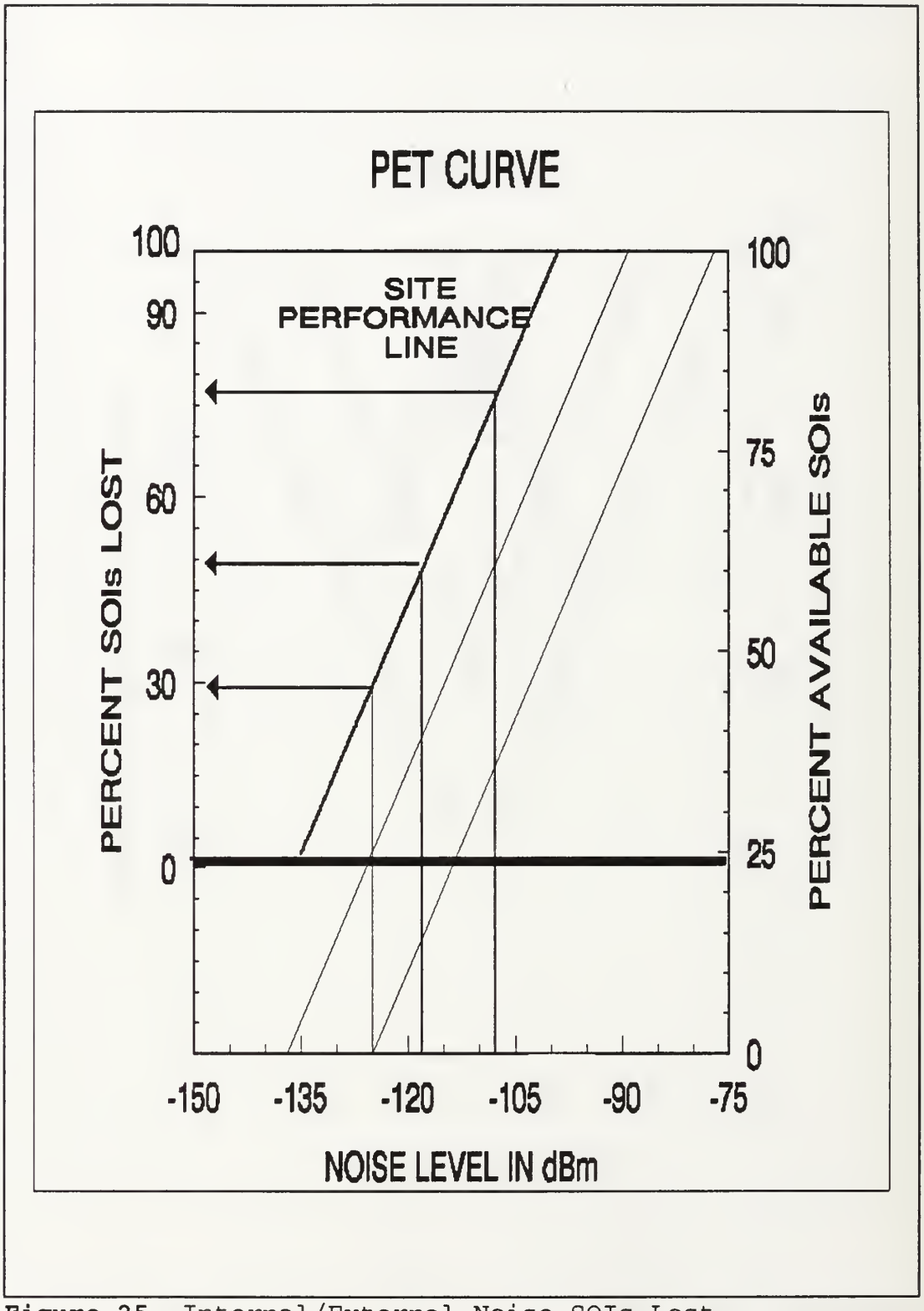


Figure 25. Internal/External Noise SOIs Lost.

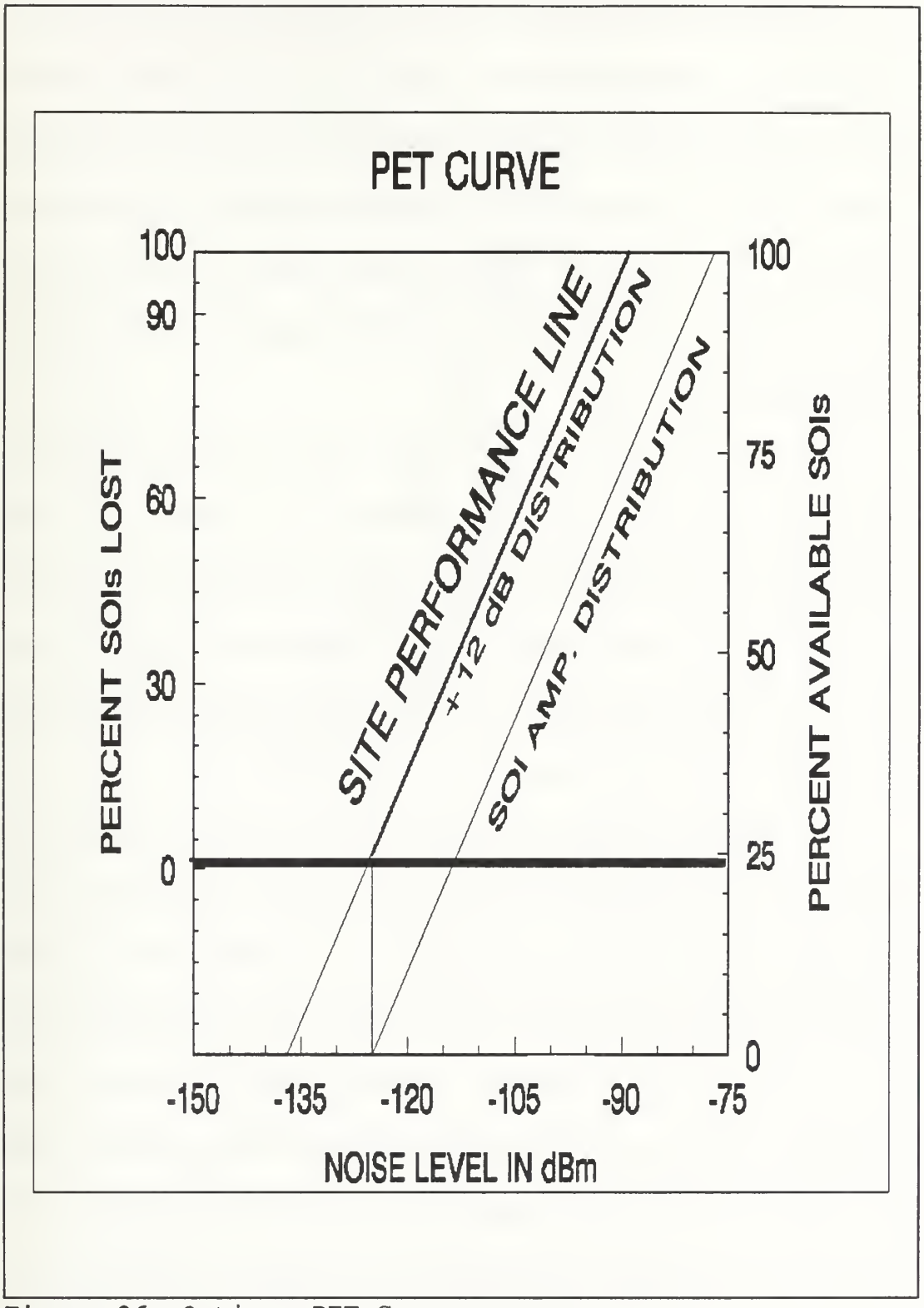


Figure 26. Optimum PET Curve.

RFD loss moves the site performance curve left by the amount of the loss. Since the optimum operating point for the system is where the reference noise floor intersects the Site SOI Performance line, the added RFD noise produces a corresponding percentage of SOIs lost. Figures 27-29 show examples of RFD loss in dB steps and the corresponding percent of SOIs lost. One can plainly see that the best performance attained is when there is no RFD loss and the Site SOI Performance line is the same as the +12 dB amplitude distribution.

The impact of excess noise floor on the reception of SOIs is determined by entering the excess noise into the x-axis and establishing a new operating point on the Site Performance line. Figure 30 shows the effect of an excess noise floor of 6 dB. The percent of SOIs lost due to the changing noise floor to an excess of 8 dB is shown in Figure 31. The system can perform best when there is no excess noise floor and the reference noise floor sets the operating point.

The presence of internal and external man-made noise also degrades site performance. The noise amplitude can vary with frequency and bearing, and the examples address both factors. The man-made noise level is entered on the x-axis. The point where the noise level intercepts the Site Performance line is determined and the resulting loss in SOI reception is established. The effect here is the same as an excess noise floor level. The presence of man-made noise masks or hides the signals of weaker strength. Figure 32 shows another example of the spectral shape of power-line noise. All the signals below the level of the power-line noise are effectively hidden in the noise and cannot be detected because of the noise. The photograph is scaled to the settings of

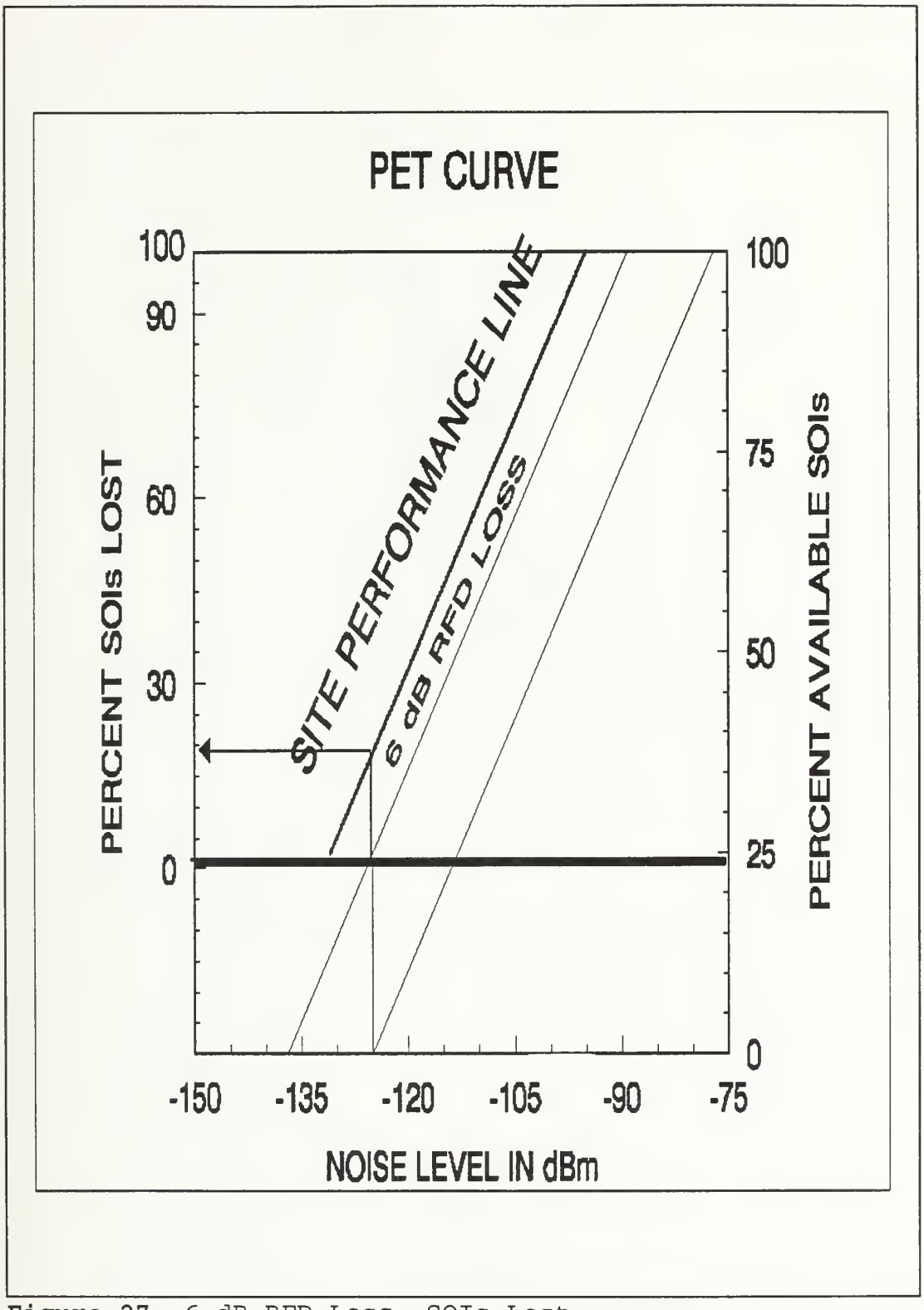


Figure 27. 6 dB RFD Loss, SOIs Lost.

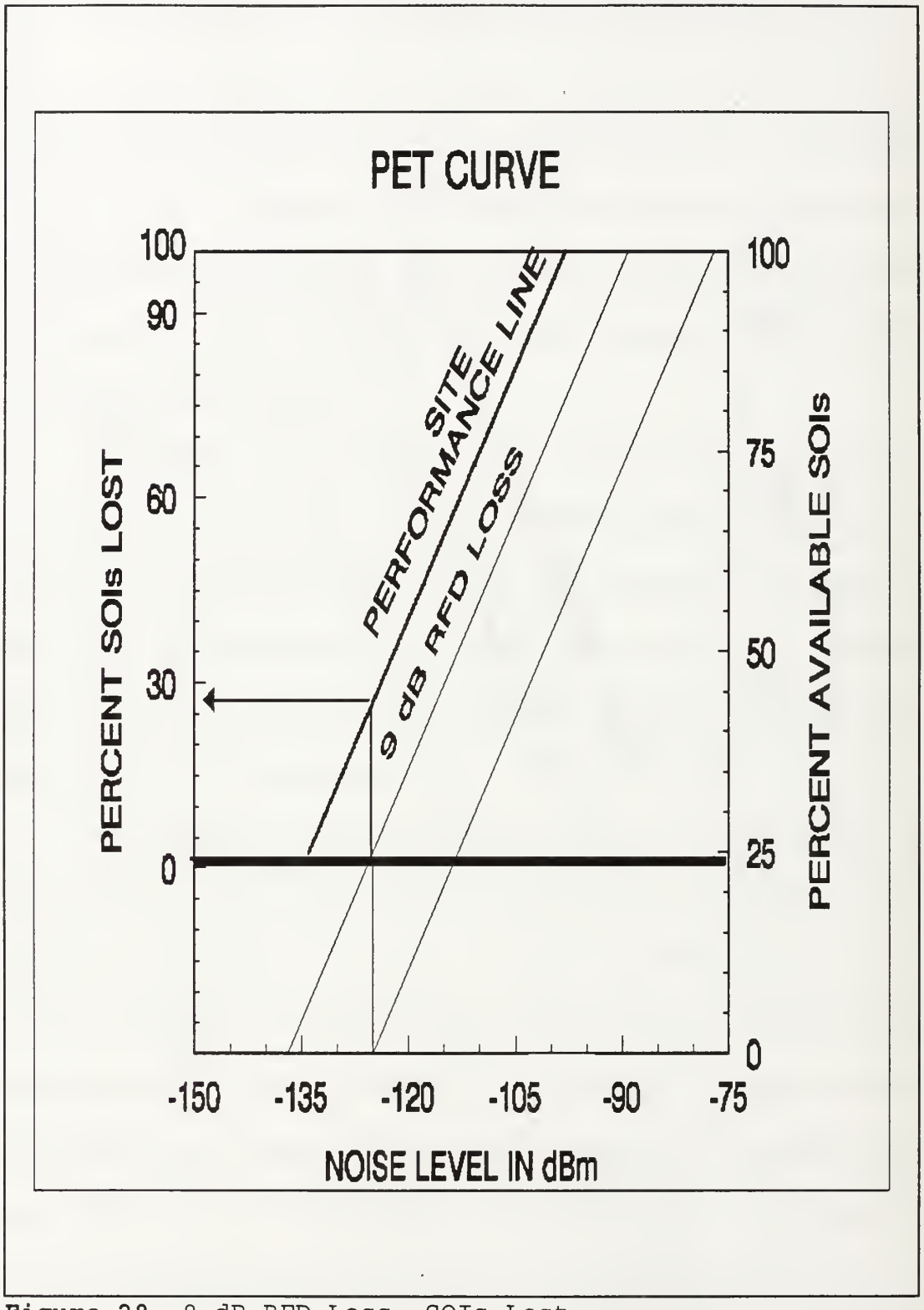


Figure 28. 8 dB RFD Loss, SOIs Lost.

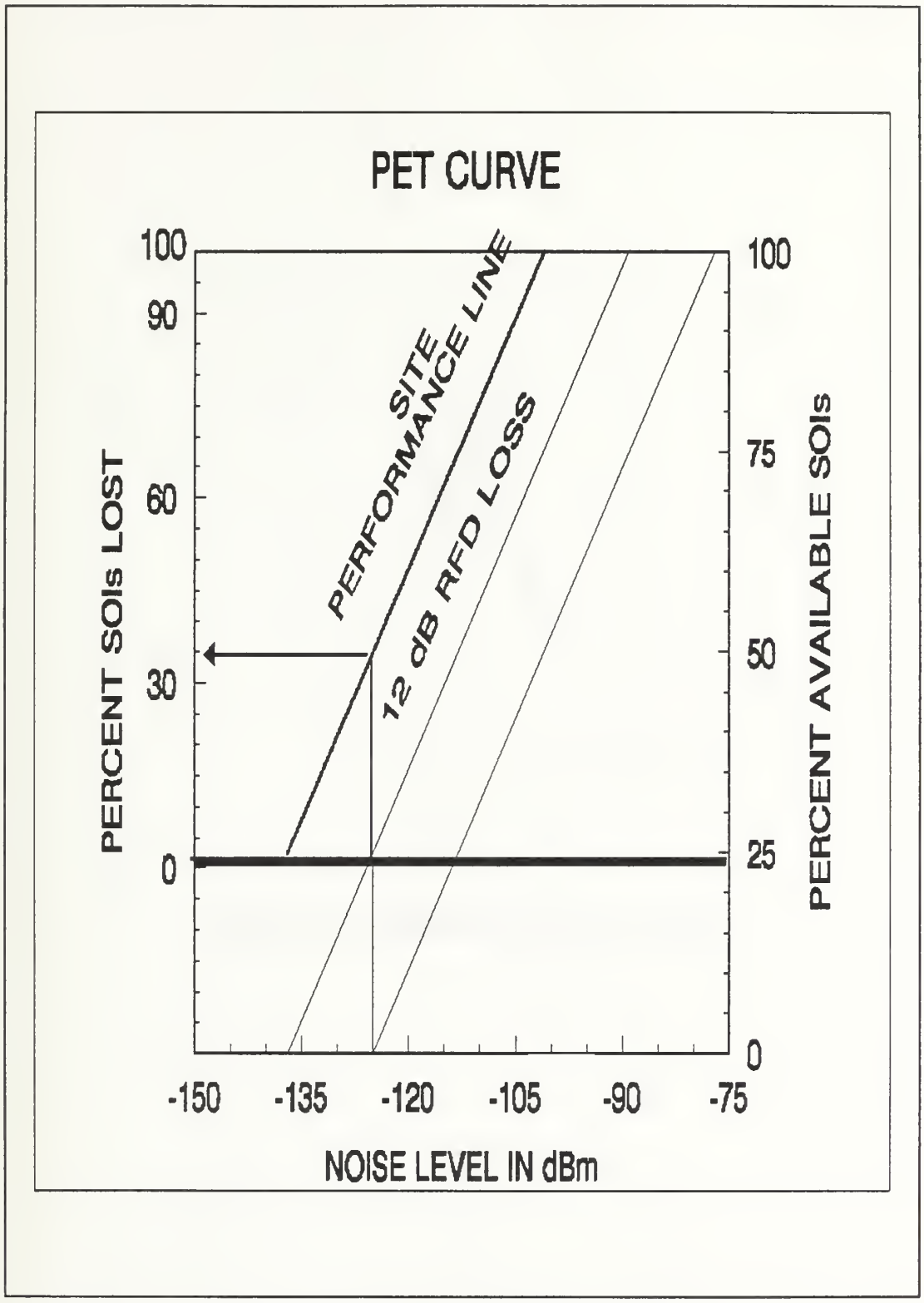


Figure 29. 12 dB RFD Loss, SOIs Lost.

VI. AUTOMATED PET ANALYSIS OF SABANA SECA DATA

The SNEP team visited NSGA Sabana Seca, Puerto Rico in early December 1991 to conduct a quick-look survey. Quick-Look Report #911213 was prepared for the Commanding Officer of NSGA Sabana Seca and Commanding Officer of G-43 at Naval Security Group Headquarters in Washington, D.C. Using the manually generated PET curves, an assessment of its performance was presented to those concerned. The survey results identified a number of specific problems affecting the performance of the receiving site. A detailed account of the actual SNEP survey steps can be found in the quick-look report.

This appendix will use the Sabana Seca data and the techniques developed for the automated PET, expand the results and provide a more detailed analysis of the individual factors affecting the overall site performance. The steps to be followed will be the applicable sections from Chapters III and IV.

The target used to produce the SOIs was a ship located approximately 2000 km northeast of the site, operating with the parameters as set in Appendix B. The maximum signal strength data from the PROPHET calculation was used to generate the PET curves. Figure 40 shows the diurnal variation of the maximum signal strength based upon the 4-hour intervals selected from all the data points. The resulting six associated PET curves corresponding to the 4-hour intervals are shown in Figures 41-46. This completes the preliminary work.

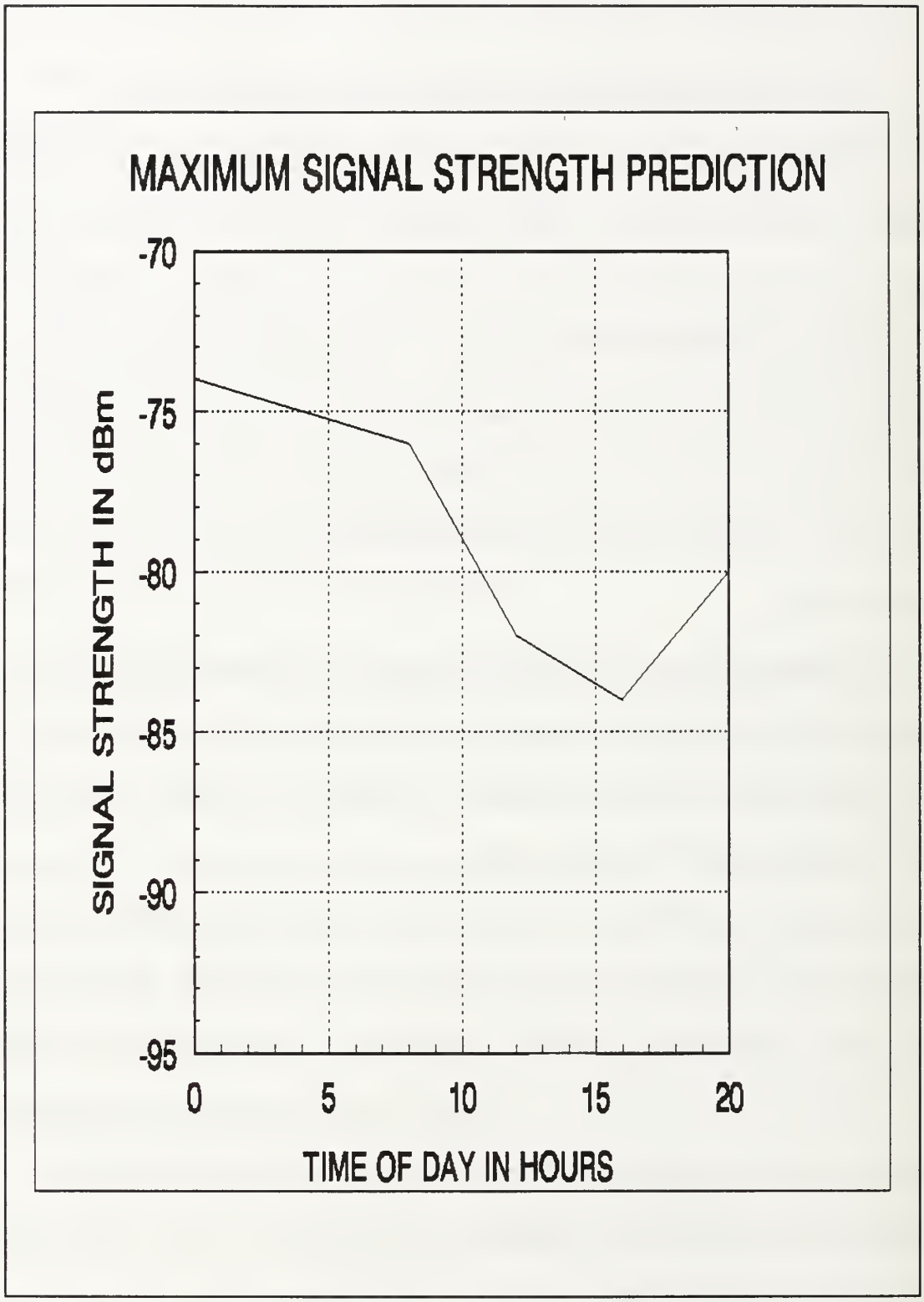


Figure 40. Maximum Signal Strength Predicted.

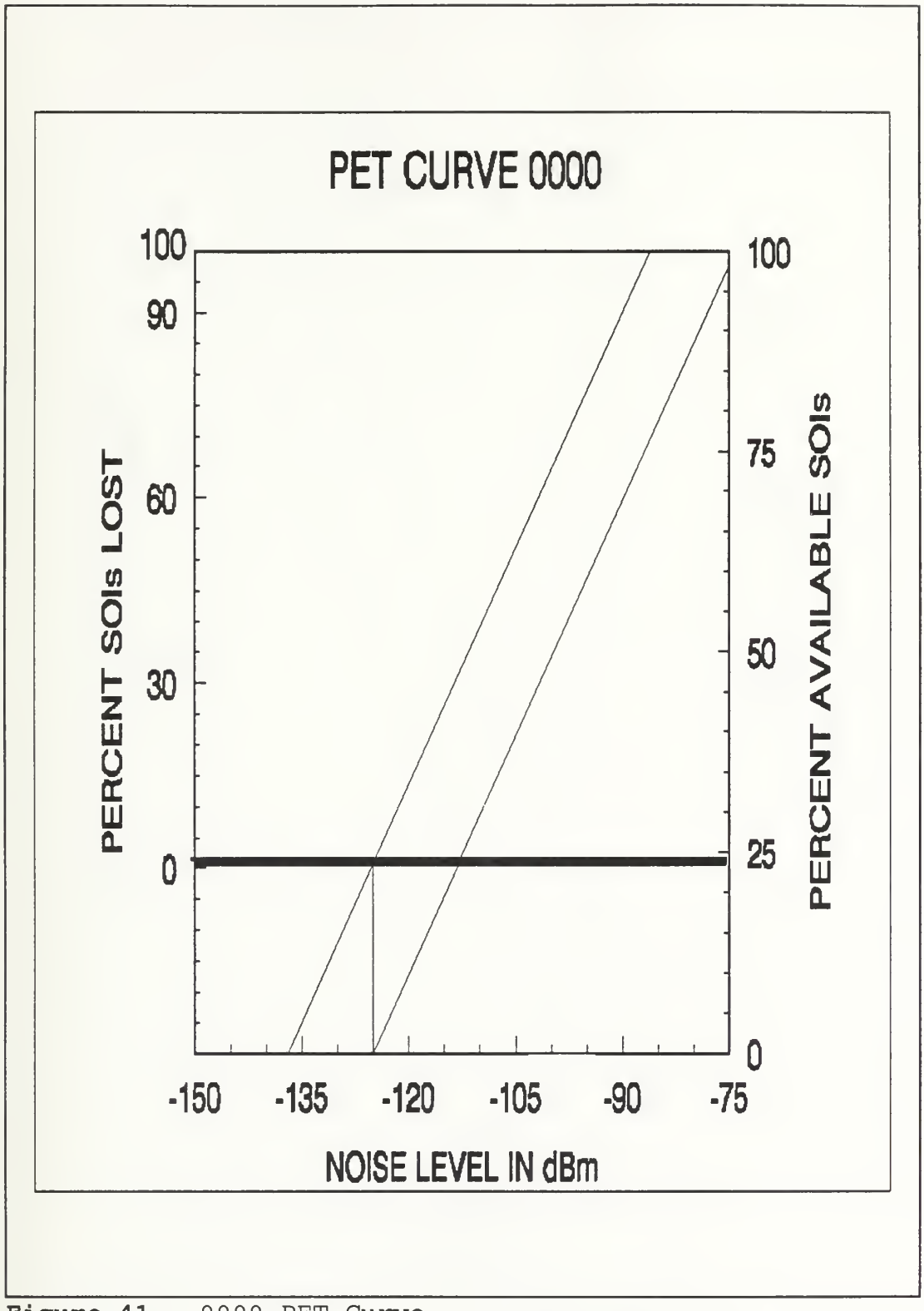


Figure 41. 0000 PET Curve.

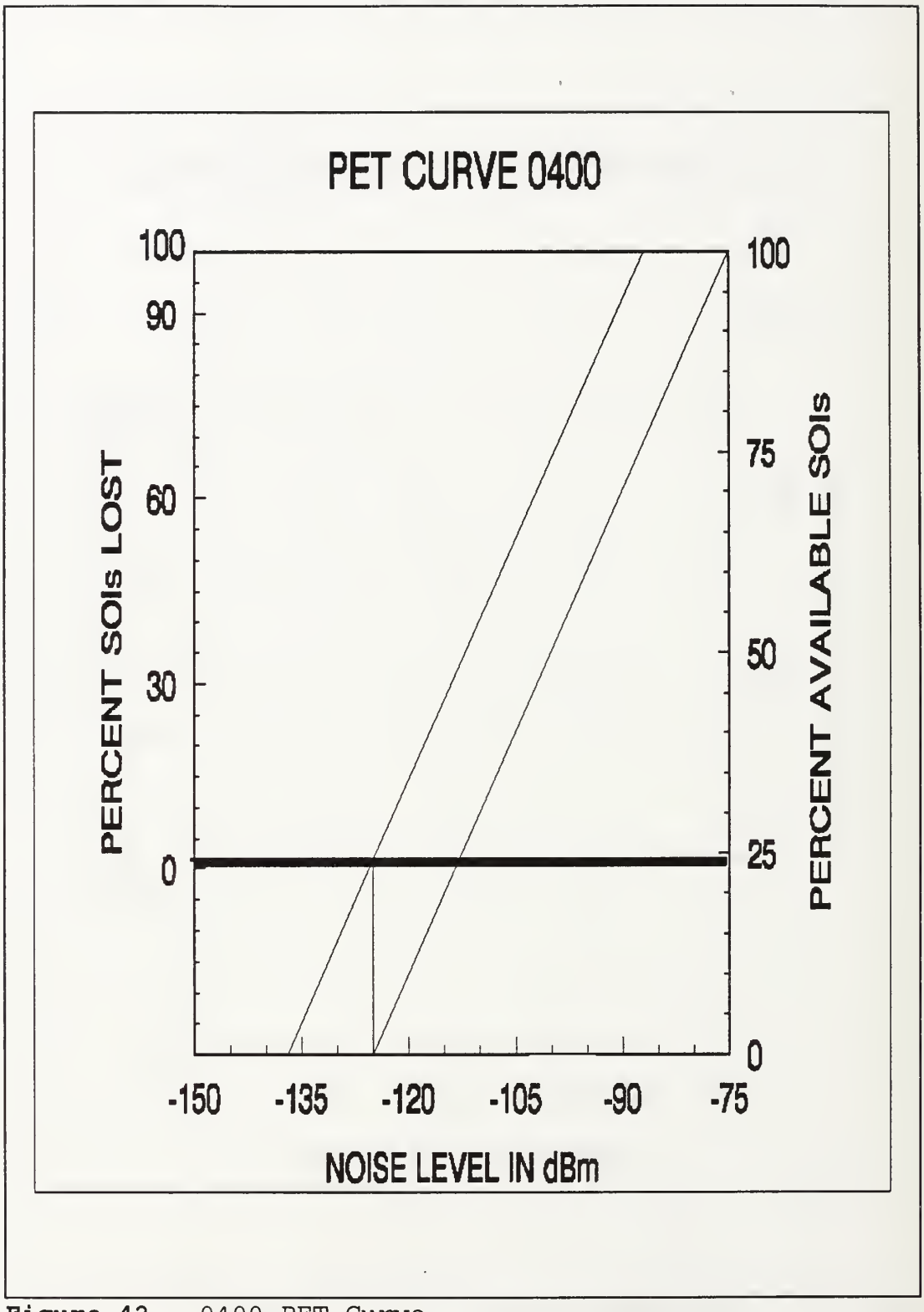


Figure 42. 0400 PET Curve.

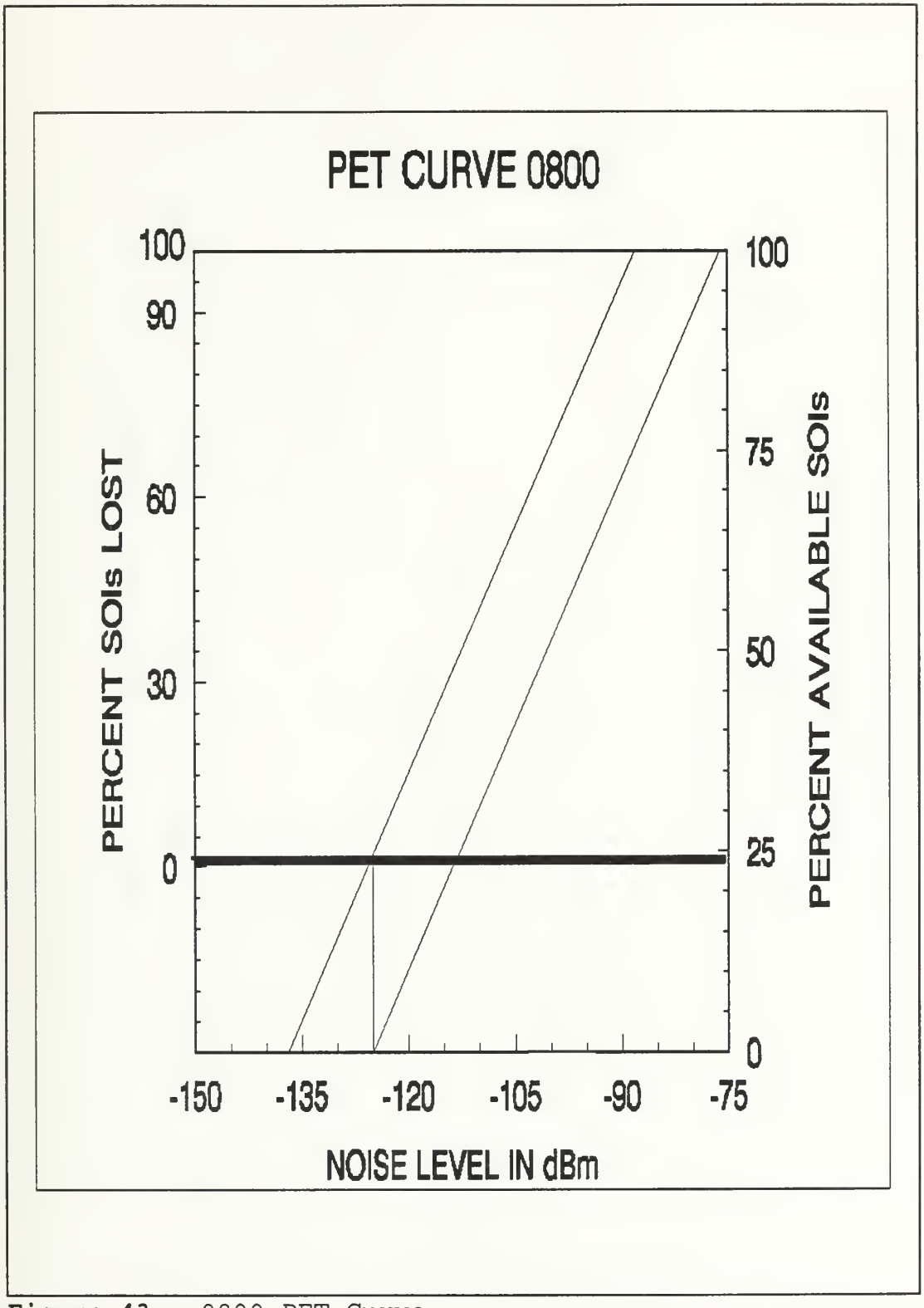


Figure 43. 0800 PET Curve.

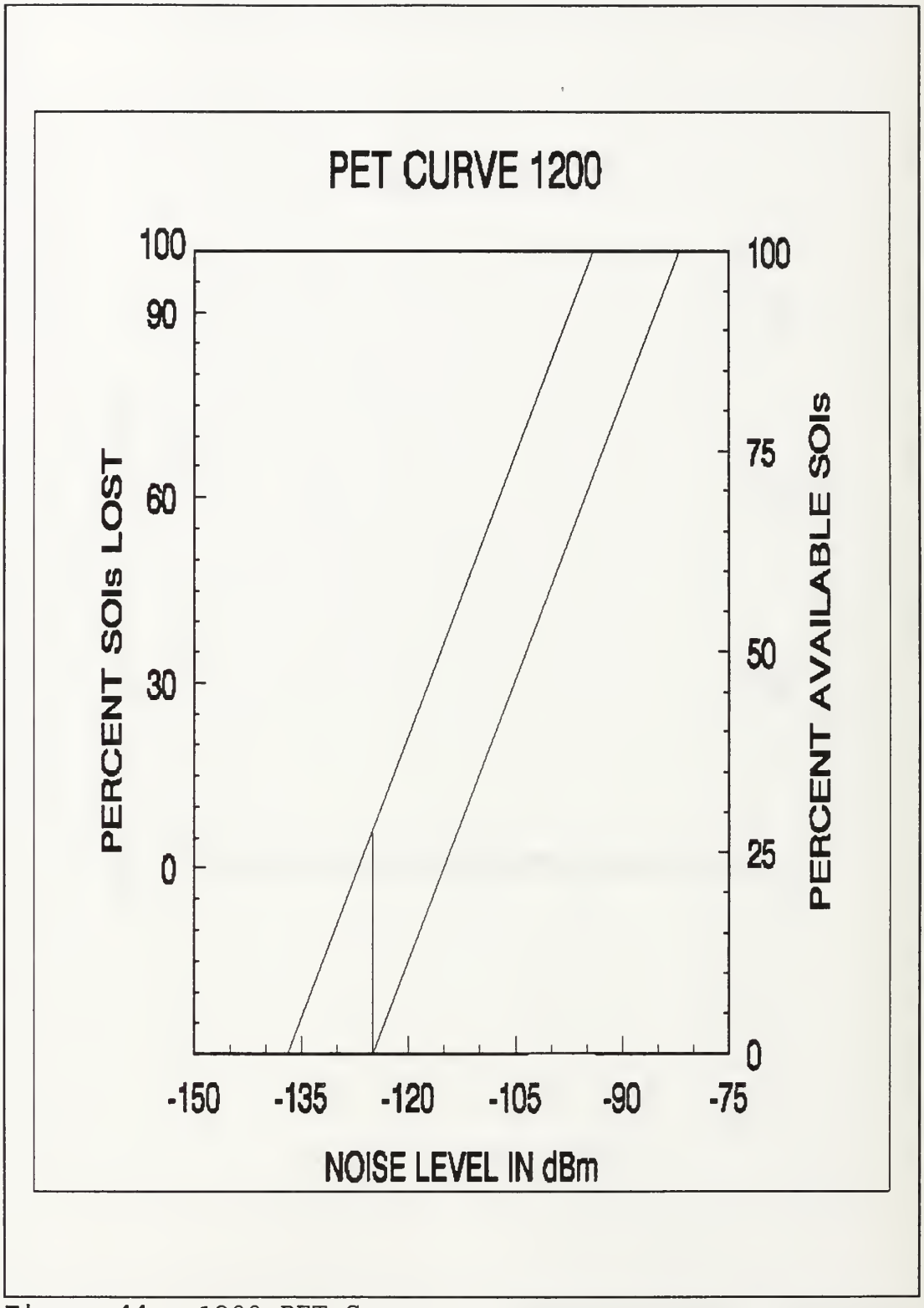


Figure 44. 1200 PET Curve.

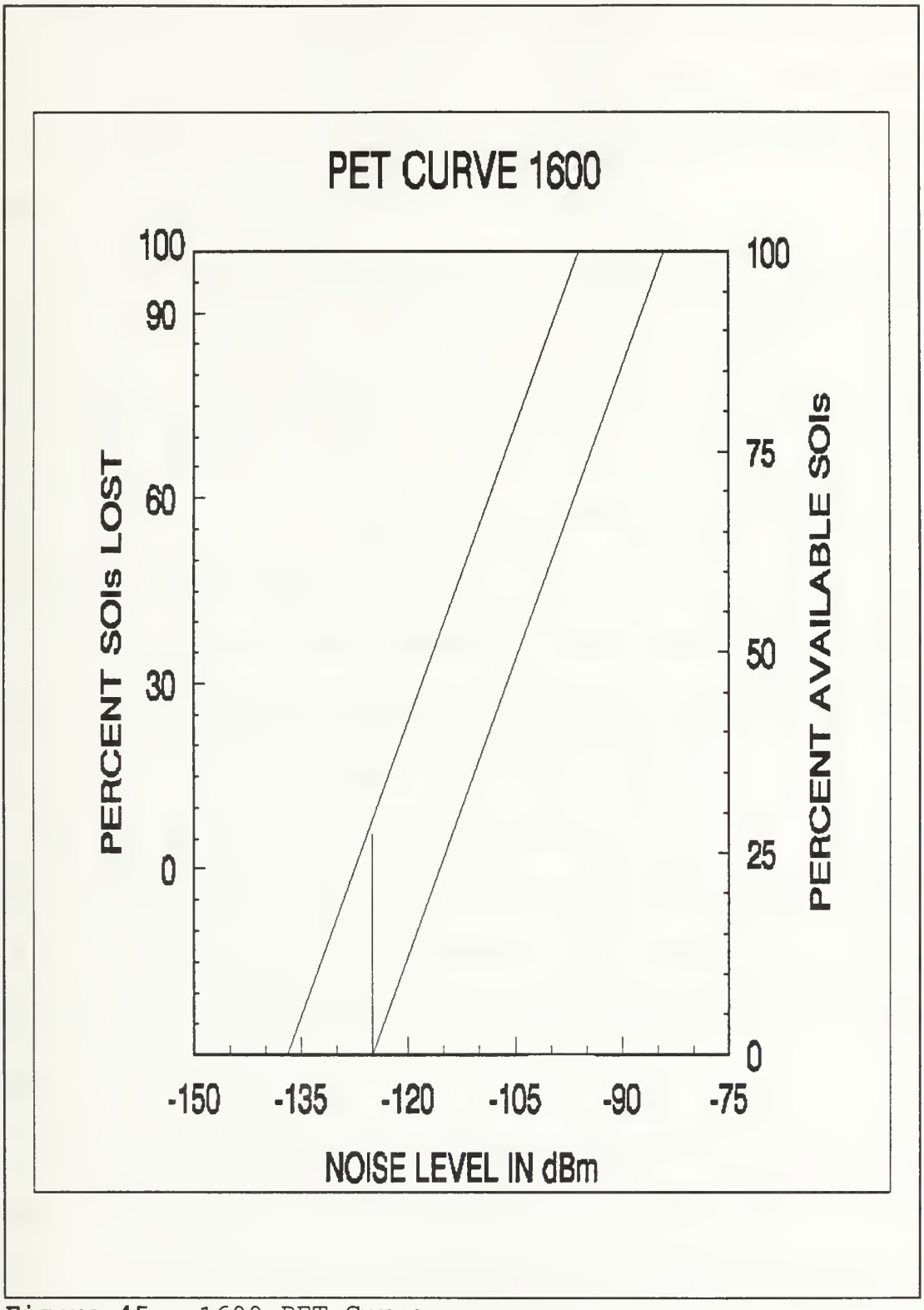


Figure 45. 1600 PET Curve.

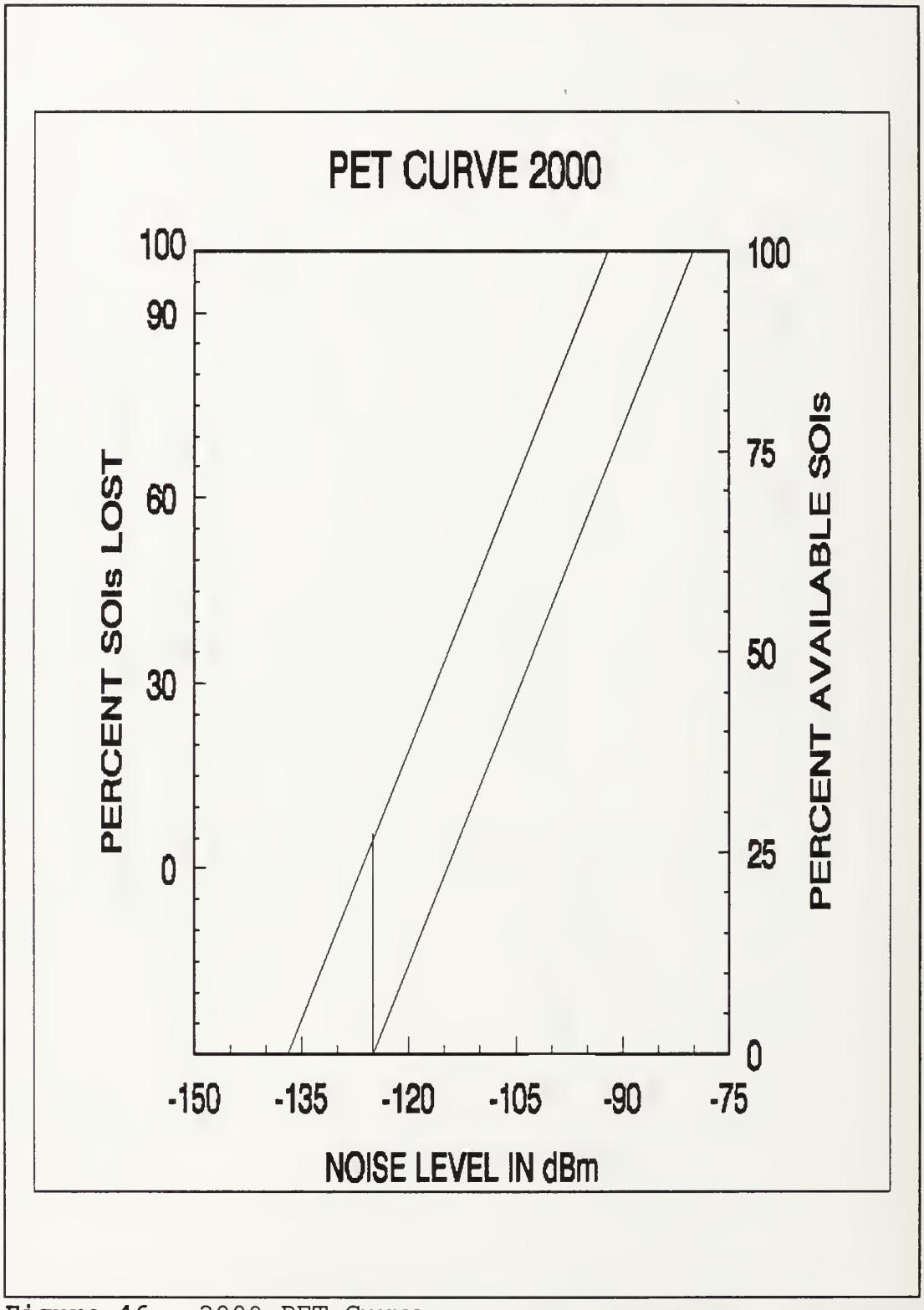


Figure 46. 2000 PET Curve.

The results of the various RFD losses and noise source measurements taken at Sabana Seca are plotted in Figures 47-50. The performance evaluation will be made for the Omni and Beam A/C-060 over a 24 hour period. The performance levels of other beams can be assessed as desired.

The results from the automated PET are shown in Figures 51-86. The performance trend for a full 24 hours is now established, which had not been done previously due to the excessive amount of time needed to compile the data. Summary presentations of the 24-hour curves are shown in Figures 87 and 88. These summary curves show the diurnal variations of lost SOIs as well as frequency variations. The curves show only the impact of site-related factors.

Since the source of each factor degrading performance is identified, a cost-to-effect-repairs can now be assigned to each factor. The resulting gain in percent SOIs lost can be measured and the most cost-effective repairs can be implemented.

The effects of man-made noise on performance were not included in this partial analysis. The performance of the system is degraded even more by identified problems such as power-line noise and noise from internal sources. These problems are beam-dependent and were not included, because the primary objective here was to show the baseline performance.

There are many combinations of mitigation actions that can be assessed using the automated PET. The data is stored in files that can be recalled easily for additional analysis. The expanded database for SOIs lost provides a greater understanding of site performance problem.

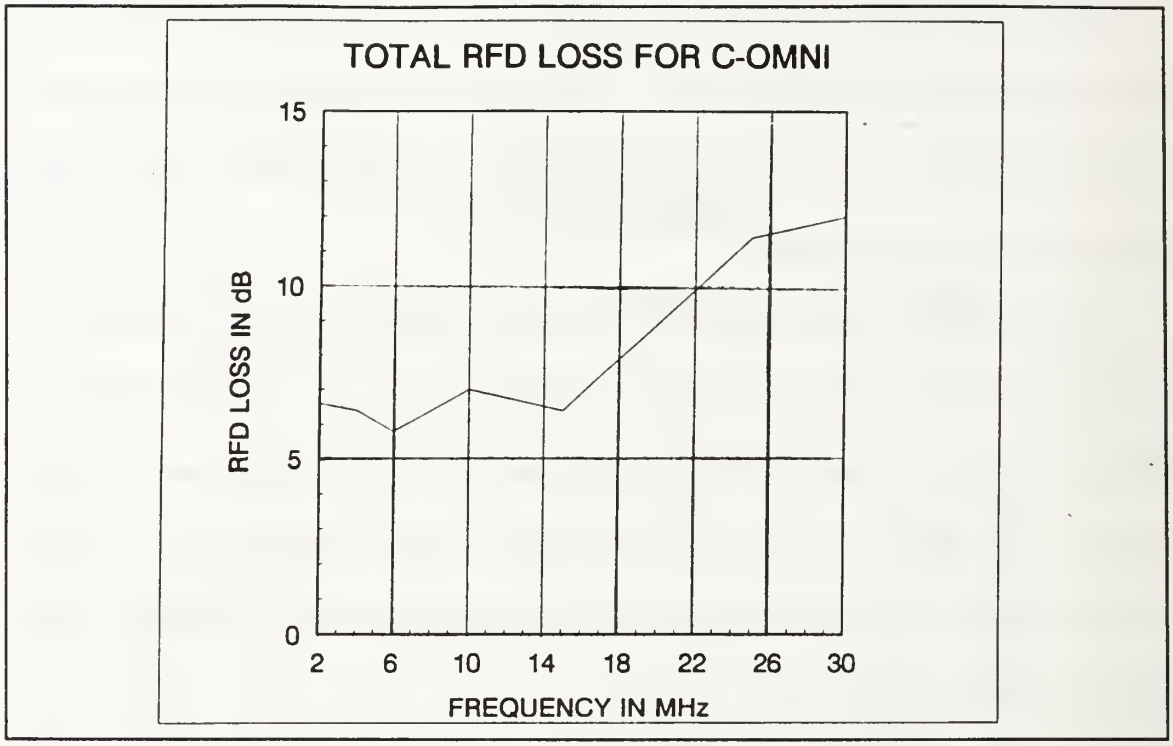


Figure 47. C-OMNI, RFD LOSS.

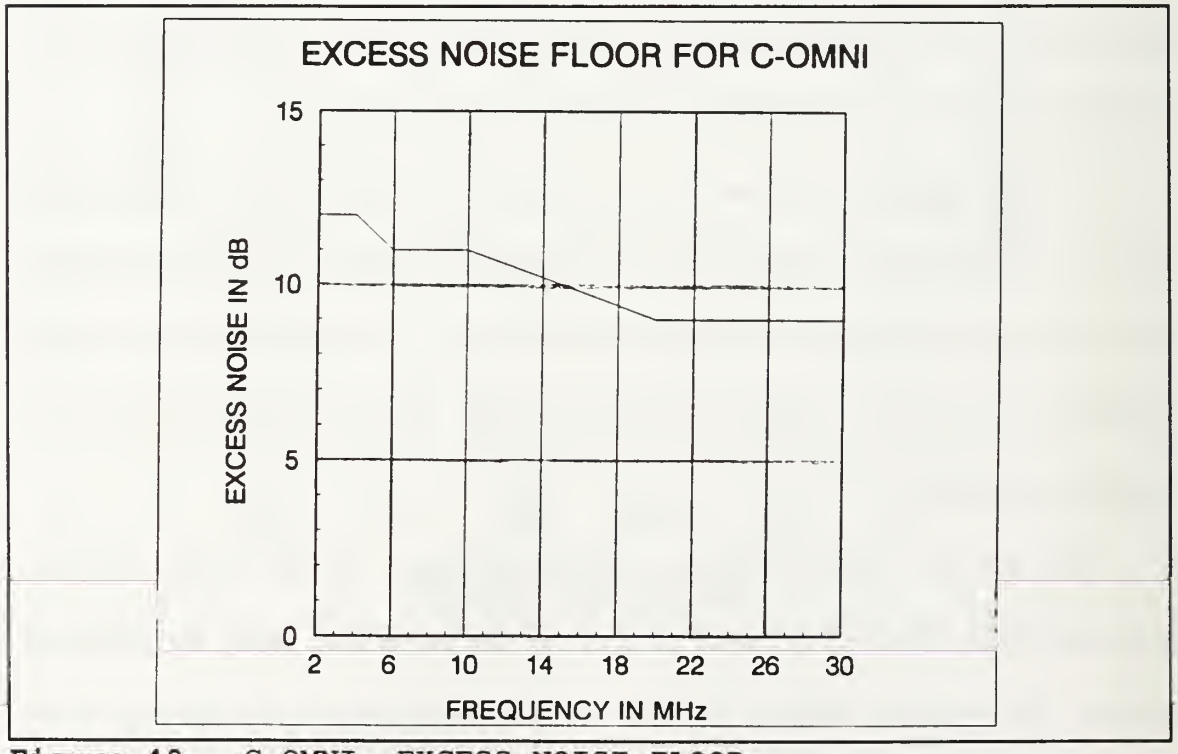


Figure 48. C-OMNI, EXCESS NOISE FLOOR.

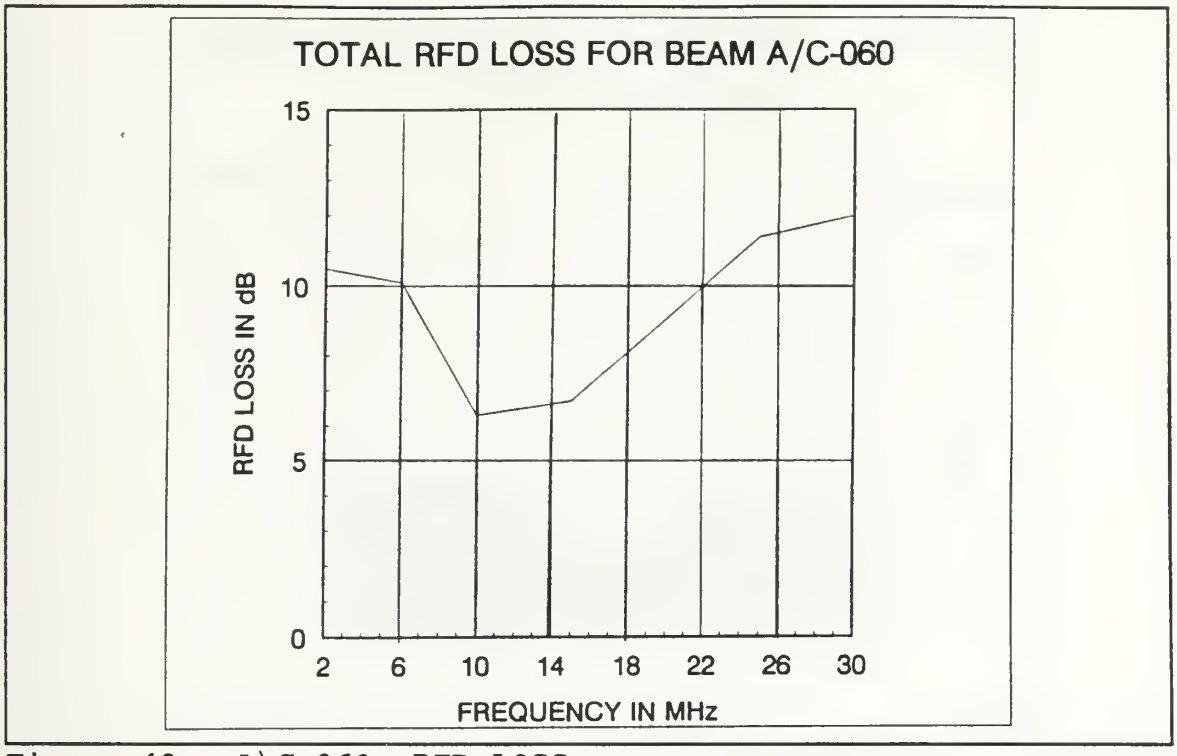


Figure 49. A\C-060, RFD LOSS.

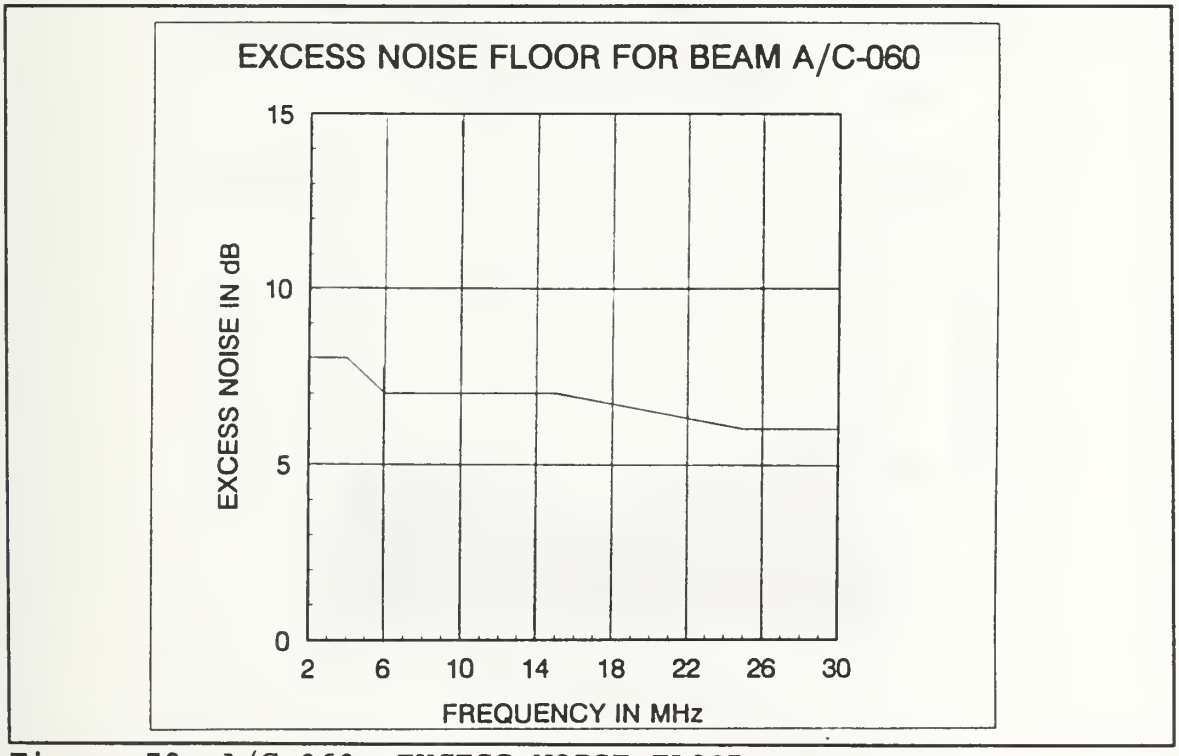


Figure 50. A/C-060, EXCESS NOISE FLOOR.

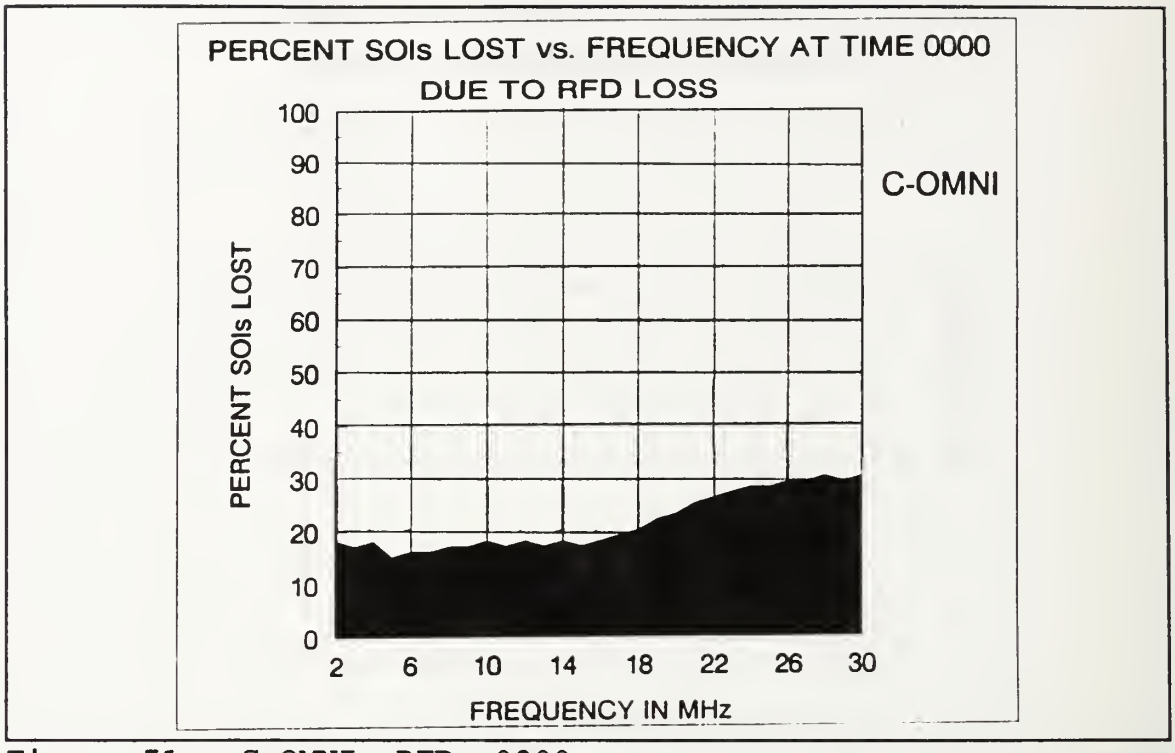


Figure 51. C-OMNI, RFD, 0000.

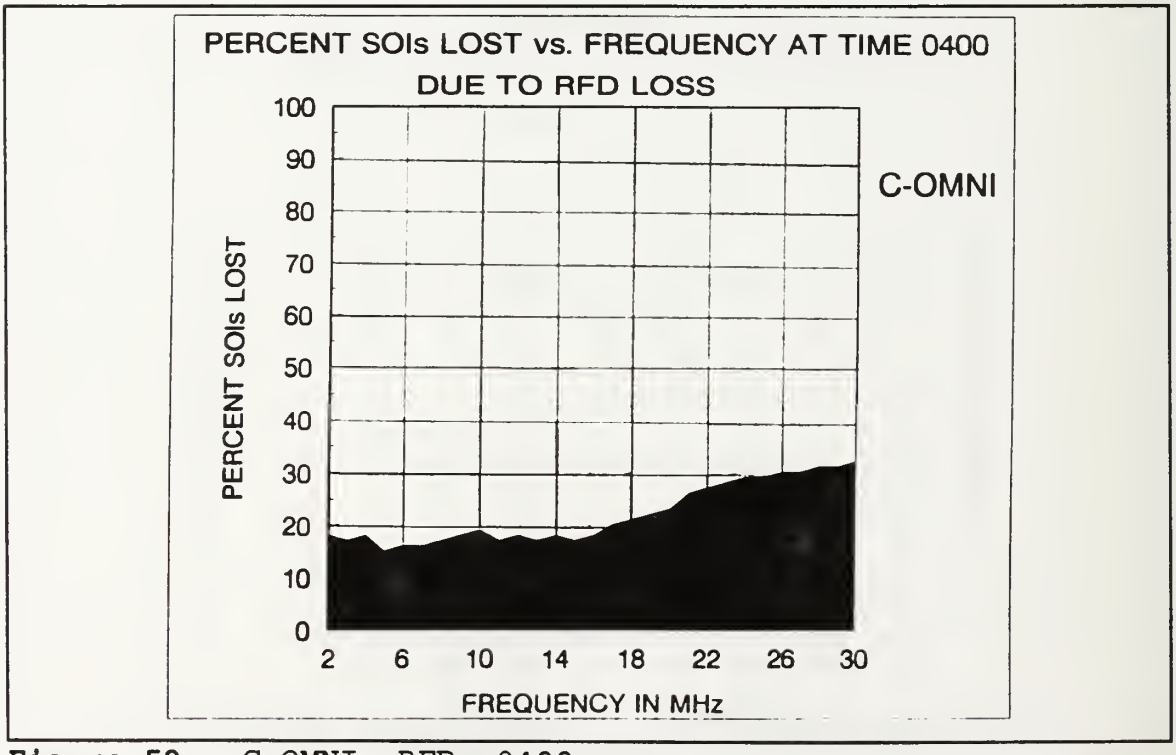


Figure 52. C-OMNI, RFD, 0400.

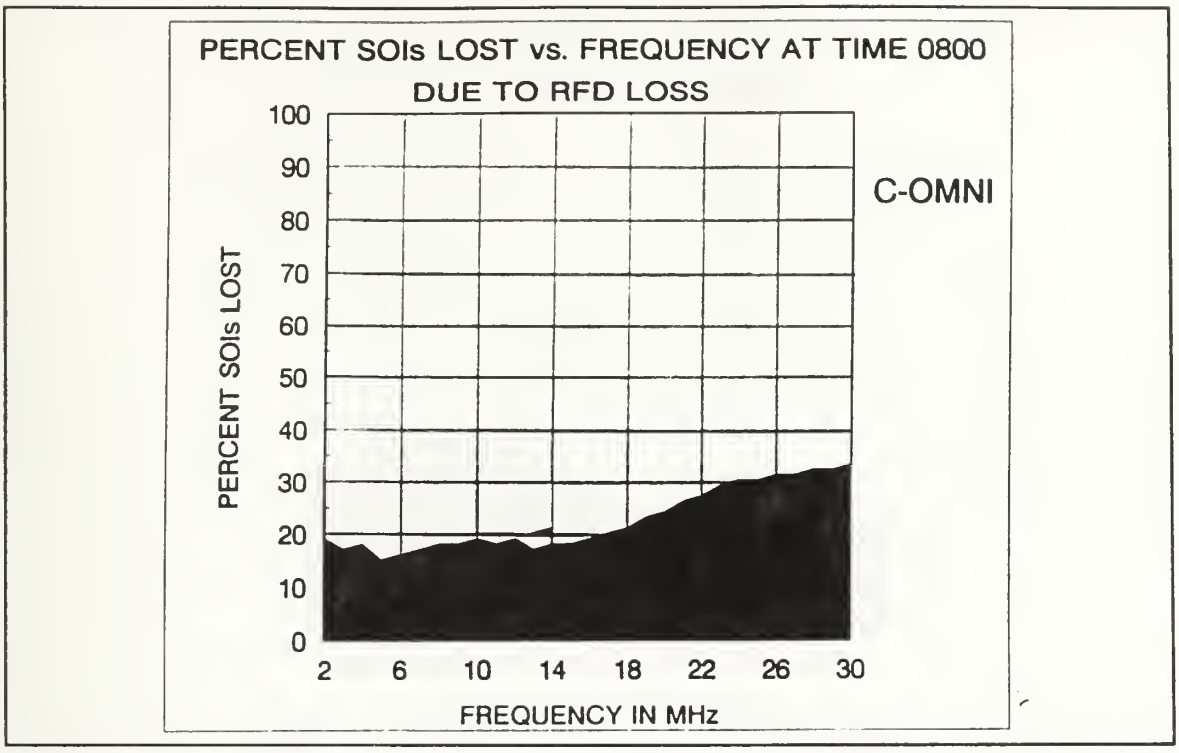


Figure 53. C-OMNI, RFD, 0800.

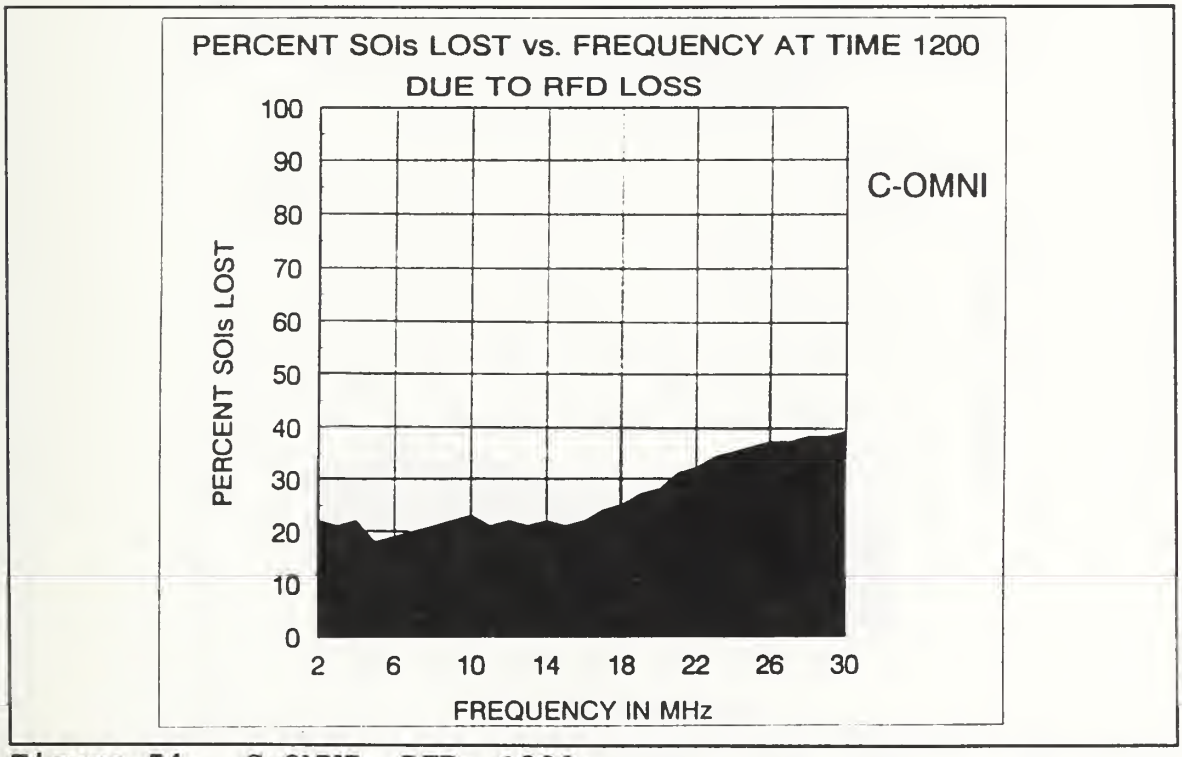


Figure 54. C-OMNI, RFD, 1200.

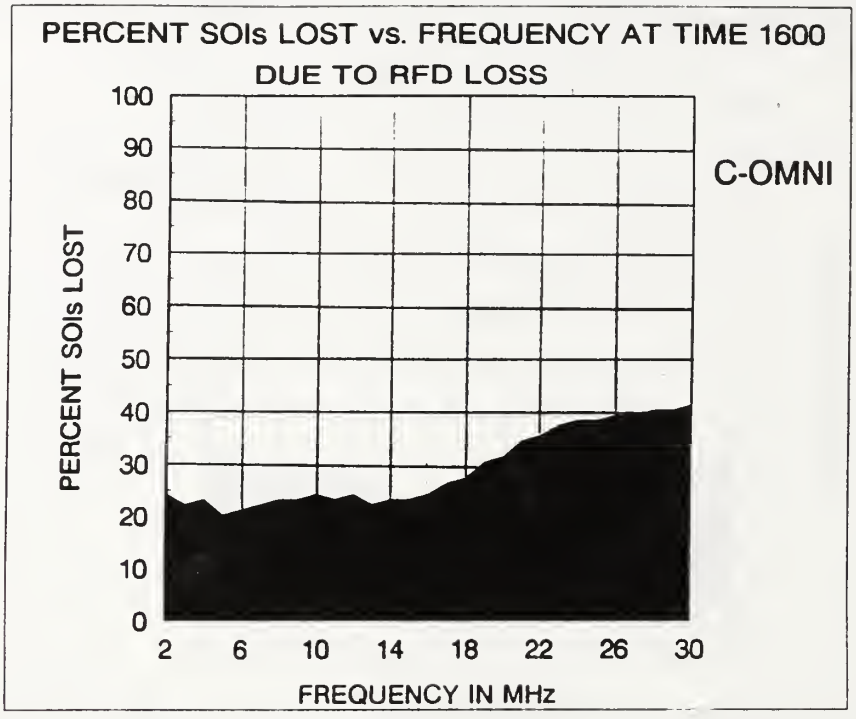


Figure 55. C-OMNI, RFD, 1600.

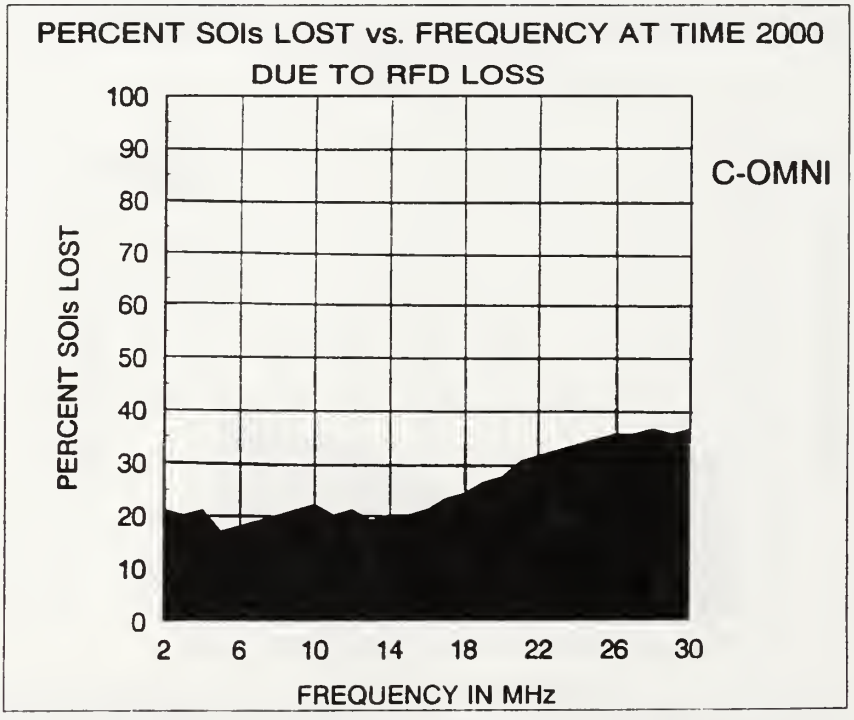


Figure 56. C-OMNI, RFD, 2000.

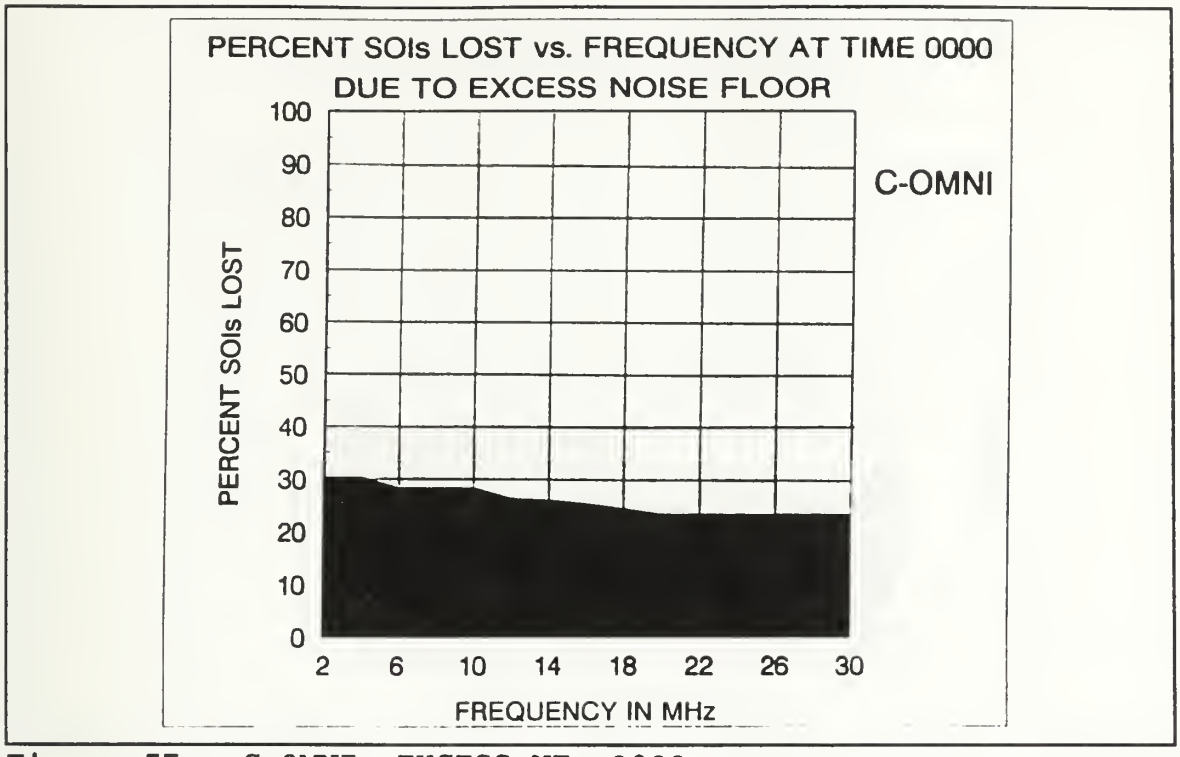


Figure 57. C-OMNI, EXCESS NF, 0000.

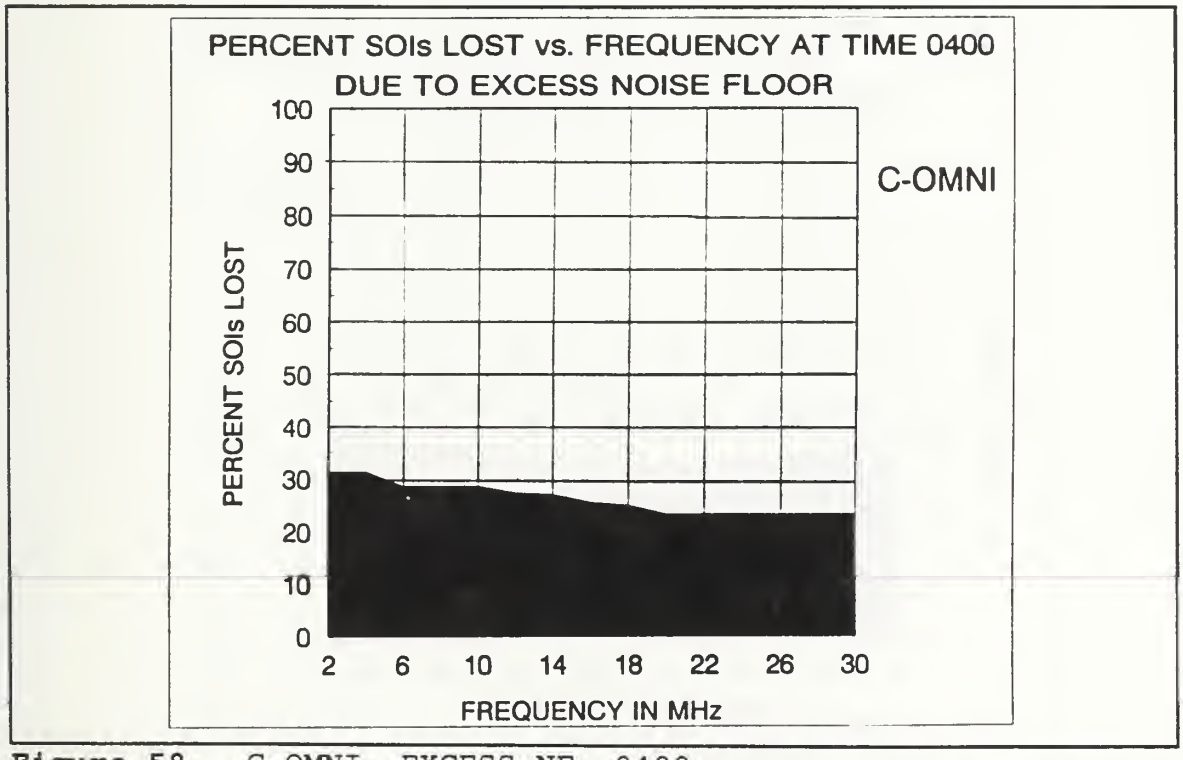


Figure 58. C-OMNI, EXCESS NF, 0400.

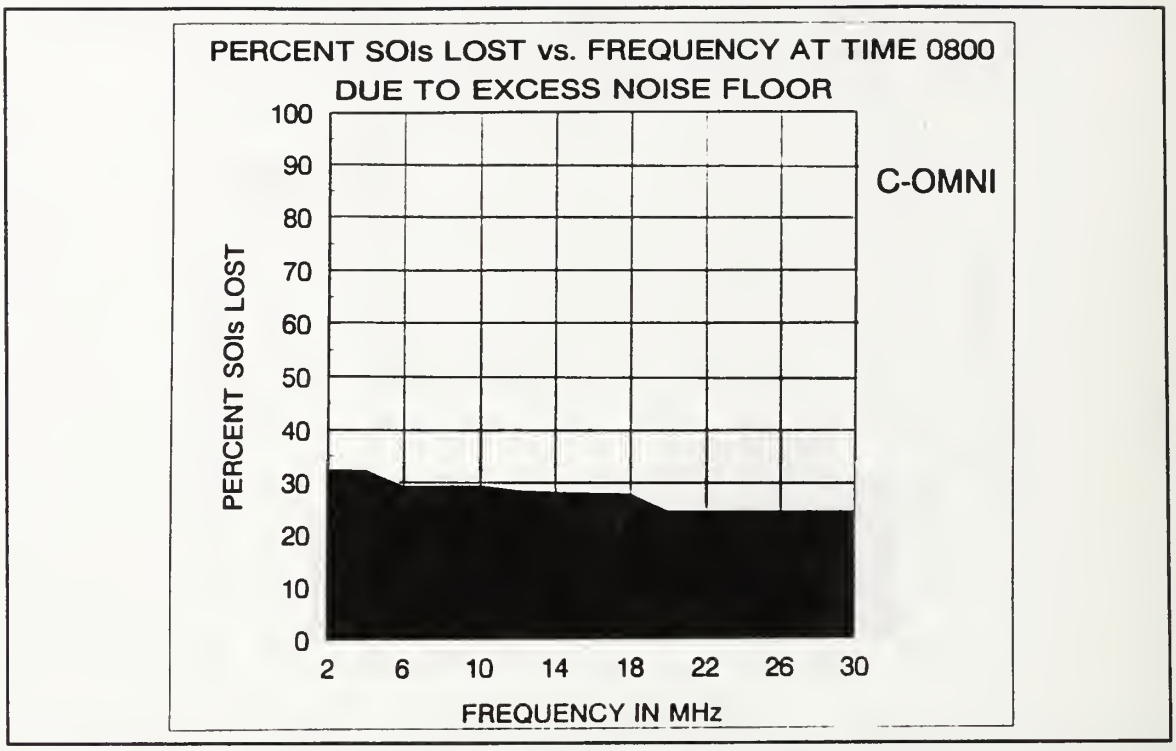


Figure 59. C-OMNI, EXCESS NF, 0800.

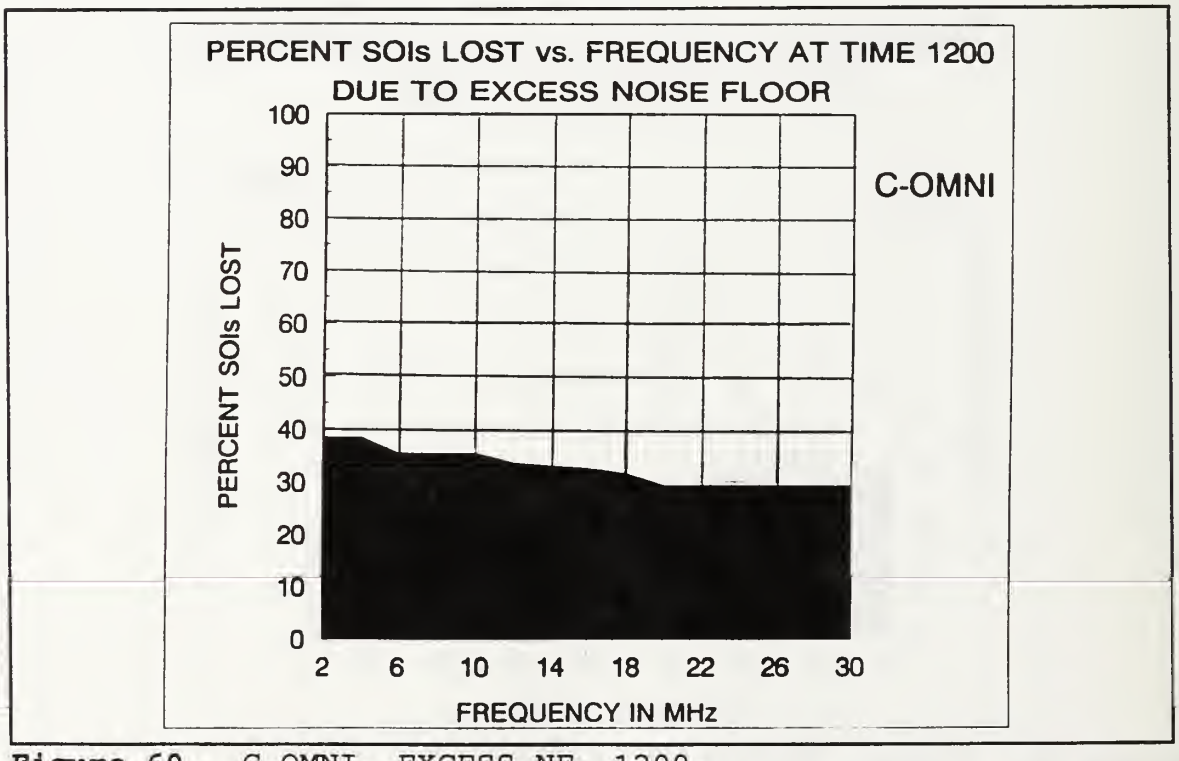


Figure 60. C-OMNI, EXCESS NF, 1200.

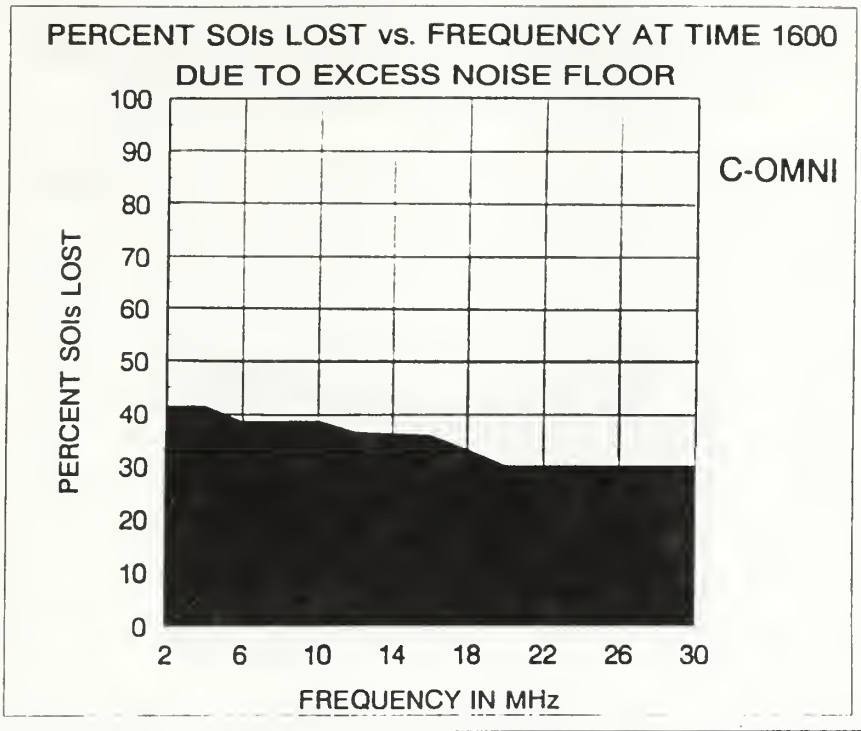


Figure 61. C-OMNI, EXCESS NF, 1600.

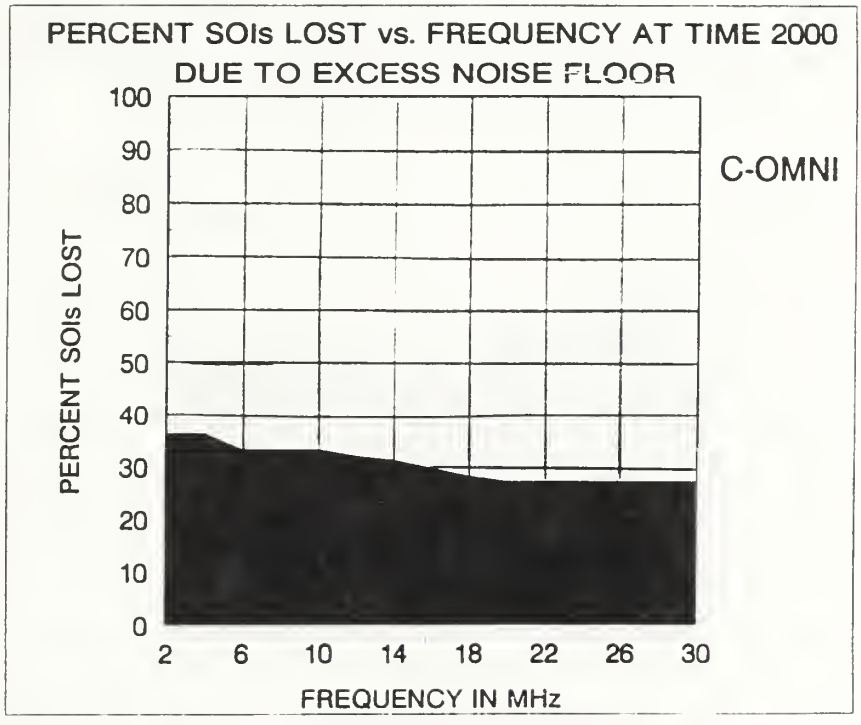


Figure 62. C-OMNI, EXCESS NF, 2000.

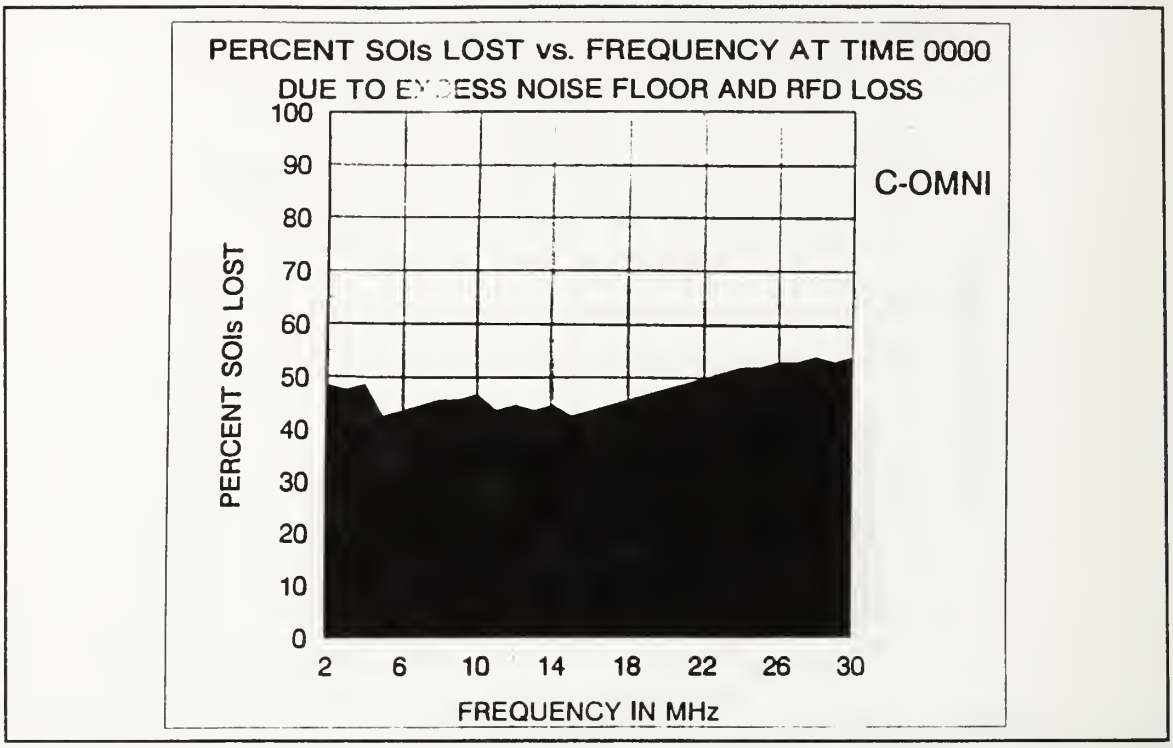


Figure 63. C-OMNI, RFD AND EXCESS NF, 0000.

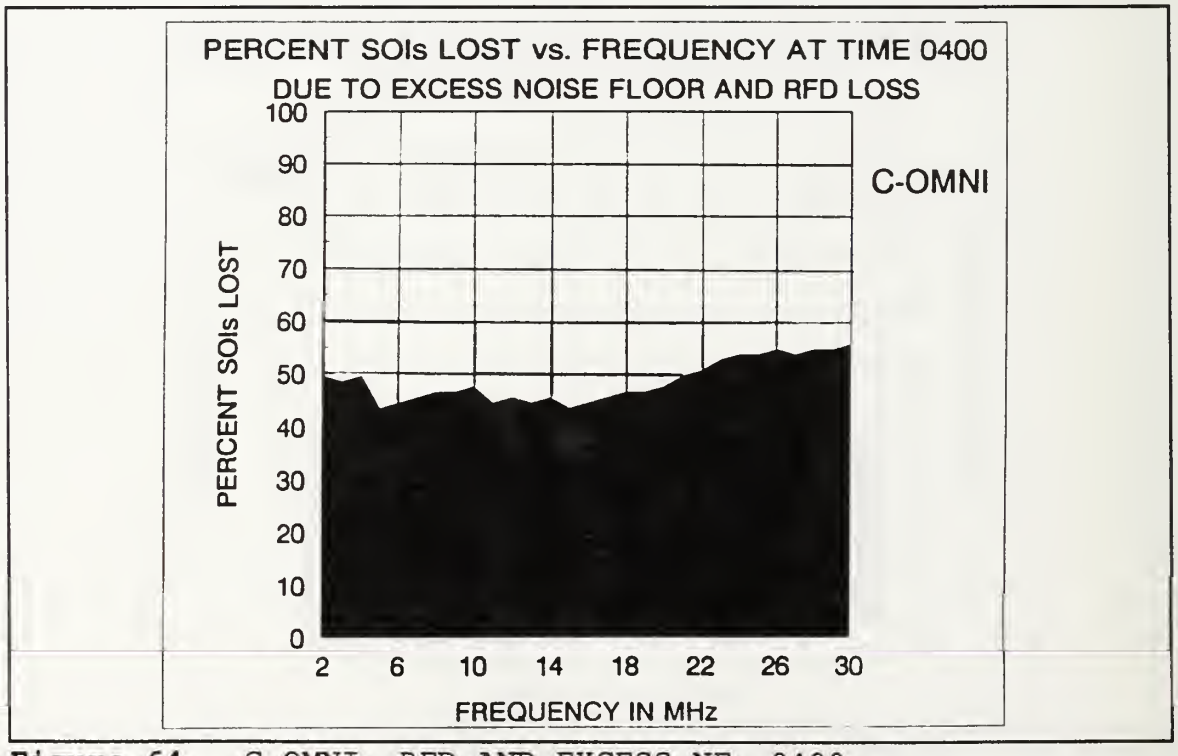


Figure 64. C-OMNI, RFD AND EXCESS NF, 0400.

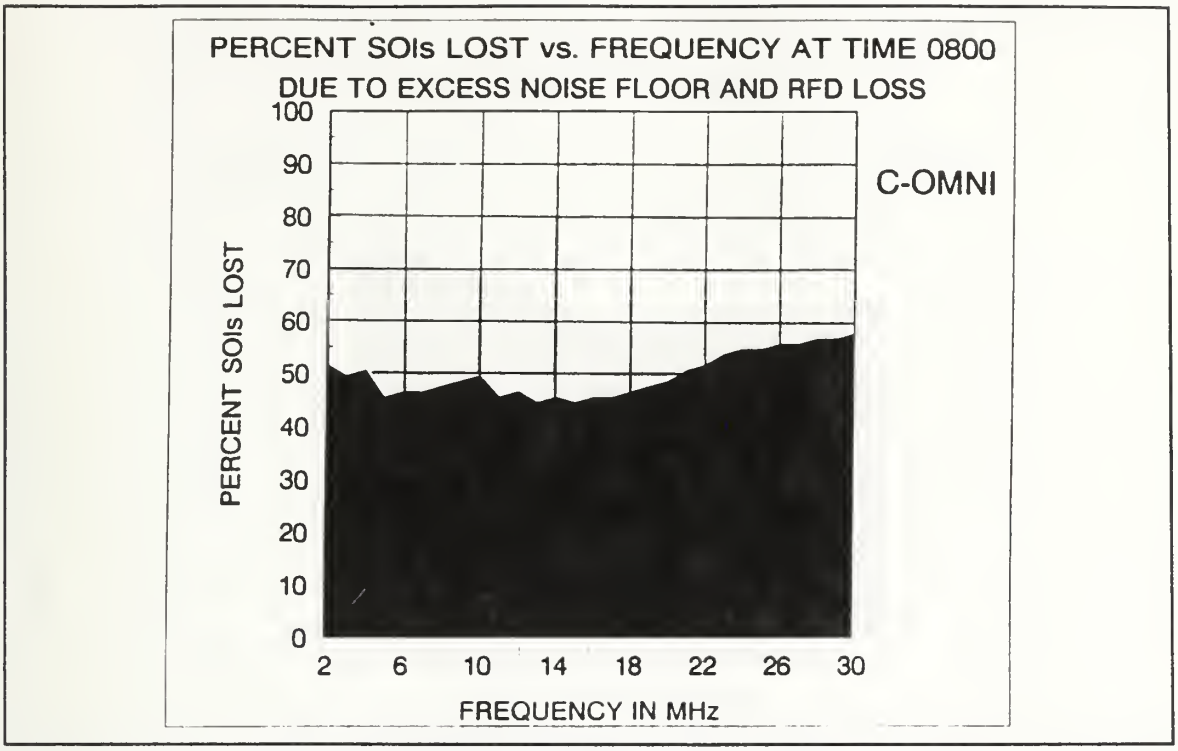


Figure 65. C-OMNI, RFD AND EXCESS NF, 0800.

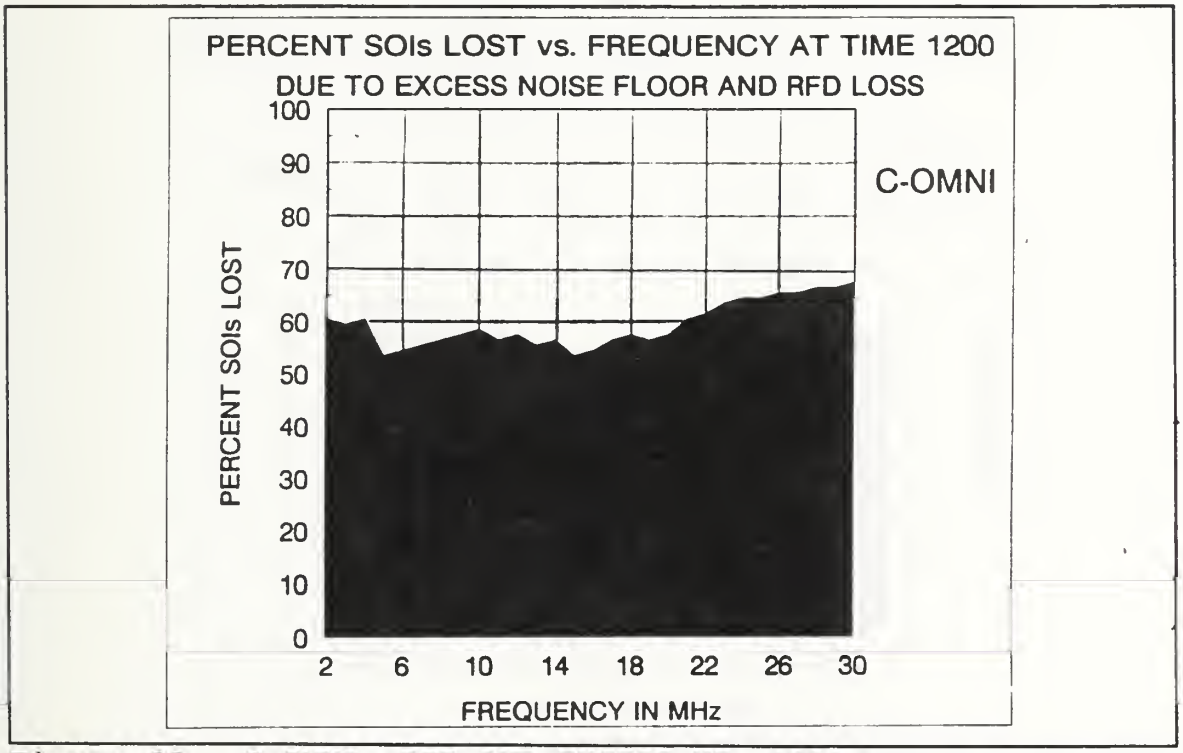


Figure 66. C-OMNI, RFD AND EXCESS NF, 1200.

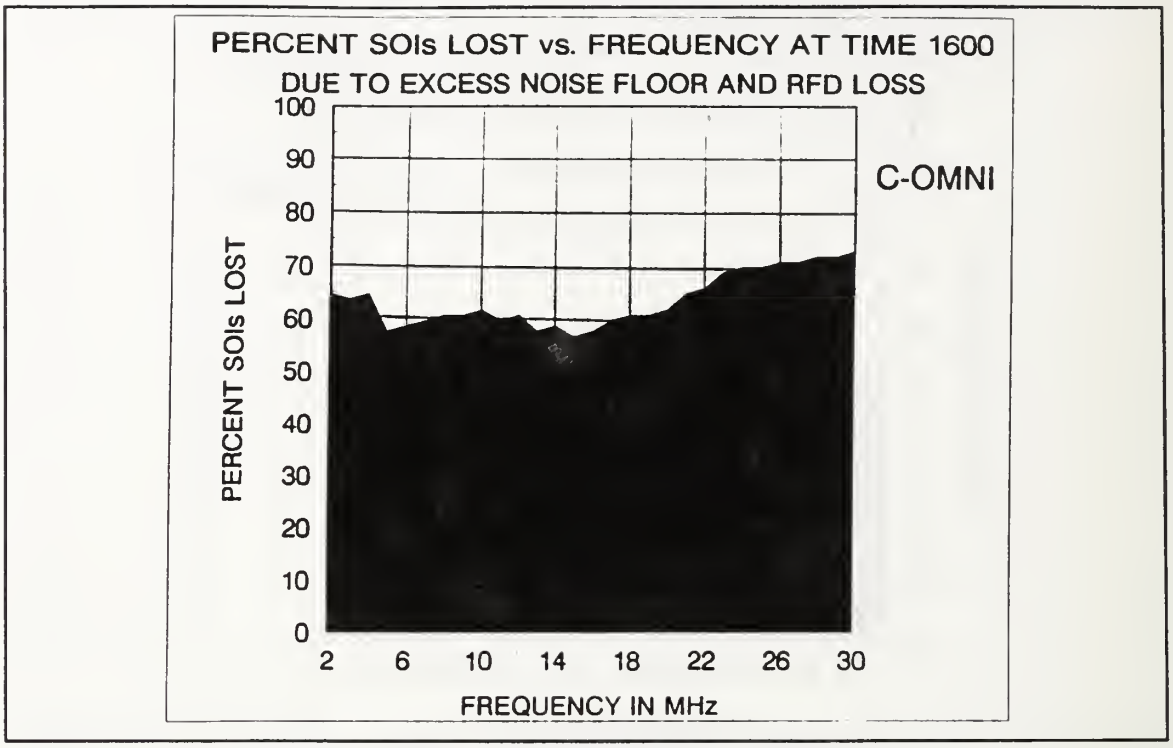


Figure 67. C-OMNI, RFD AND EXCESS NF, 1600.

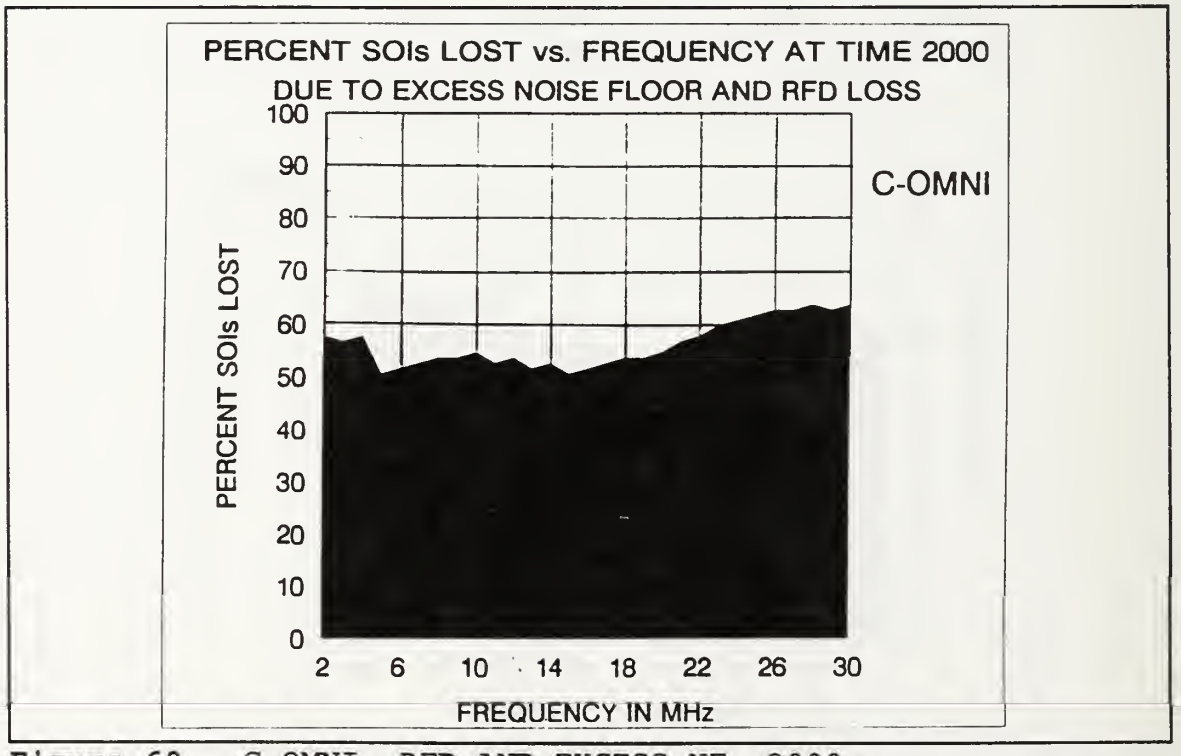


Figure 68. C-OMNI, RFD AND EXCESS NF, 2000.

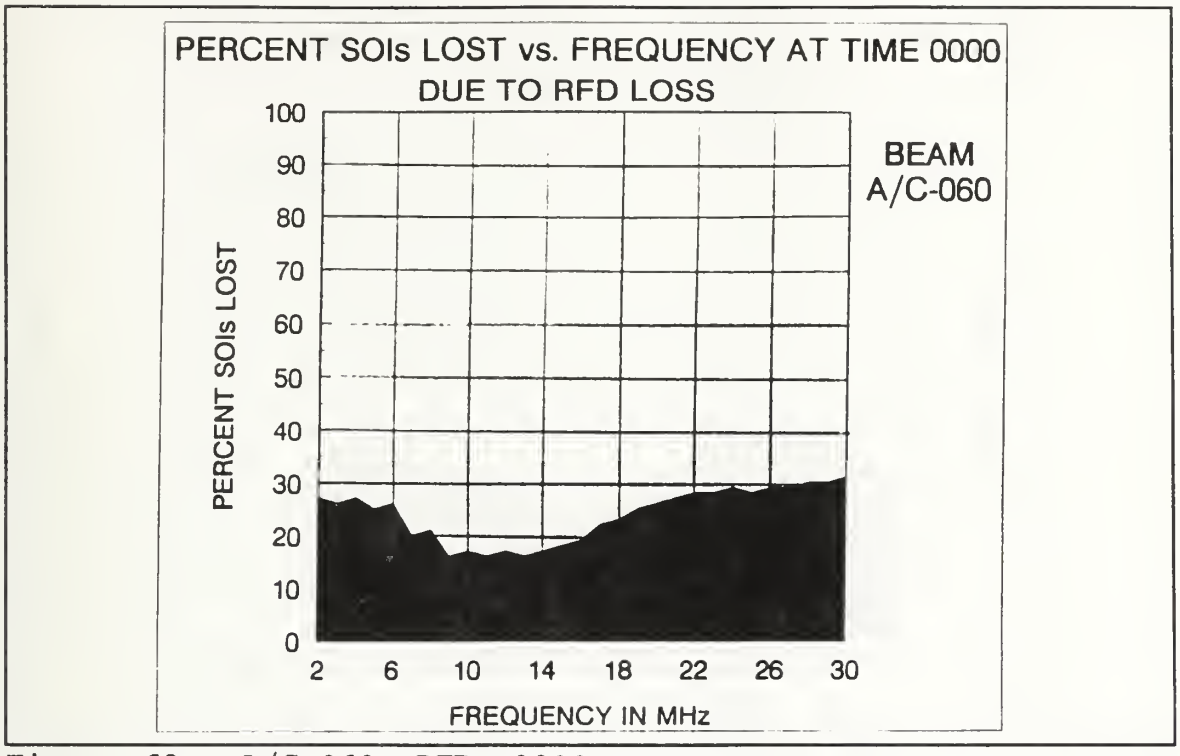


Figure 69. A/C-060, RFD, 0000.

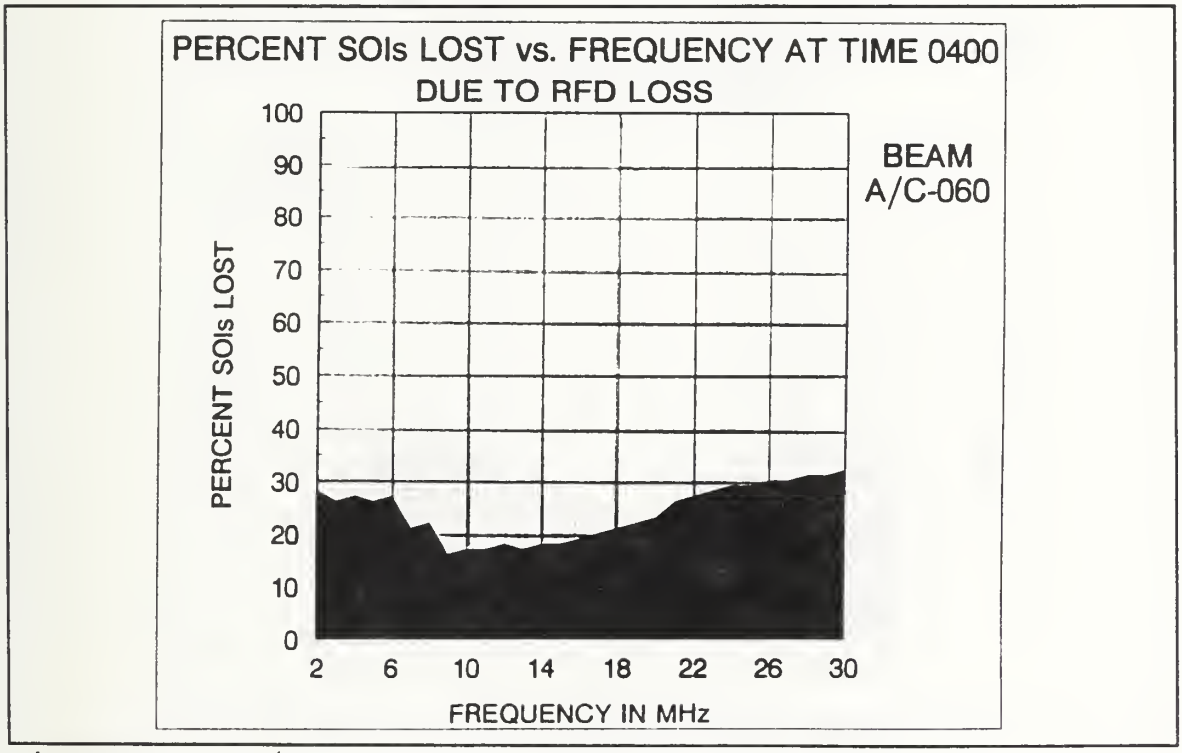


Figure 70. A/C-060, RFD, 0400.

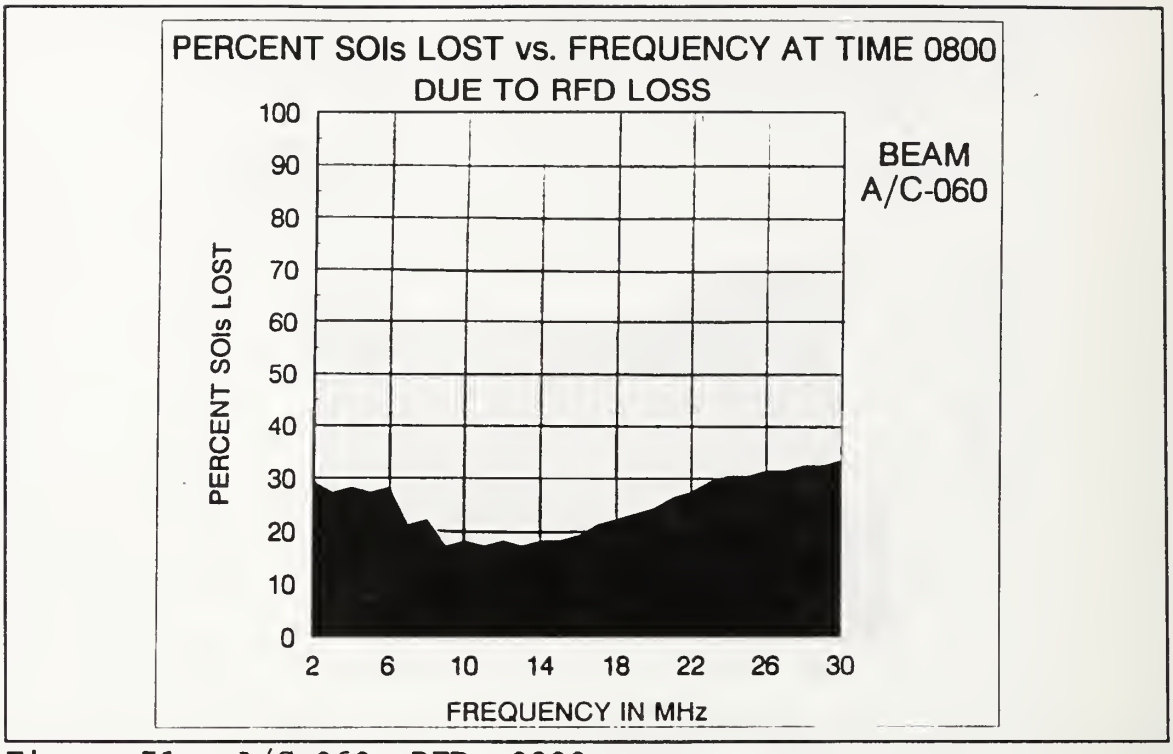


Figure 71. A/C-060, RFD, 0800.

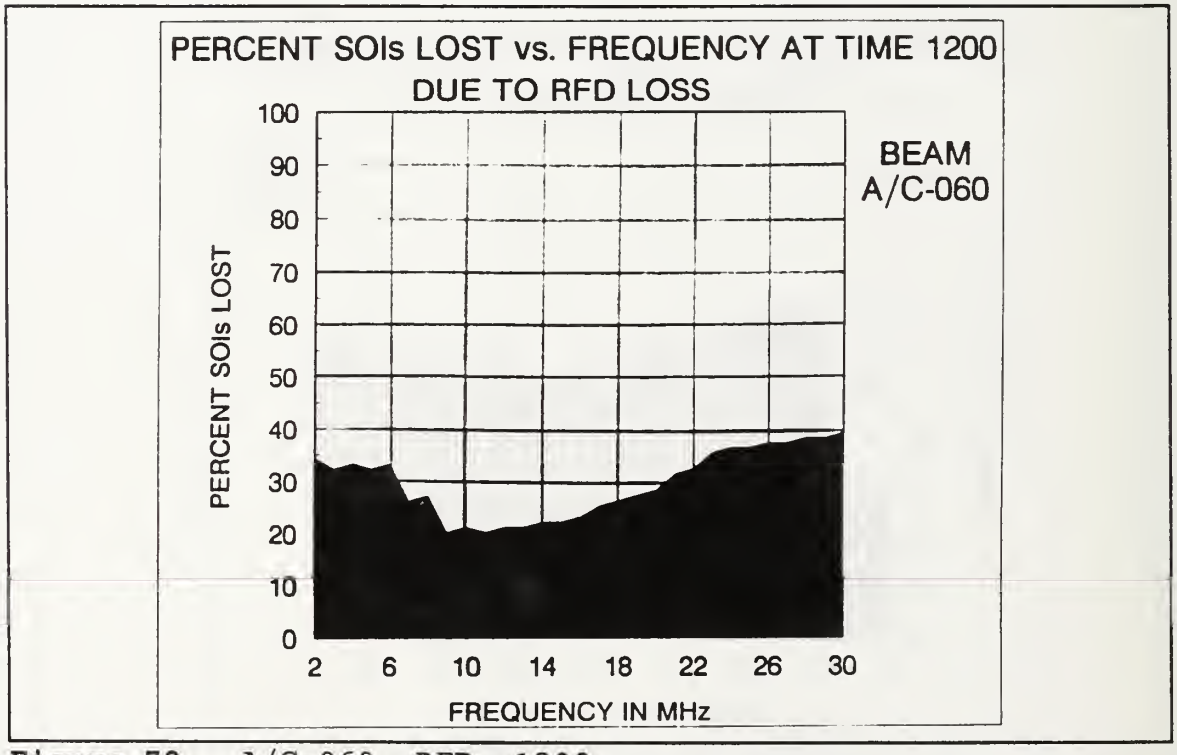


Figure 72. A/C-060, RFD, 1200.

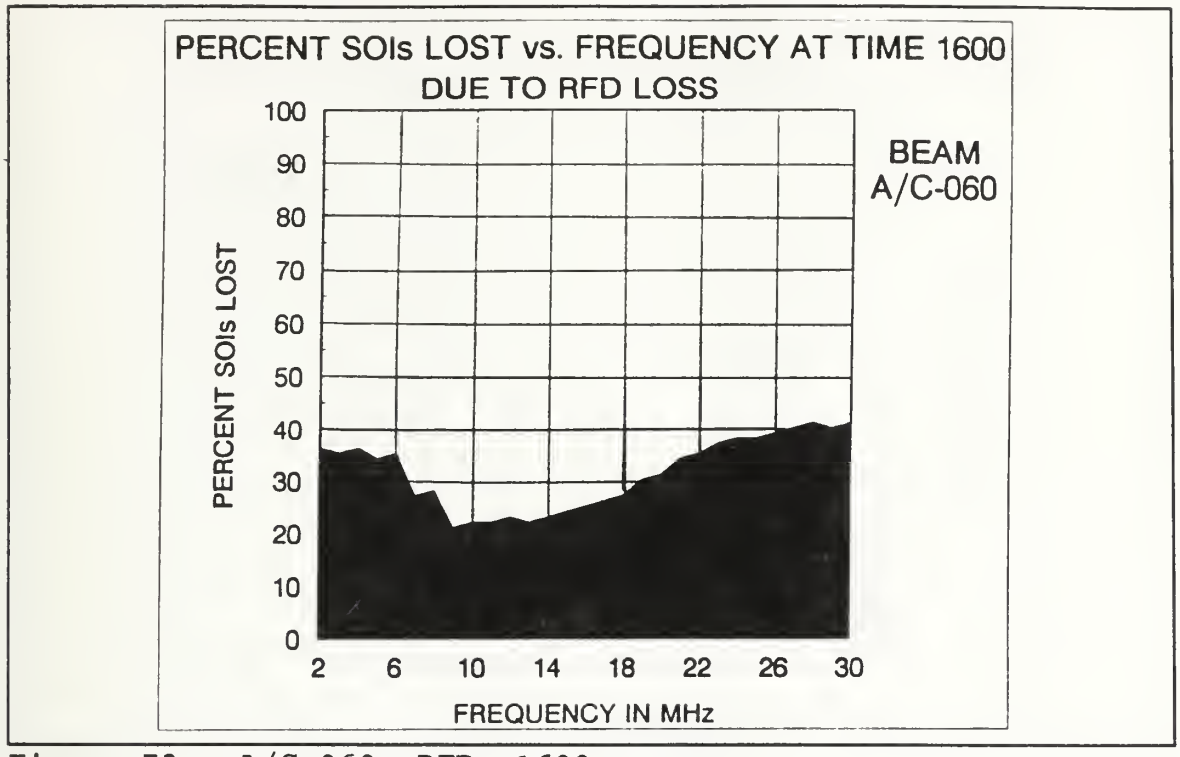


Figure 73. A/C-060, RFD, 1600.

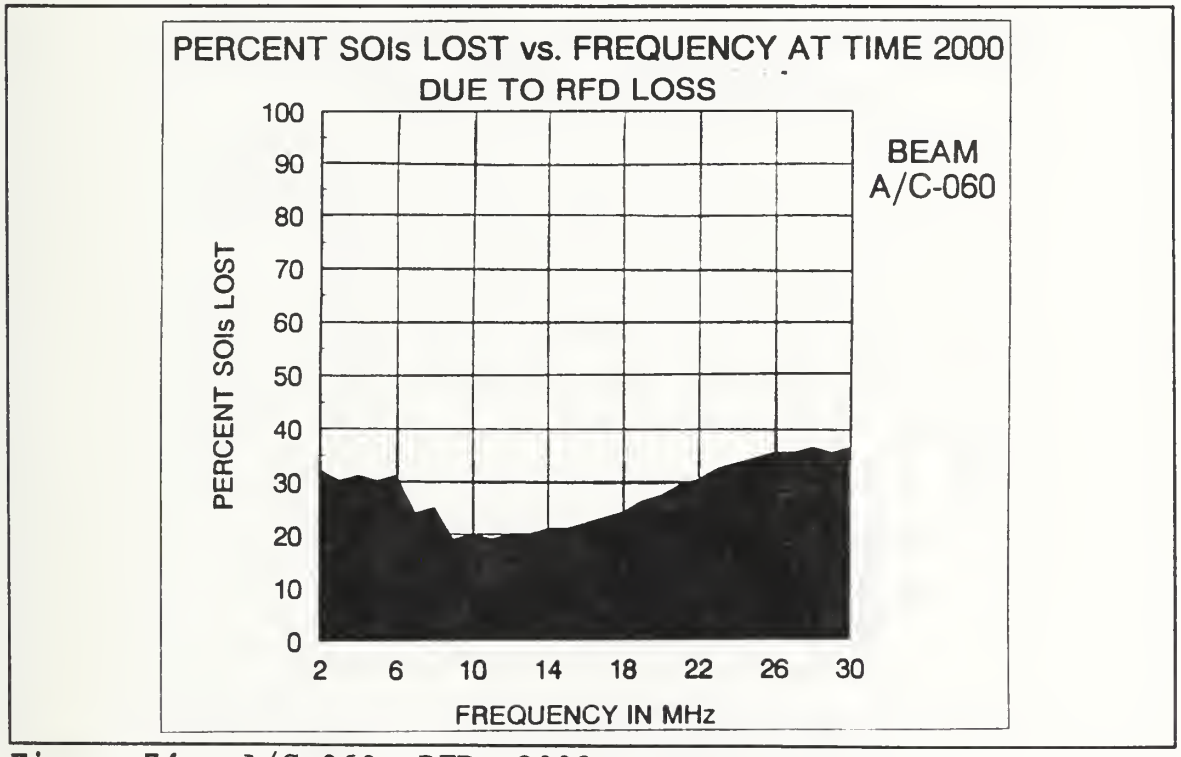


Figure 74. A/C-060, RFD, 2000.

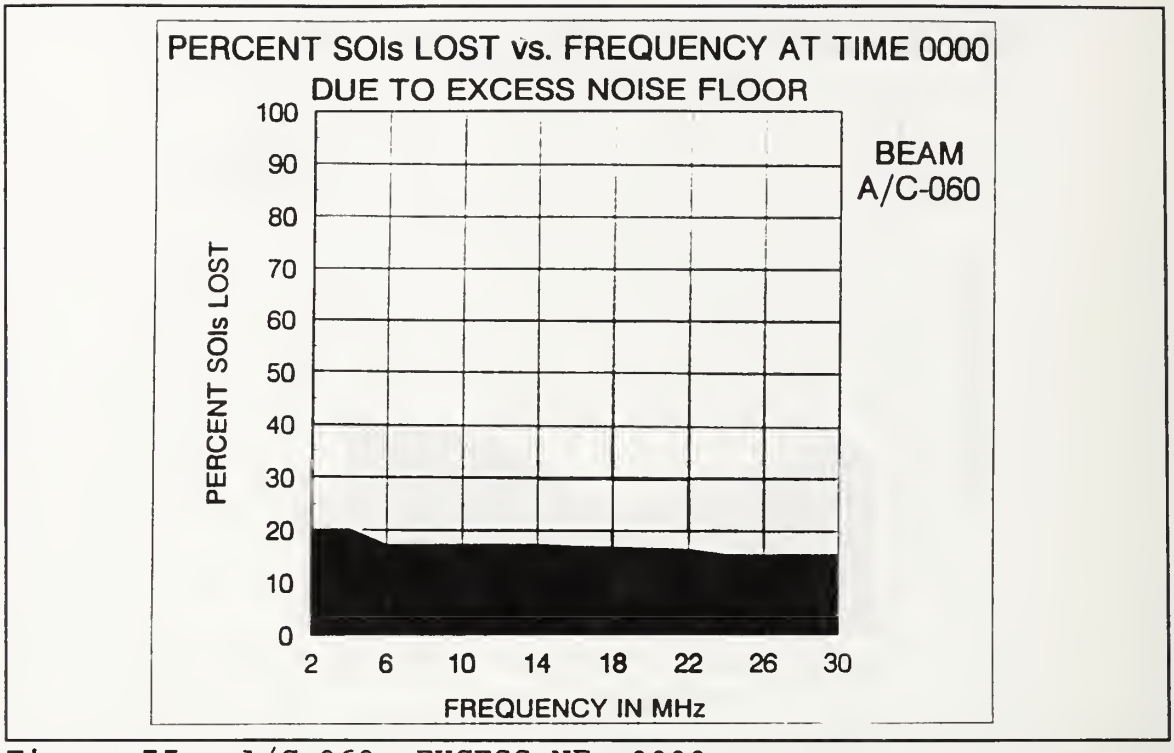


Figure 75. A/C-060, EXCESS NF, 0000.

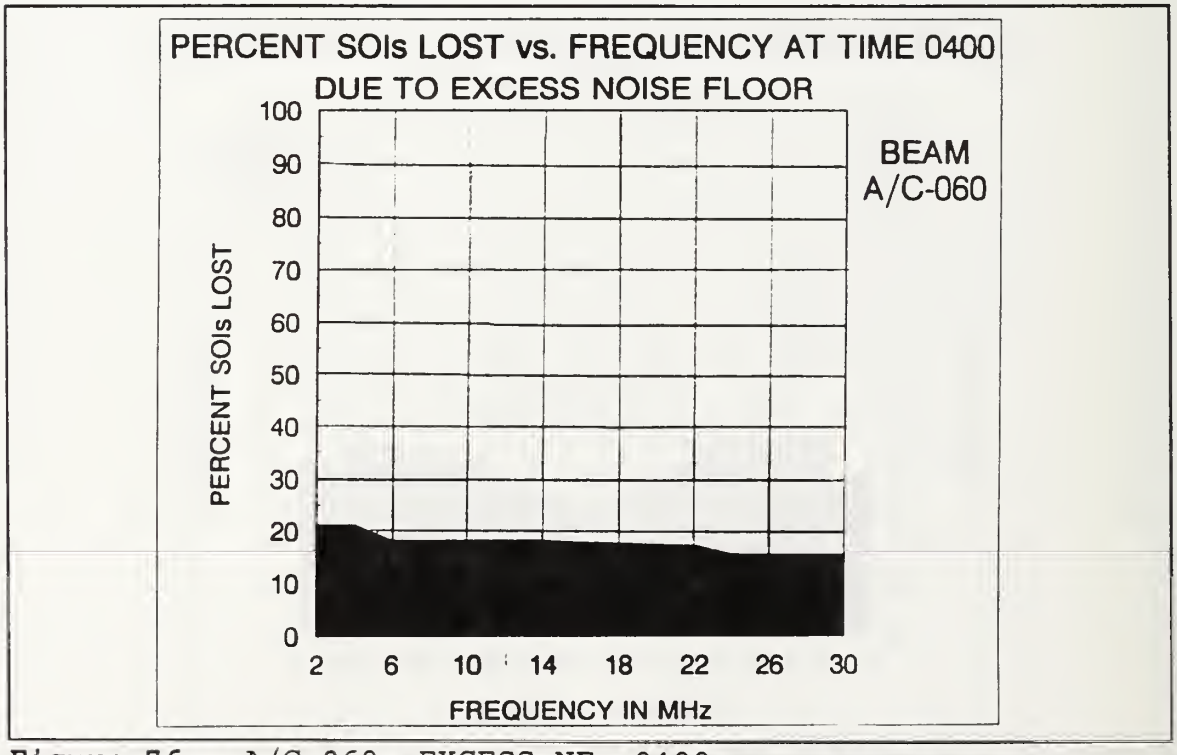


Figure 76. A/C-060, EXCESS NF, 0400.

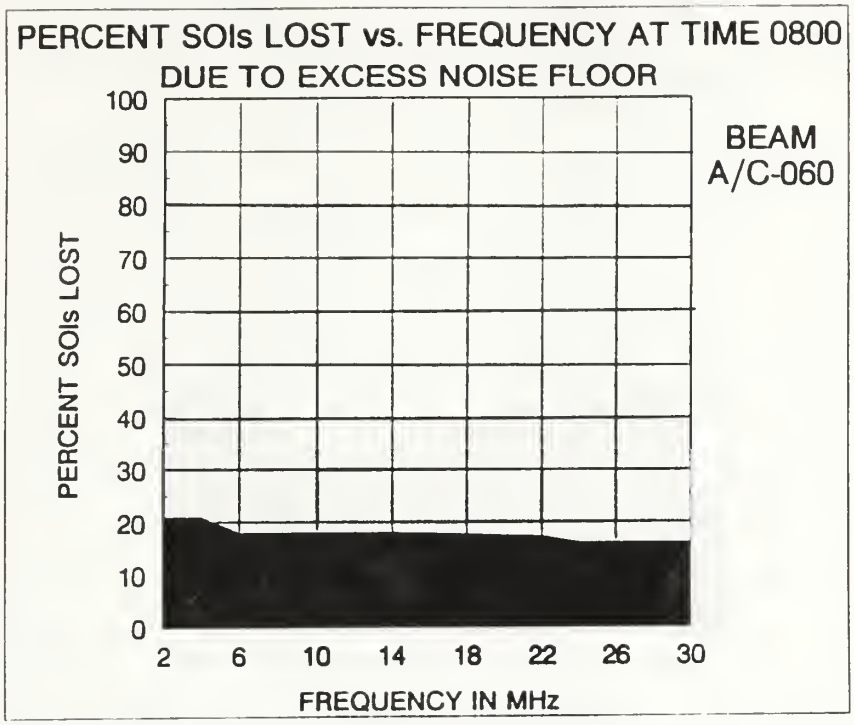


Figure 77. A/C-060, EXCESS NF, 0800.

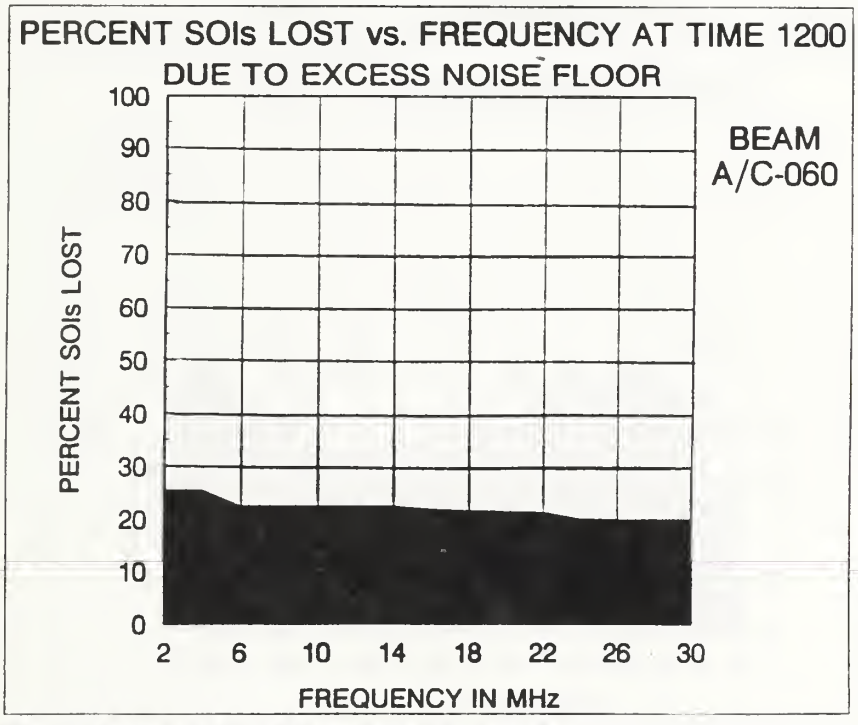


Figure 78. A/C-060, EXCESS NF, 1200.

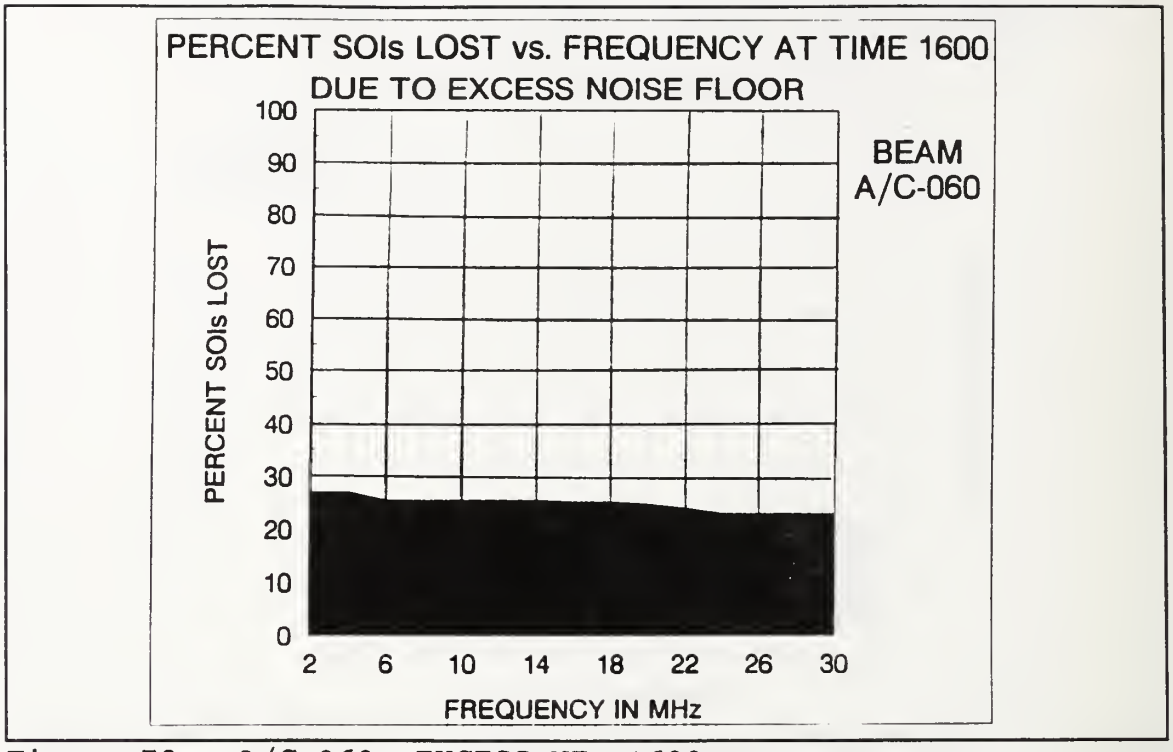


Figure 79. A/C-060, EXCESS NF, 1600.

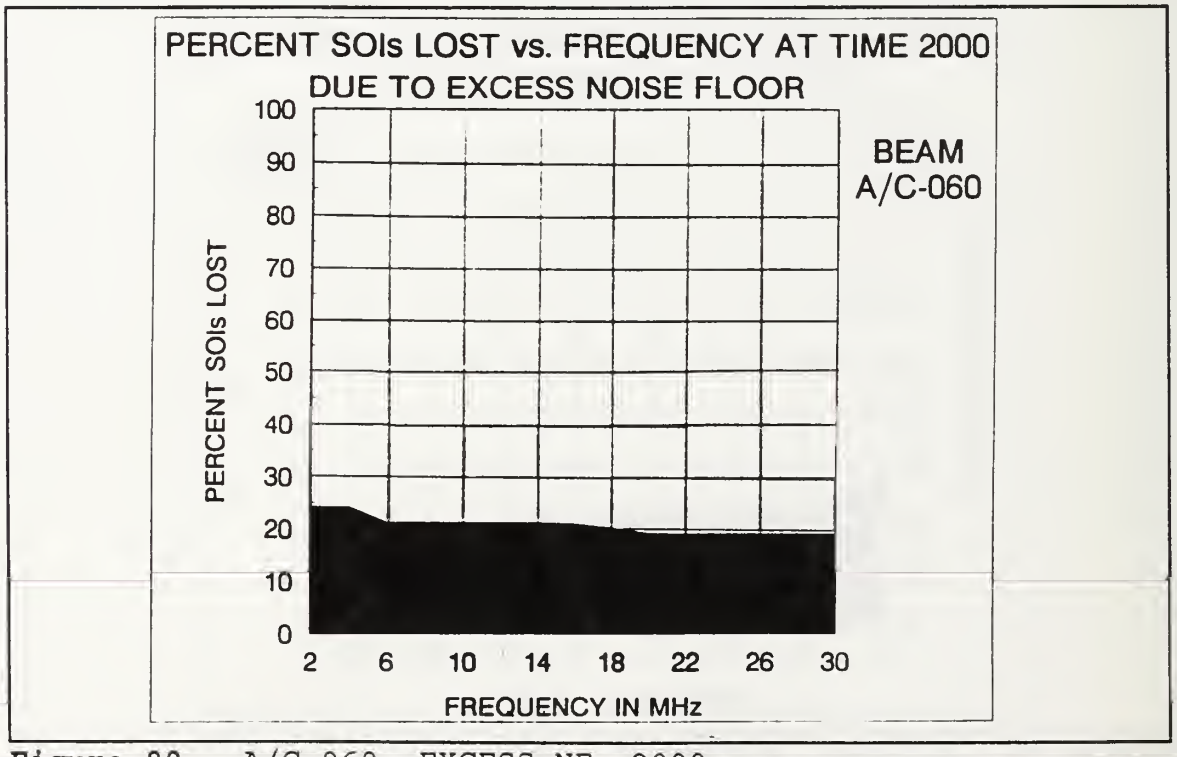


Figure 80. A/C-060, EXCESS NF, 2000.

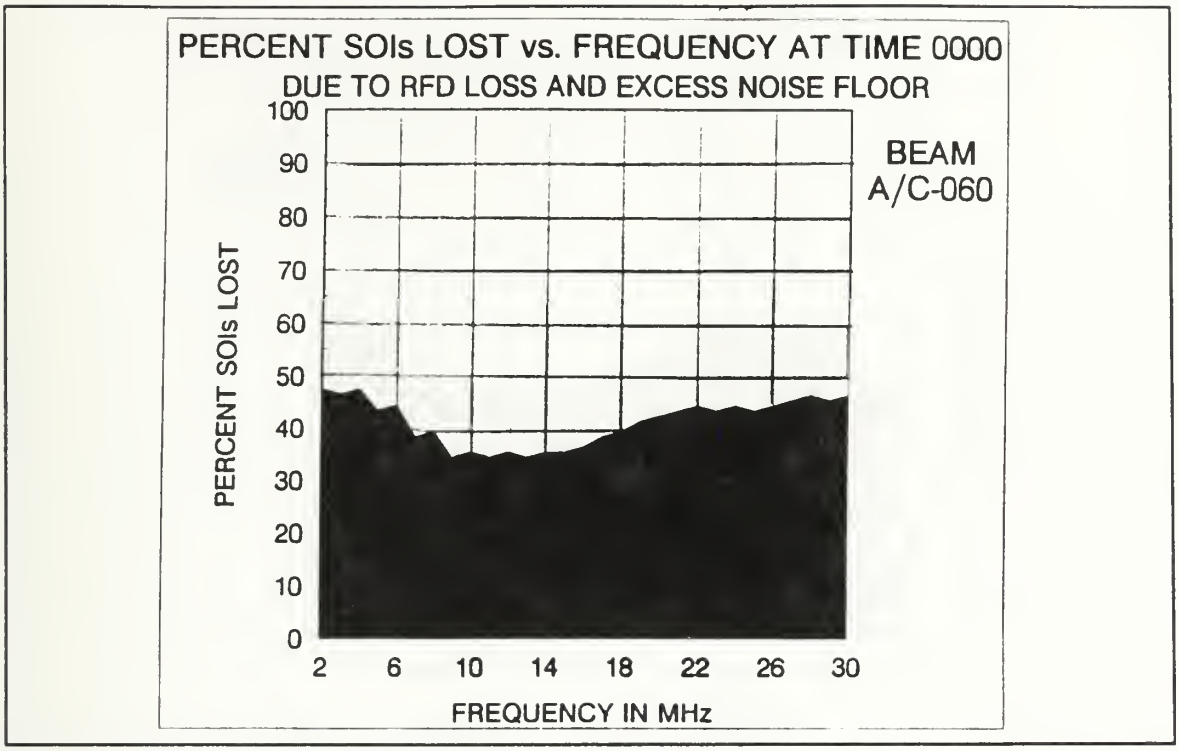


Figure 81. A/C-060, RFD AND EXCESS NF, 0000.

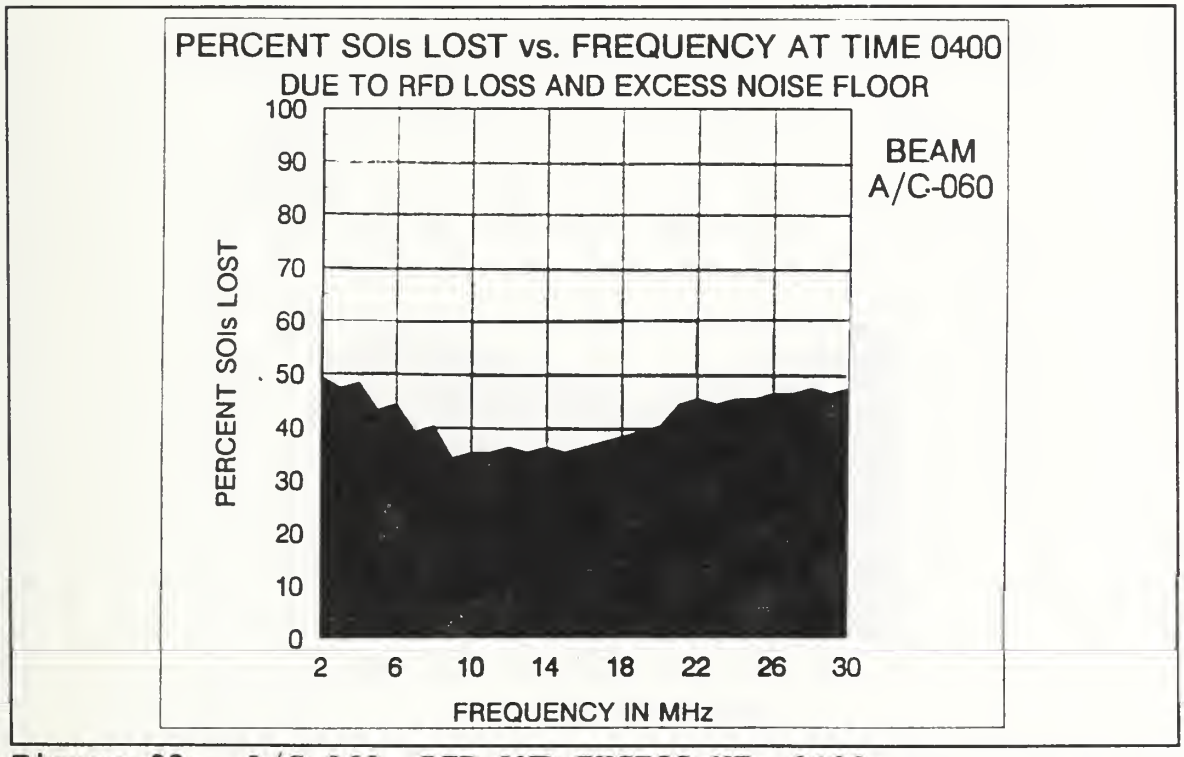


Figure 82. A/C 060, RFD AND EXCESS NF, 0400.

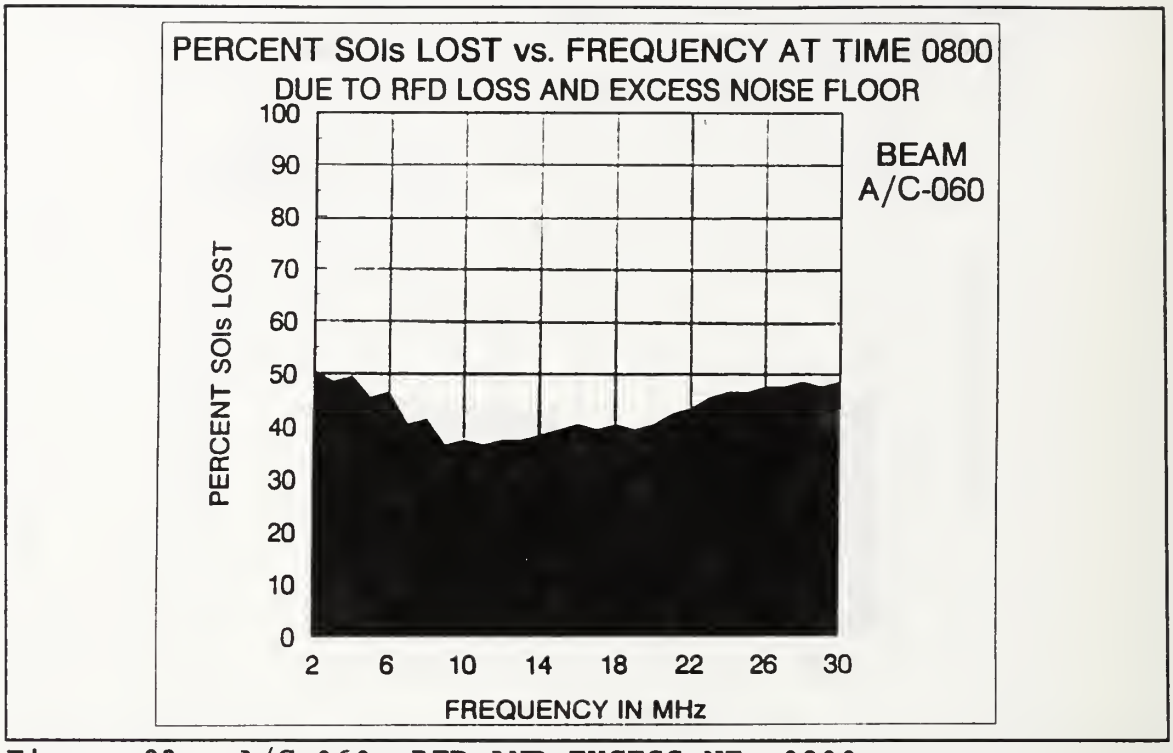


Figure 83. A/C-060, RFD AND EXCESS NF, 0800.

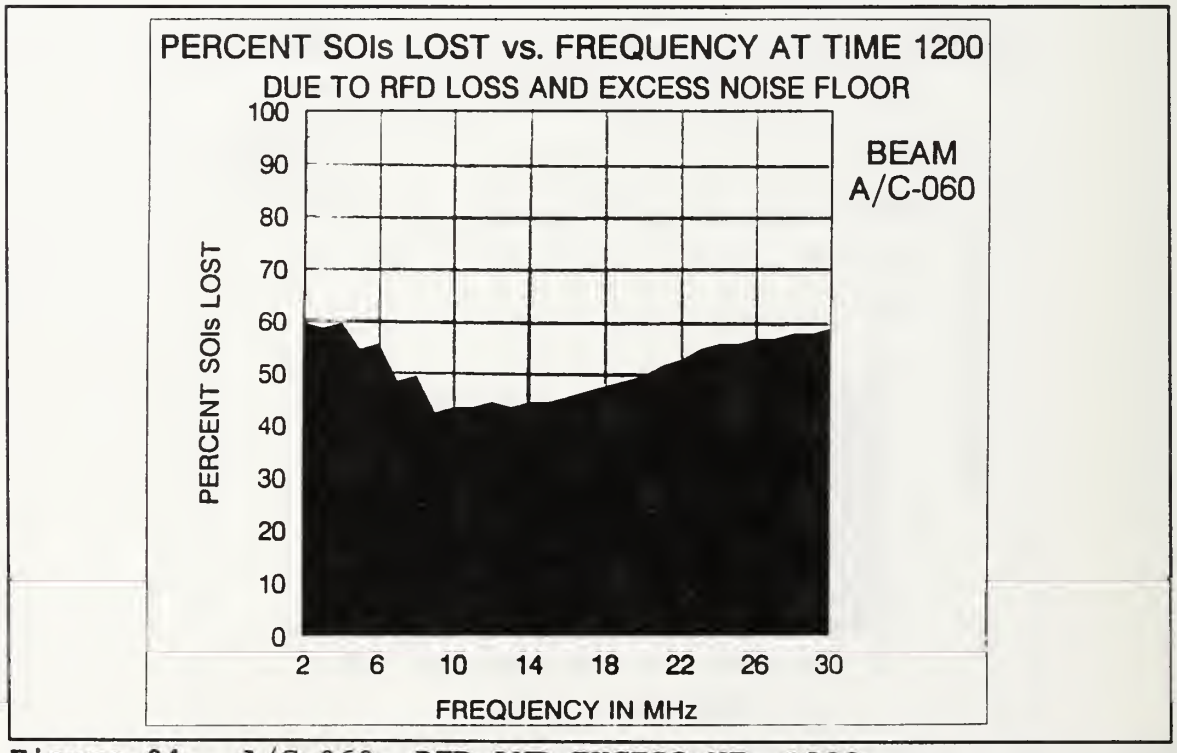


Figure 84. A/C-060, RFD AND EXCESS NF, 1200.

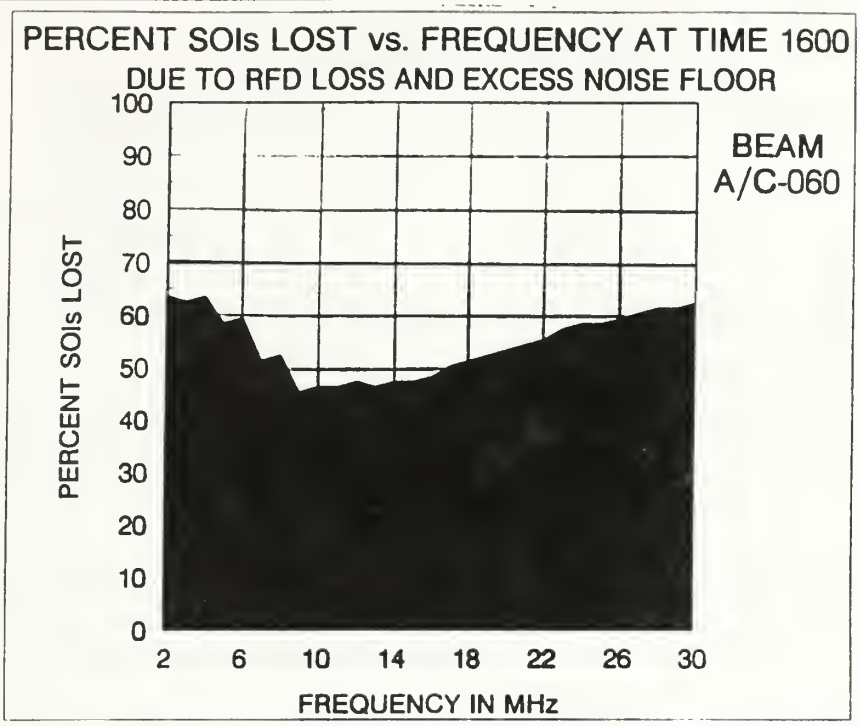


Figure 85. A/C-060, RFD AND EXCESS NF, 1600.

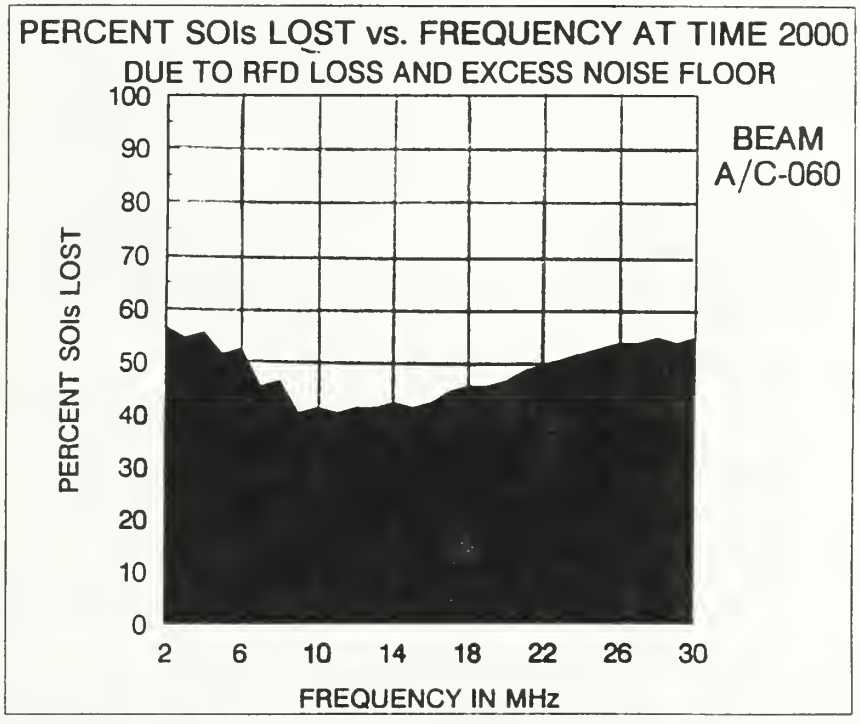


Figure 86. A/C-060, RFD AND EXCESS NF, 2000.

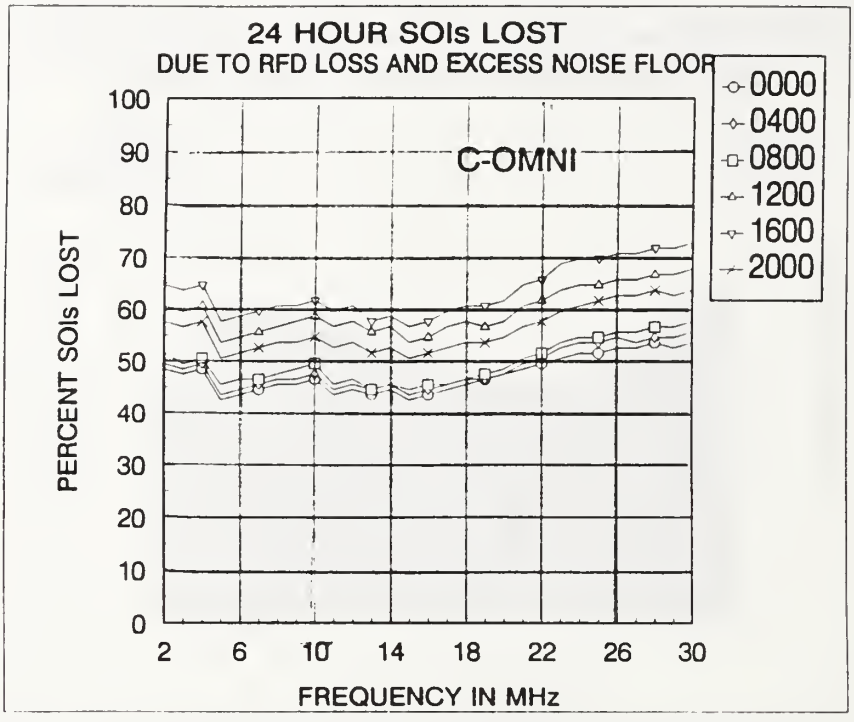


Figure 87. C-OMNI, RFD AND EXCESS NF, 24 HOURS.

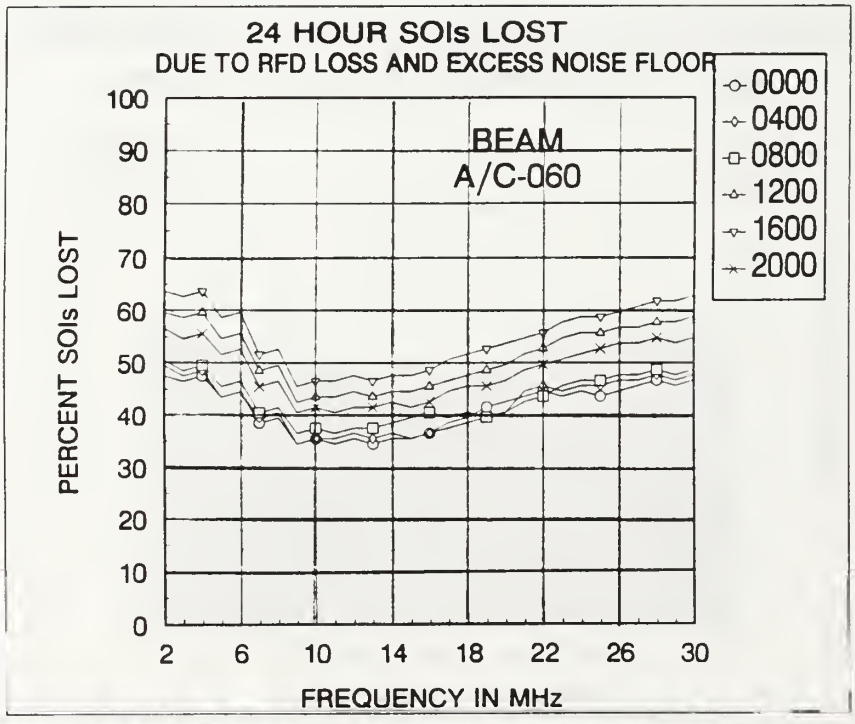


Figure 88. A/C-060, RFD AND EXCESS NF, 24 HOURS.

VII. CONCLUSIONS AND RECOMMENDATIONS

A. CONCLUSIONS

Work accomplished under this thesis reached a number of conclusions. They are:

- It was verified that the amount of data required to complete a comprehensive study of factors affecting the performance of a receiving site is too large to handle by manual techniques. Only simple problems with restricted objectives can be handled by manual means.

- The usefulness of automated techniques for processing and formatting data needed for a comprehensive analysis of site performance was demonstrated. Practical examples were produced from field data.

- The ability to define the impact of each factor that degrades site performance was demonstrated.

- It was shown that a cost can be associated with each factor that degrades site performance. This allows site managers to conduct accurate and meaningful cost-benefit analyses of the mitigation actions required to restore a site to higher levels of performance.

- While the present automated PET process has been shown to be of high value, even further benefits can be obtained by writing custom computer software to replace the standard data processing software used in this effort.

B. RECOMMENDATIONS

Based on the conclusions reached in this thesis, specific recommendations are:

- Dedicated computer software should be designed and written specifically to perform PET curve analyses.

- A number of problems exist in all CDAA sites, and in other receiving sites too, that need to be corrected. The PET process should be used to aid in planning all site upgrades, modifications, improvements, and repairs that might impact performance. Site managers should use the PET process to determine the amount

of performance improvement or degradation caused by each factor and relate this to the cost of implementing each action.

- Additional studies of the amplitude probability distributions of certain classes of SOIs are needed to support the full use of the PET.

- The methods used to predict and verify the maximum amplitudes of SOIs and other signals need to be improved.

- A user's manual should be completed that describes all aspects of the PET process and provides simplified implementation procedures. This manual should accompany the existing computer software and future dedicated software.

- A library of photos showing the spectral and temporal detail of noise from a large number of man-made sources is needed. The availability of such a library will significantly aid in the identification and location of the sources of noise.

APPENDIX A. NOISE MEASUREMENT SYSTEMS

SNEP teams have found it necessary to use special equipment to measure and define the primary characteristics of man-made radio noise. This equipment provides the amplitude versus frequency data needed for the PET process. It also provides sufficient information to distinguish between external and internal sources of noise and to identify the types of sources involved. The identification of the types of sources and their individual impact on site performance is a key factor in developing effective mitigation activities to correct the man-made noise problems.

A second source of noise data is also available. The Automatic Noise Measurement System (ANMS) developed by the Naval Electronic Engineering Activity, Pacific (NEEACT PAC) is available at many sites, and it provides routine measurements of RFD noise levels. The objectives of the ANMS are to:

- Document changes to the ANMS measured site noise baseline over time or after mitigation procedures are performed.
- Automatically measure strong signal levels at NAVSECGRU CDAA sites to determine if they may cause intermodulation products in the system.
- Develop a standard measurement technique which can be used to establish a database and compare measurements between NAVSECGRU sites.

The ANMS records noise power, and it provides limited noise analysis capabilities. The current version of the ANMS does not provide the temporal and spectral information required to identify sources of noise. Future versions of this system may provide sufficient information for the complete PET analysis effort.[Ref. 1]

APPENDIX B. SNEP NOISE DEFINITION EQUIPMENT AND CONFIGURATION

This entire appendix was drawn from Appendix A of the Doctoral Dissertation of LCDR G. Lott [Ref. 3:pp. 172-178].

Figure A.1 shows the equipment configuration used to provide detailed time- and frequency-domain measurements. The input voltage is the voltage present on the coaxial cable feeding signals to a typical receiver. The receiver is usually fed by the facility's RF distribution system which may include primary multicouplers, beam-forming networks, secondary multicouplers, path switching, and connecting cabling.

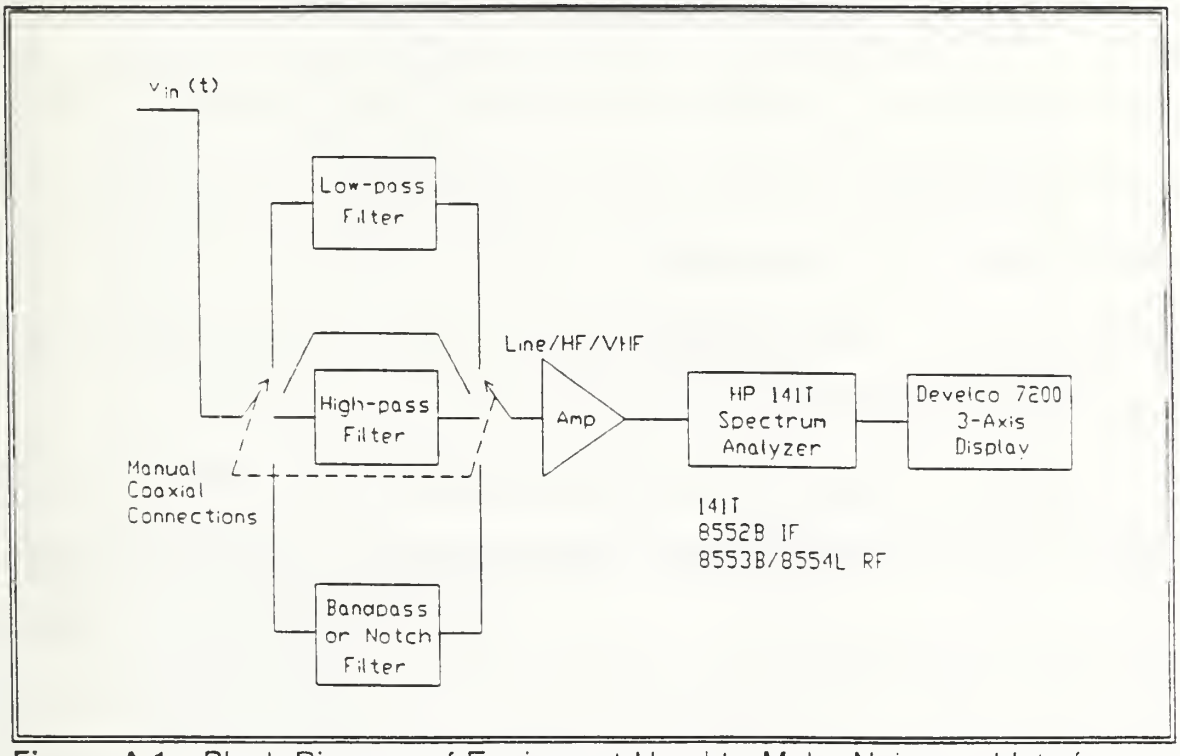


Figure A.1 - Block Diagram of Equipment Used to Make Noise and Interference Measurements

While measurements are made with the spectrum analyzer connected directly to the RF distribution system, filters and amplifiers can modify the input voltage. The filters commonly used include a lowpass filter with a cutoff frequency of 1 MHz, a highpass filter with a 35 MHz cutoff frequency, and a bank of bandpass filters designed to pass non-international broadcast bands from 2 to 30 MHz. Strong signals may require the use of an external attenuator.

The amplifiers include a low frequency (10 Hz to 500 kHz) line amplifier, an HF amplifier (such as the Olektron Model B-HIA-11-HF, 500 kHz to 50 MHz), and a VHF amplifier (50 MHz to 500 MHz). The line and VHF amplifiers are used primarily to make intermodulation products measurements above and below the HF spectrum. The HF amplifier must have a large dynamic range, requiring a third order intercept point of at least +52 dBm.

As shown in Figure A.1, the Hewlett-Packard (HP) Model 140/141 spectrum analyzer acts as a scanning receiver. Along with the HP 141T Display Section, typical HF measurements require two plug-in modules, the HP 8552B Intermediate Frequency Section and the HP 8553B RF Section. The operator can adjust the RF attenuation, scan rate, scan width, IF gain, IF bandwidth, and other controls to give the best presentation of the noise or signal under observation.

The Develco 7200 3-axis display provides a real time display of noise and signals received with the spectrum analyzer. As shown in Figure A.2, the three axes are usually frequency (horizontal axis), signal or noise power (vertical axis),

and time (depth or Z axis). The horizontal axis is also the time for each spectrum analyzer sweep which allows measurement of repetition rate and duration of wideband interference such as distribution power-line related noise.

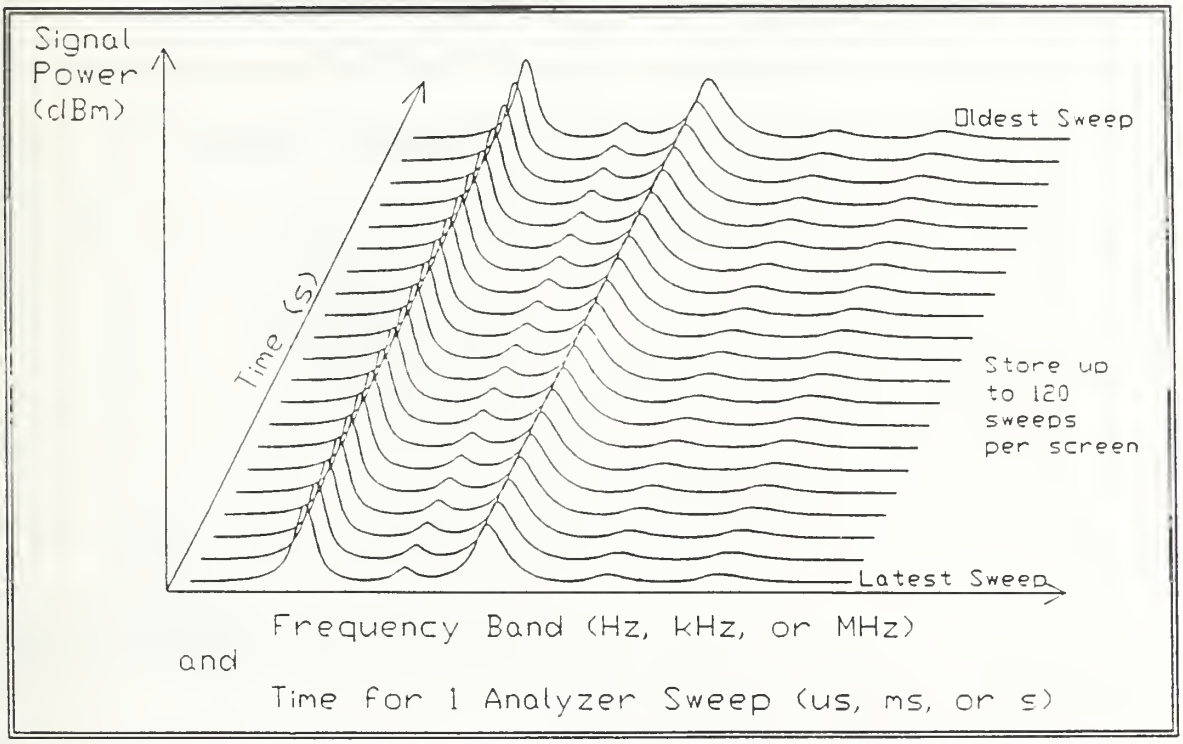


Figure A.2 - Units of Measure Associated with Each Axis in Photographs Made with the 3-Axis Display System

The HP141 spectrum analyzer provides two signals to the 3-axis display, video and synch. The 3-axis display takes 512 equally spaced samples of the video signal from each complete analyzer scan, and the sample resolution is eight bits. As shown in Figure A.3, the Develco 7200 is a first-in, first-out (FIFO) display. The latest scan appears as line one. Line one moves to line two with the newest scan again appearing as line one. The 3-axis display can typically store up to 60

spectrum analyzer scans. There are 120 line versions of the Develco 7200. With each scan update, the oldest scan data on the top line is discarded.

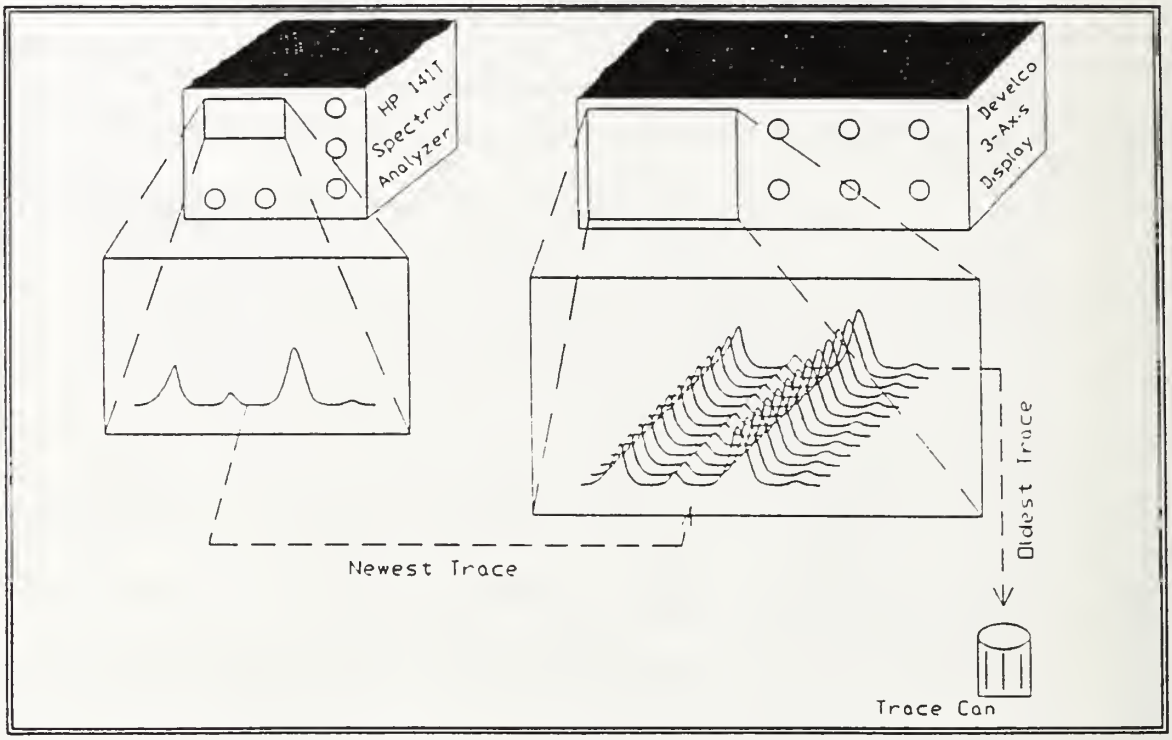


Figure A.3 - Combined Operation of HP 141T and Develco 7200 Showing FIFO Movement of Spectrum Analyzer Scans

The time (depth) axis is the elapsed time for the 60 traces. However, spectrum analyzer retrace time adds to the total. Measurements show that on one HP 8553B with a scan rate of 5 ms per division (50 ms per scan), the actual time for one scan and retrace in the auto synch mode was 56.5 ms. For the same unit with the same setting, the actual time for one scan and retrace in the line synch mode was 66.94 ms. When displayed on the Develco 7200, the depth time axis limit for measurements made with a 5 ms per division scan rate on the specific HP

8553B are 60 times the actual time for one scan plus retrace, or 3.4 s and 4.0 s respectively.

There is no simple expression that one can use to determine the actual scan time as a function of the instrument control scan rate. Prior to making measurements, the operator must measure the actual scan times for each scan rate in both the auto and line synch modes. The actual scan times will be different for each HP 8553B, and experience shows that the times will change each time a unit undergoes calibration.

Measurements require accurate frequency, amplitude, and time calibrations for use as standards for manually scaling the photographs taken of the 3-axis display's screen. Calibrations include the total scan time measurements and a 10 dB step amplitude calibration photograph. Calibrations are good only for the specific instruments used. Operators should make daily checks to ensure that the calibration photographs are accurate. Changing the oscilloscope camera may require a new amplitude calibration photograph because image compression may occur due to small differences in the camera lens.

Figure A.4 shows a sketched example for 25 spectrum analyzer scans as displayed on the Develco 7200. The figure shows the temporal changes for six signals in the 50 kHz part of the HF spectrum. Actual signal identification for some modulation types is difficult using only the 3-axis display. To make signal identification easier, a separate HF communications receiver augments the measurement system.

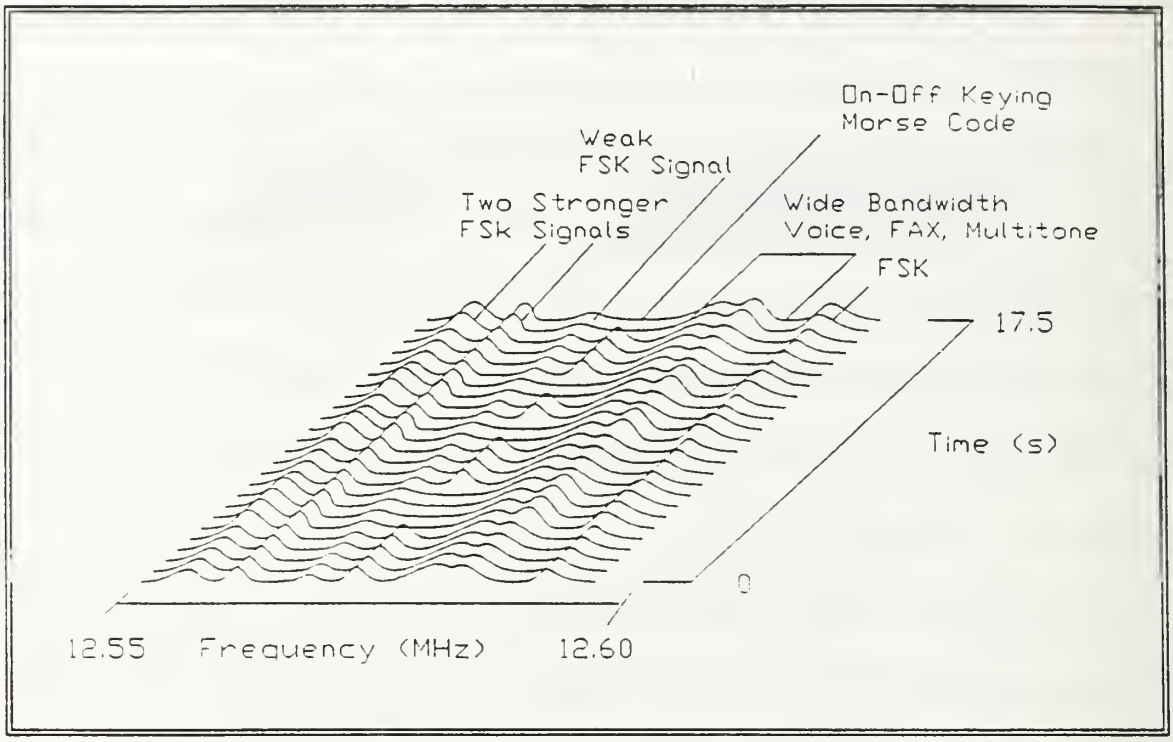


Figure A.4 - Example of 3-Axis Display of HF Signals

The 3-axis display controls allow for:

- freezing the data in memory for photographing or detailed viewing
- changing amplitude compression
- changing the elevation and azimuth of the depth axis
- adjusting the background level.

To make photographs for amplitude measurements, the display elevation and azimuth are set to zero. This results in viewing all 60 traces as if they were superimposed into one trace. Using a card made from the 10 dB calibration step photograph, knowing the equipment settings, and using the trace baseline as a reference, one can manually scale the amplitude photographs.

Controls also allow for the selection and display of subsets of the 60 spectrum analyzer scans stored in 3-axis display memory. Experience using the 3-axis display while viewing various types of signals and noises results in the operator being able to adjust the 3-axis display controls to optimize the presentation. A typical measurement requires two photographs, one for amplitude measurement and one with the time (depth) axis elevated to show temporal variations.

APPENDIX C. PROPHET SIGNAL STRENGTH COMPUTATION

PROPHET provides a convenient way to predict the value of the maximum signal strength of received signals. The following parameter list specifies the input information for a signal strength calculation. A sample set-up procedure is also provided.

- AT- Atmospheric Noise- No
- BW- Bandwidth- 3.00 kHz
- DA- Set Date- 12/1/91
- FL- 10.7 cm Flux- 145.0
- FR- Frequency Input- 2-30 MHz
- LA- Launch Angle- 1.0 Deg. Min., 87.0 Deg. Max.
- NM- Numeric Units- Kilometers
- NP- Propagation Modes- 6
- RN- Receiver Name- Sabana Seca
- TN- Transmitter Name- TEMPXMTR
- WI- Wind Velocity- 1 Knot
- XF- X-Ray Flux- 1.0E-03

The previous list of set-up information can be listed by typing LI while in the PROPHET program. Assign the receiver as PTRICO and designate a new transmitter

as TEMPXMTR with the desired antenna characteristics. The following is the set-up definition of TEMPXMTR:

- TEMPXMTR
  Lat. 29.5 W., Lon. 51.3 N., OMNI Ant., 1000 W.

The resulting Signal Strength calculation for the times listed is in dBuV.

To convert the signal strength in dB above a microvolt into dBm use the conversion

$$\text{SS dBuv} - 107 = \text{SS dBm} \qquad (2)$$

The value that is obtained is the maximum signal strength expected to be used in the PET curves to set the amplitude distribution of SOIs. Figures 89 and 90 are the desired outputs from PROPHET.

```
*** UNCLASSIFIED ***
DATE: 12/ 1/91          ATMOSPHERIC NOISE:  NO
10.7 CM FLUX: 145.4     X-RAY FLUX:  .0010    MAN-MADE NOISE: QM
TEMPXMTR        LAT:  29.5    LON:   51.3 ANT: 101 @ *OMNI* PWR:    1000.00
PTRICO          LAT:  18.0    LON:   66.5 ANT:   0 @ *OMNI* RANGE:  2003 KM

                SIGNAL STRENGTH  (DB ABOVE 1 MICROVOLT)

                                    FREQUENCY
TIME 2          8           16          24          32          40  LF MF
00  29 33 32 31 29 26 11-15                                         2 13
01  29 32 32 30 28 24  0                                           2 12
02  29 32 32 30 27 24 -2                                           2 12
03  29 32 31 29 26 15-14                                           2 11
04  29 32 31 28 25  6                                              2 11
05  29 32 31 29 25 11-18                                           2 11
06  29 32 30 28 24 -2                                              2 10
07  29 32 30 27 20 -9                                              2 10
08  29 31 29 25 -1                                                 2  8
09  29 31 28 24 -2                                                 2  8
10  31 33 33 32 31 30 28 26 24  3                                  2 19
11     -2 18 24 27 27 27 27 26 25 23 18-17                         3 24

                SIGNAL STRENGTH  (DB ABOVE 1 MICROVOLT)

                                    FREQUENCY
TIME 2          8           16          24          32          40  LF MF
12        -3 13 20 23 24 25 25 24 23 21 11-11                       4 26
13       -19  4 14 19 22 24 24 24 23 22 12 10-16                    5 28
14           -3 10 16 20 22 23 23 23 22 13 11 -5                    6 29
15           -6  8 15 19 22 23 23 23 22 13 12  0                    6 29
16           -7  7 14 18 22 23 23 23 22 13 12  0                    6 29
17           -5  8 15 19 22 23 23 23 22 13 12 -6                    6 29
18            0 12 17 21 23 24 24 23 22 13  9-16                    5 28
19       -12  8 16 21 23 25 25 24 23 22 13 -7                       5 27
20         6 18 23 25 26 27 26 25 24 22 -4                          4 25
21 -17 21 28 30 30 30 29 29 27 25 23 -2                           2 22
22  31 33 33 32 31 30 28 26 19 -8                                 2 18
23  29 33 33 31 30 28 25 10-18                                    2 15
FS>
```

Figure 89. Maximum Signal Strength Prediction.

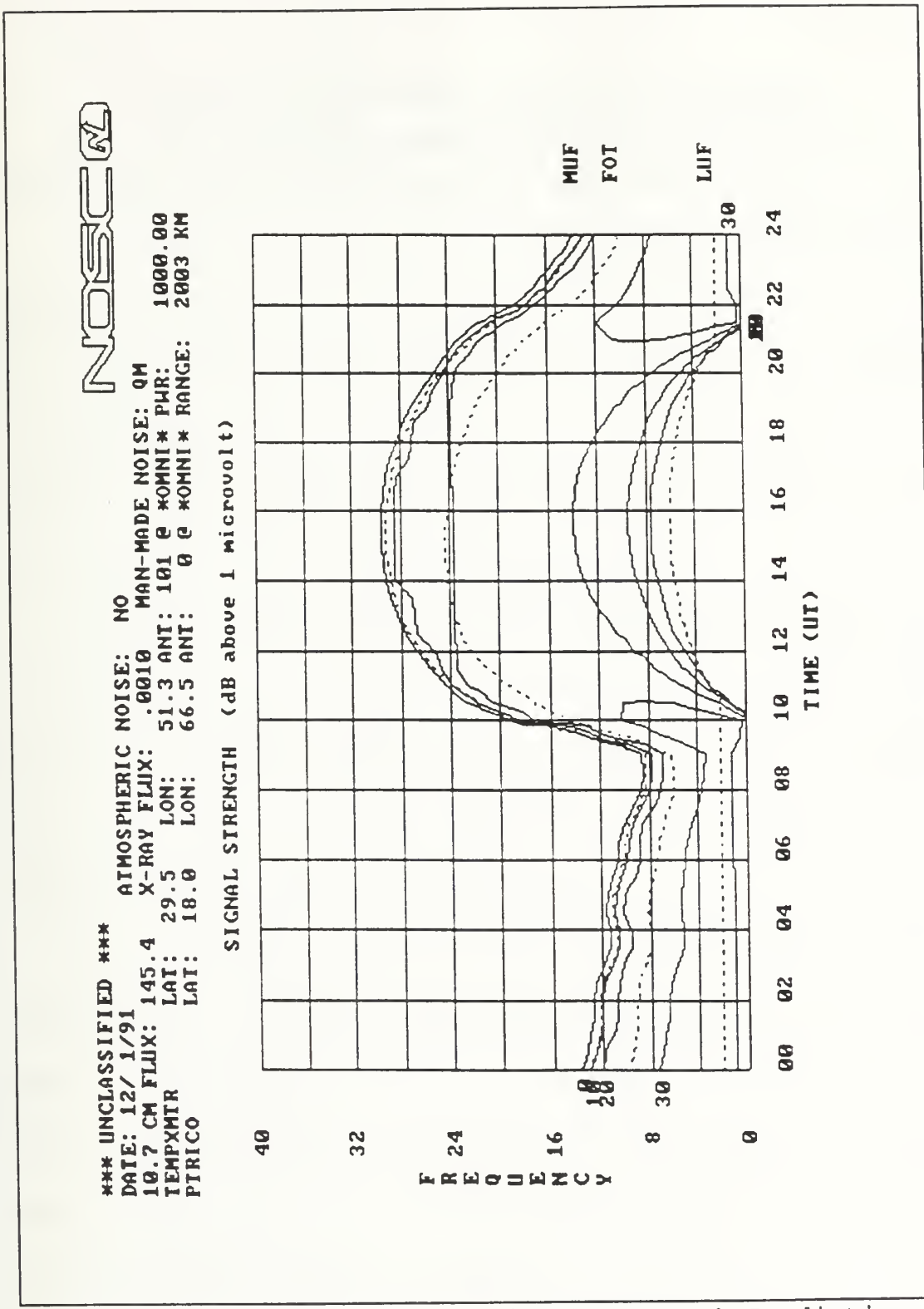


Figure 90. Graph Of Maximum Signal Strength Prediction.

APPENDIX D. HF SIGNAL AMPLITUDE STATISTICS

This entire appendix was drawn from Chapter III of the Doctoral Dissertation by LCDR G. Lott [Ref. 3:pp. 28-45].

III. HF SIGNAL AMPLITUDE STATISTICS

This dissertation will use the random variable v_{in} as the root-mean-square (RMS) amplitude of the total, intercepted HF voltage applied to a receiver. In a wideband receiver searching the HF spectrum for new signals, v_{in} represents a voltage comprised of all broadcast signals, non-broadcast signals, and noise. Distortion in non-linear RF system components, losses in cables and connectors, and induced noise add an undesired component to v_{in}.

A wideband receiver and the first stages of many narrowband receivers must be capable of processing the maximum peak value of v_{in}. A narrowband receiver with pre-selection will reject signals and noise outside the pre-selector bandwidth. A much lower value of the input voltage will reach the front-end components of a narrowband receiver with pre-selector filtering.

The RMS voltage produced only by signals of military interest is considerably different than v_{in}. It will have a smaller dynamic range than v_{in}. Analog-to-digital (A/D) converters designed to optimally quantize signals of military interest should not waste limited quantization dynamic range on the high amplitude broadcast band signals. Instead, the A/D design should optimize the ability to receive and process the adversary's most clandestine transmitter.

A. HF SIGNAL STUDIES

As part of the Navy's Signal-to-Noise Enhancement Program, Prof. W. Ray Vincent and LT John O'Dwyer estimated an initial distribution of HF signal amplitudes. Using photographs taken of spectrum analyzer displays, they developed an amplitude distribution function by counting the number of signals exceeding threshold levels in 10 dB steps. This technique yielded a logarithmic distribution with a slope of approximately 0.1 per 10 dB of signal amplitude change. [Ref. 16]

In 1980, Dutta and Gott studied HF spectrum occupancy to determine the congestion levels. They compared the percentage of 1 kHz windows which had signals with amplitude greater than threshold slicing levels. This data, when viewed as an amplitude probability function, suggests a logarithmic distribution with a slope of 0.15 per 5 dB change between -125 and -110 dBm. [Ref. 17]

In 1981, Wong and others conducted an HF spectral occupancy study which provides spectrum occupancy information as a function of frequency. Their goal was to predict the probability of finding a vacant frequency for military use. A vacant frequency would have to have a signal level less than a specified amount. Wong's data includes the percentage of time a 1 kHz bandwidth has a signal level greater than specified thresholds. [Ref. 4]

Figure 3.1 displays Wong's data differently from that used in Reference 4. Figure 3.1 plots Wong's data as a two dimensional probability distribution of frequency and the amplitude as a random variable. Figure 3.2 is a plot of the 0.5

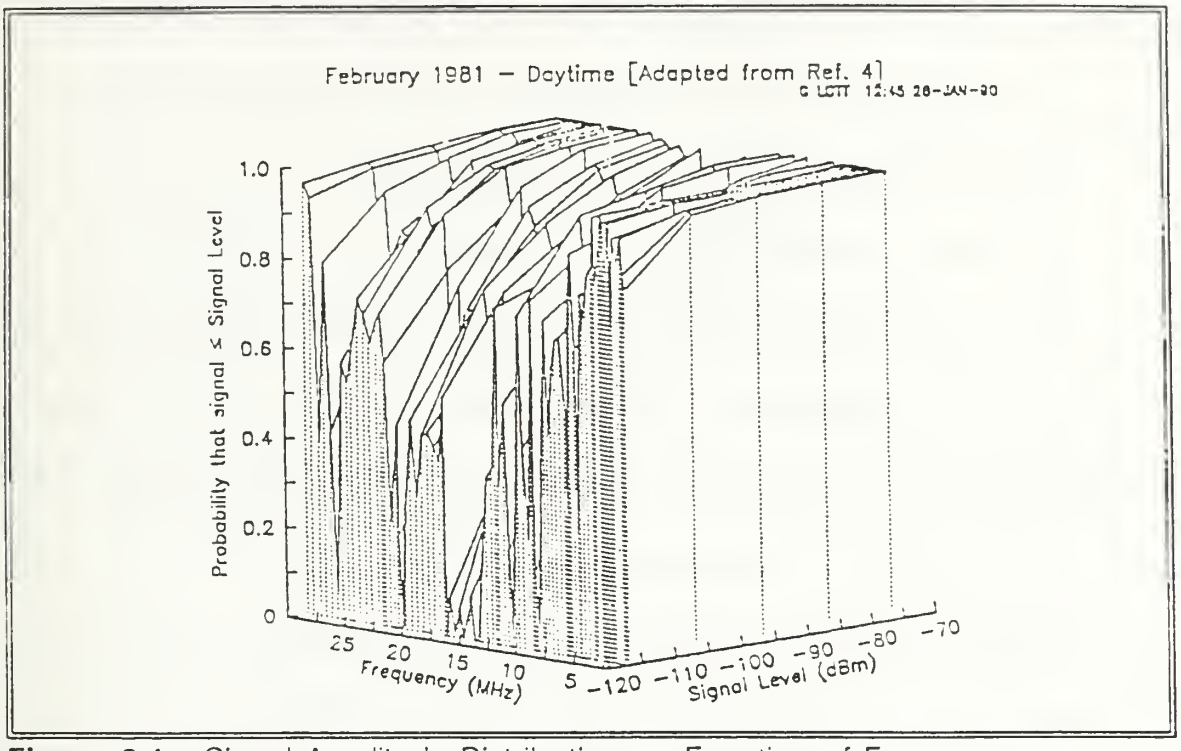


Figure 3.1 - Signal Amplitude Distribution as Function of Frequency

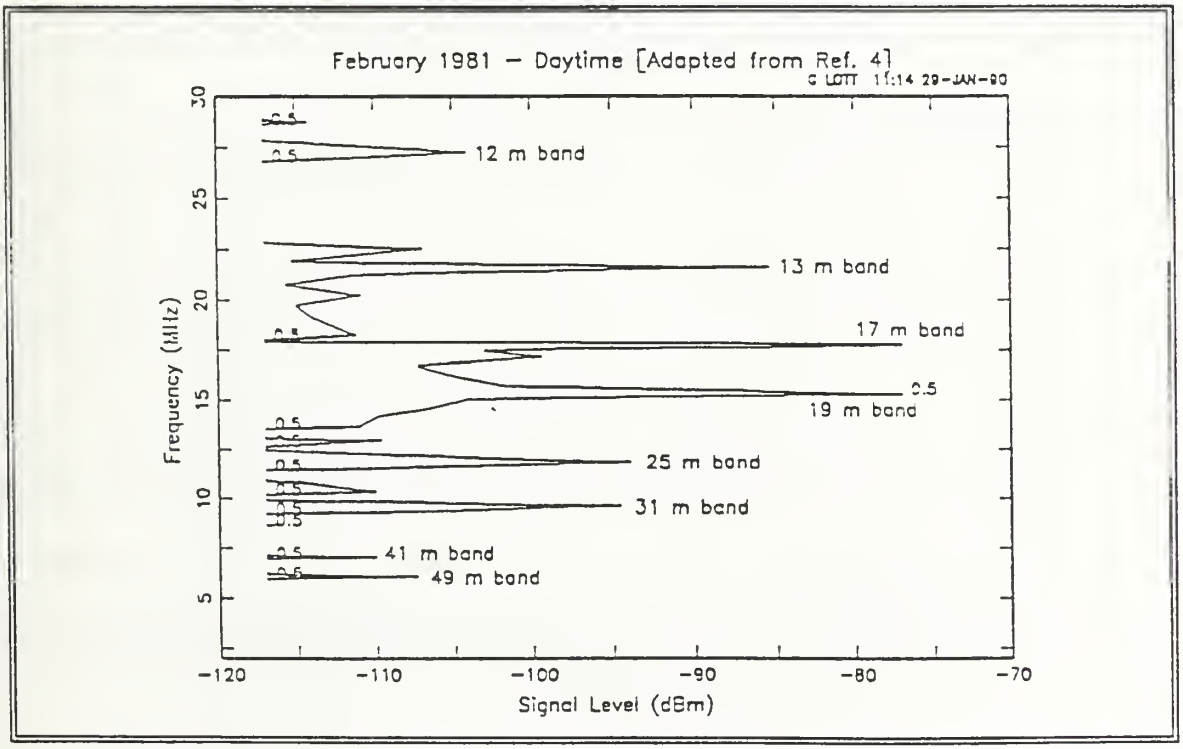


Figure 3.2 - Plot of 0.5 contours from Figure 3.1 Showing Dominance of International Broadcasting Bands

probability contours from the surface in Figure 3.1. It clearly shows the dominance of signals in the international broadcasting bands. Nearly all signals exceeding the 0.5 contours are within ITU allocated broadcasting bands.

P.A. Bradley, analyzing Wong's data, concluded "...that occupancy (or congestion) varies with the threshold level (expressed in dBm) approximately in accordance with a log-normal law." Of particular note is the limitation in Wong's measurement system that allowed it to revisit each 1 kHz frequency window only once every 3 to 5 days for one second duration. [Ref. 4]

Wilkinson performed a spectral occupancy study in which he separated data by frequency and receiver bandwidth. Figure 3.3 displays Wilkinson's data using the same type of presentation as that in Figure 3.1. He found that cumulative signal level distributions remain log-normally distributed for receiver bandwidths from 0.1 to 100 kHz. [Ref. 18]

Gibson and others conducted one of the few spectral occupancy studies using a large aperture antenna, namely a circularly disposed antenna array (CDAA) or Wullenweber antenna. After analysis, they concluded that the cumulative amplitude distributions "...are found generally to follow a log-normal law." [Ref. 19]

Moulsley used an active-antenna-based observation system to make his spectral observations. As shown in Figure 3.4, he found signals in the international broadcasting band to have power levels more than 20 dB higher than signals in the

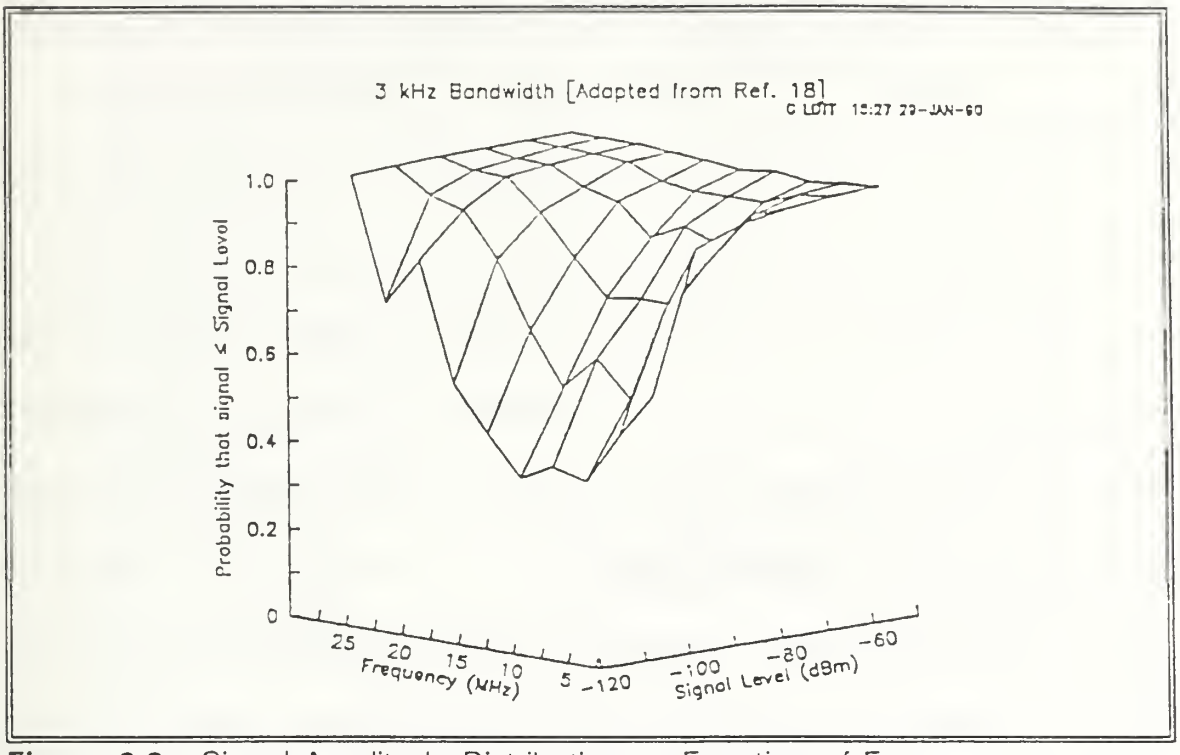


Figure 3.3 - Signal Amplitude Distribution as Function of Frequency

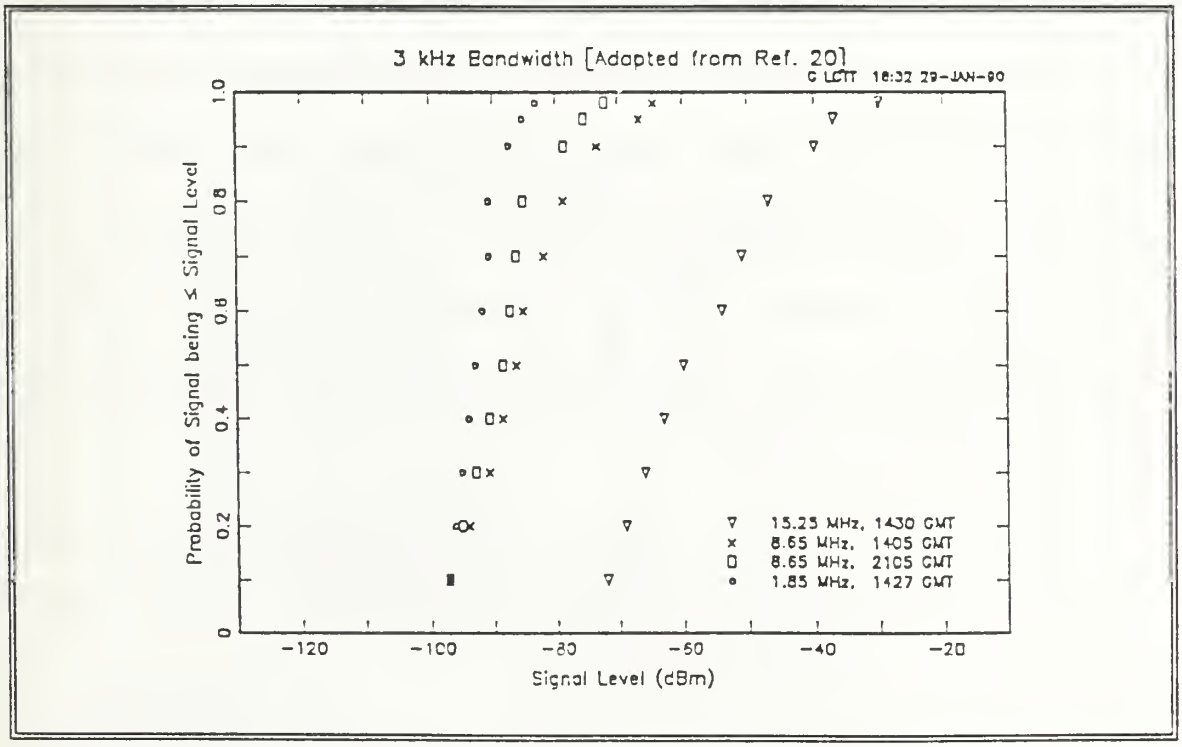


Figure 3.4 - Broadcasting vs. Non-Broadcasting Signal Amplitude Distributions

fixed, mobile, and maritime service bands. Moulsley's data shows an amplitude cumulative probability distribution which follows a log-normal law. [Ref. 20]

During the summer of 1987, Gibson performed a new spectral survey using a technique different from his 1981 observations. This study found little difference in spectrum occupancy from weekdays to weekends. Gibson modeled the noise floor as incident-external noise limited and distributed according to a Rayleigh law. Even with this projection, he found that the overall amplitude cumulative probability distribution followed a log-normal law. He eventually used a log-normal model for the noise floor. This survey considered specifically signals in non-broadcast portions of the HF band. This signal distribution should be similar to that expected from signals of military interest discussed earlier. Figure 3.5 displays the results. [Ref. 21]

Laycock and others made additional spectrum occupancy measurements in central England using a format similar to Wong's 1981 survey. From this they developed a model of channel occupancy, which is binomially distributed. While similar, channel occupancy is different from amplitude cumulative probability. Figure 3.6 shows the results of this study in a format similar to that used to show data from Wong's study. [Ref. 22]

Another study in 1987 by Perry and Abraham suggests that the channel occupancy statistics change when using bandwidths less than 150 Hz. The HF channel-occupancy to power-level relationship found in this study is log-log

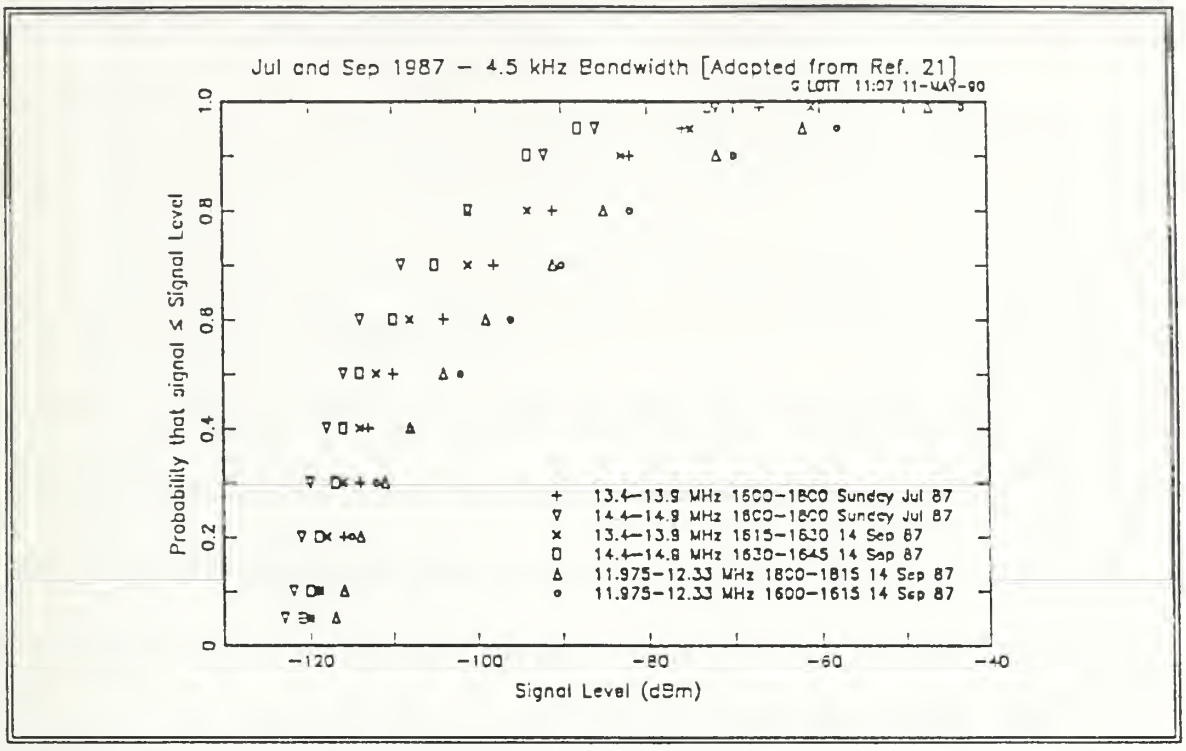


Figure 3.5 - Non-Broadcasting Signal Amplitude Distribution

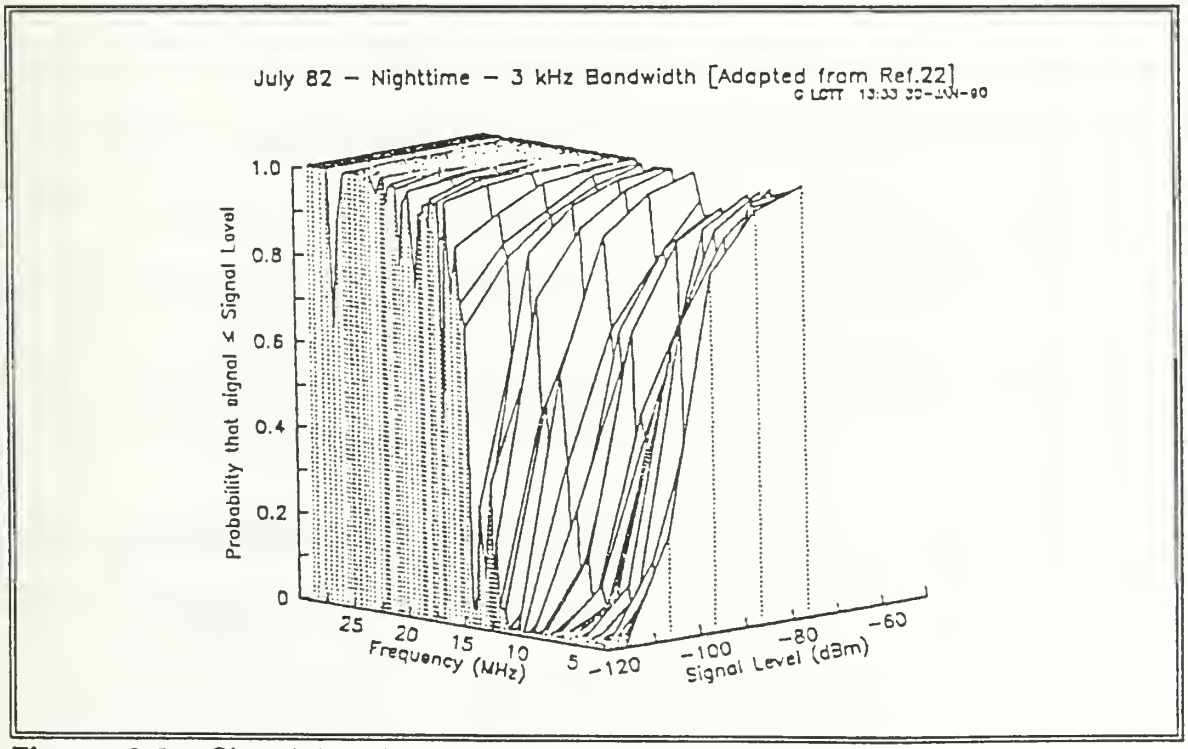


Figure 3.6 - Signal Amplitude Distribution as Function of Frequency

distributed. However, the model ignores curvature at the lower power levels due to external noise. To simplify the data required for their work, Perry and Abraham normalized all measurements to the largest interferer, or signal, present. This relationship is nearly log-normal after adding curvature on the extremes. [Ref. 23]

The most exhaustive HF signal level study published is that by Hagn and others using measurements from Europe and the U.S. taken during the Fall 1987. Most earlier studies used time averaged amplitude values, or they had long revisit times to each 1 to 3 kHz window. Hagn's survey used instrumentation that allowed rapid revisit. "Each of the 9333 3-kHz channels in the band from 2 to 30 MHz was sampled 150 times/hour...." [Ref. 24]

Figure 3.7 displays some of Hagn's data, and it reveals three significant results. First, Hagn's data follow a log-normal distribution. The slope, which indicates variance, is similar to the other tests conducted in Europe. However, the slope is steeper for the U.S. tests. The smaller variance indicates a smaller dynamic range requirement for receivers at sites in the continental U.S. environment.

Second, the mean signal level in the fixed and maritime service bands are about 20 to 30 dB below the mean of signals in the international broadcast bands. This agrees well with Moulsley's data as shown in Figure 3.4.

Third, there is a 10 to 30 dB difference in mean between signal levels in Europe and signals in the U.S.. One would expect this since most European area

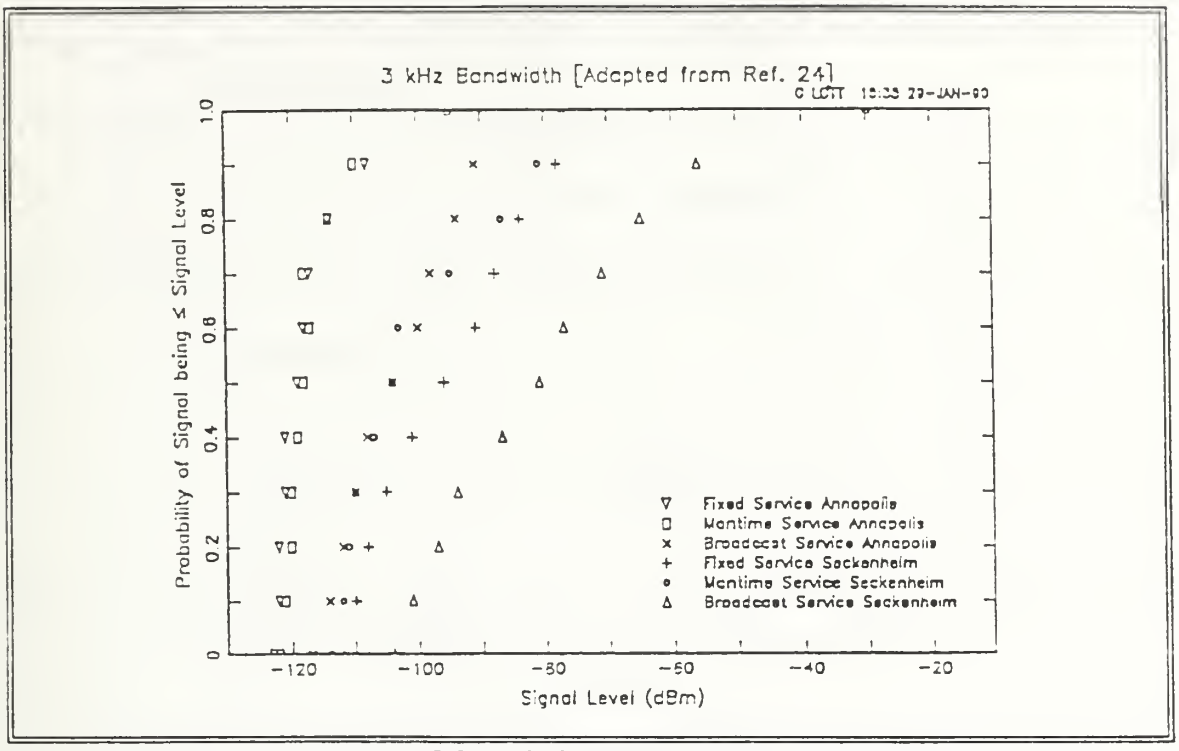


Figure 3.7 - European and CONUS Signal Amplitude Distributions

transmissions are a single ionospheric hop from many powerful transmitters, and many of the U.S. received signals are multi-hop from such sites.

Figure 3.8 shows the composite distributions from the various studies of non-broadcast signals. To reduce the number of data points displayed in Figure 3.8, the data representing Wong's and Laycock's studies (from References 4 and 22) are displayed as the arithmetic mean over all frequency bins calculated with each non-broadcast frequency bin as an independent observation.

B. THE LOG-NORMAL DISTRIBUTION

One common thread for all the studies is that they are normally distributed when plotted as a function of received signal power in dBm. This leads one to

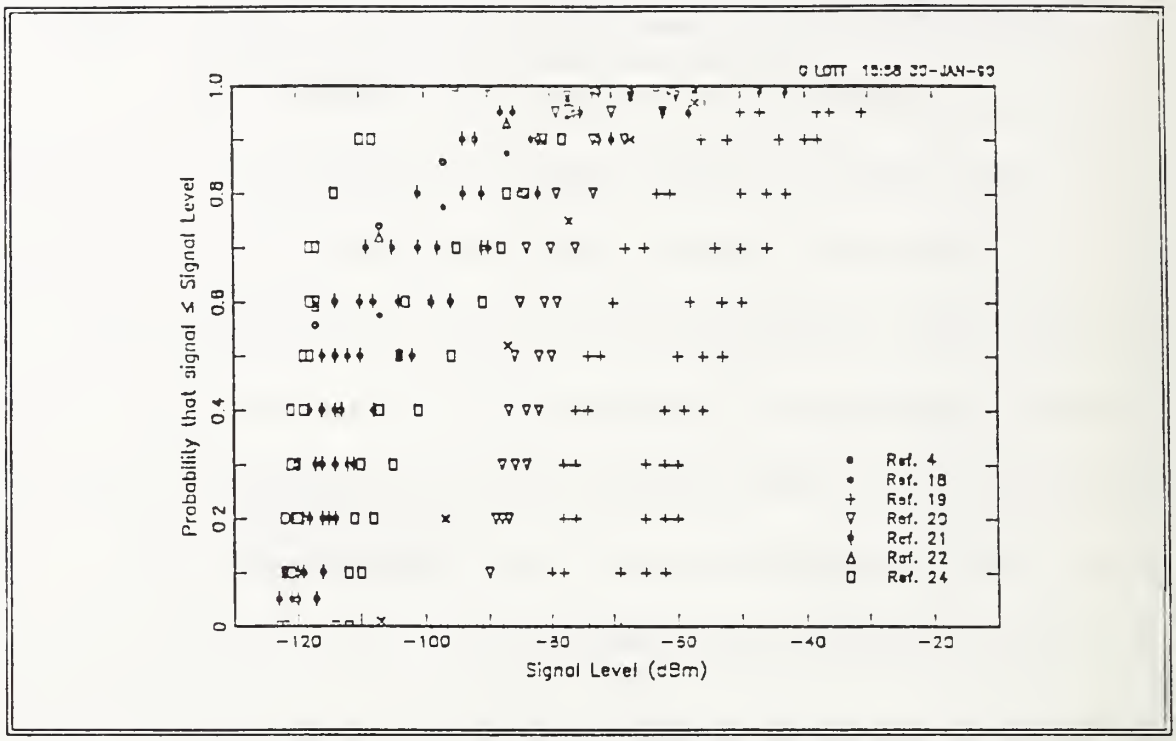


Figure 3.8 - Composite of Non-Broadcasting Signal Amplitude Distributions

the log-normal distribution for the RMS voltage v_{in} at the input to a wideband receiver.

The log-normal distribution is a positive, skewed distribution when plotted against a linear ordinate. Where the domain of the random variable for a normal distribution is all of the real numbers, the domain of the random variable for a log-normal distribution is all non-negative real numbers.

Economic trends, biological growth, and particle size commonly describe statistics that appear to be log-normally distributed [Ref. 25]. Reference 25 is the universally accepted reference on the subject. Many other references which

mention the log-normal distribution simply summarize the Aitchison and Brown [Ref. 25] work.

The random variable v_{in} represents the composite RMS voltage amplitude as described before, and w_{in} is the composite power received. With a 50 Ω load at the receiver, the relationship between w_{in} and v_{in} is given by the expression:

$$w_{in} = 20 \log_{10}\left[\frac{v_{in}}{\sqrt{(50)(10^{-3})}} \right] \qquad (3.1)$$

where w_{in} is in dBm, v_{in} is in RMS volts such that $v_{in}>0$, and $\log_{10}$ is the logarithm to base 10.

When plotted as w_{in}, a normal distribution shape is the first indication that v_{in} may be log-normally distributed. The next step in fully describing the distribution is to calculate the mean and variance of the distribution of w_{in}, denoted as μ_{dBm} and σ^2_{dBm} respectively. Assuming normality in the dBm domain, the probability density of w_{in} is given by:

$$p_{w_{in}}(w_{in}) = \frac{1}{\sqrt{2\pi\sigma^2_{dBm}}} e^{-\frac{(w_{in}-\mu_{dBm})^2}{2\sigma^2_{dBm}}} . \qquad (3.2)$$

To simplify calculations, one can write w_{in} as a natural logarithm rather than the decibel expression. Converting Equation 3.1 yields:

$$w_{in} = 8.69 \ln(v_{in}) + 13.01 . \qquad (3.3)$$

Writing the density function of the RMS voltage amplitude v_{in} requires a change of variable. Using the transformation,

$$p_{v_{in}}(v_{in}) = p_{w_{in}}(w_{in}) \left|\frac{dw_{in}}{dv_{in}}\right| \tag{3.4}$$

and,

$$\frac{dw_{in}}{dv_{in}} = \frac{8.69}{v_{in}} \tag{3.5}$$

the probability density function for the RMS voltage amplitude v_{in} is given as:

$$p_{v_{in}}(v_{in}) = \frac{8.69}{v_{in}\sqrt{2\pi\sigma_{dBm}^2}}\, e^{-\frac{\left(8.69\ \ln(v_{in})+13.01-\mu_{dBm}\right)^2}{2\,\sigma_{dBm}^2}} . \tag{3.6}$$

Making the substitutions

$$\mu_{ln} = \frac{\left(\mu_{dBm}-13.01\right)}{8.69} \tag{3.7}$$

and

$$\sigma_{ln} = \frac{\sigma_{dBm}}{8.69} , \tag{3.8}$$

the resulting distribution for the RMS voltage amplitude is:

$$p_{v_{in}}(v_{in}) = \frac{1}{v_{in}\sqrt{2\pi\sigma_{ln}^2}}\, e^{-\frac{\left(\ln(v_{in})-\mu_{ln}\right)^2}{2\sigma_{ln}^2}} \tag{3.9}$$

which is the basic form of the log-normal distribution as used in Reference 25. The received RMS voltage amplitude will be positive since RMS implies the positive square root. Thus $v_{in}>0$ as required by the domain of the function.

Using the same notation as in Reference 25, one can write a mean and variance for the distribution of v_{in} which gives the mean, α, in rms volts as:

$$\alpha = e^{\left(\mu_{ln} + \frac{1}{2}\sigma^2_{ln}\right)} \tag{3.10}$$

and the variance, β^2, as:

$$\beta^2 = e^{\left(2\mu_{ln} + \sigma^2_{ln}\right)}\left(e^{\left(\sigma^2_{ln}\right)} - 1\right) \quad . \tag{3.11}$$

The mean and variance, calculated using Equations 3.10 and 3.11, provide an intuitive feel for the average RMS voltage levels of the receiver input. Otherwise, most calculations remain in the logarithmic domain where the form of the distribution is well understood. The density function in Equation 3.9 involves both v_{in} and $\ln(v_{in})$. There is no simple closed-form expression for the density function in terms only of v_{in}. [Ref. 25]

An important result to be applied for the log-normal distribution is in the application of the central limit theorem. Simply stated, in non-logarithmically related distributions, the sum of independent random variables having the same probability distribution will asymptotically become a gaussian distribution.

A similar statement for the log-normal distribution is possible for the product of the random variables. In positive log-normal independent variates having the same means and variances, the product of the variates is asymptotically log-normally distributed. [Ref. 25]

This can be an important tool in estimating the products of the random variable v_{in} caused by non-linearities in the RF system. These products are the resulting intermodulation products which add as noise to the desired signal.

C. ESTIMATING MEAN AND VARIANCE

The problem here is to match an experimentally determined cumulative probability distribution function or probability density function to a theoretical function. The two dependent variables to be applied in the match are the mean and variance. To simplify calculations, the matching for HF signal studies is done in dBm. The goal is to match a normal distribution to the experimental observations. The following summarizes the mean and variance estimation methods.

1. Quartile Estimation

A simple method exists to fit a normal probability density function to an experimentally derived histogram based on quartiles. Let N be the total number of observations. The observations are ordered in histogram form. Starting with the ordinate having the smallest value, the first quartile is the ordinate value corresponding to N/4 observations, etc. Stated differently, the first quartile is the ordinate value for which one-fourth of the observations have a value less than or equal that ordinate. The second, third, and fourth quartiles have similar definitions. The second quartile is the observational median.

Croxton used a quartile rule to provide an estimate of the mean and standard deviation of fitting a normal density based on these quartiles. [Ref. 26]

Following his derivation, we let Q_1, Q_2, and Q_3 be the quartiles of the experimental data where the data is already in logarithmic form (i.e., dBm). An estimate of mean and variance for the normal density are given as:

$$\mu = \frac{Q_1 + Q_2 + 1.2554\ Q_3}{3.2554} \tag{3.12}$$

and

$$\sigma^2 = 0.5495\ (Q_3 - Q_1)^2 \quad . \tag{3.13}$$

This rule requires the data to be in histogram, or density, form. Quartile estimation provides a computationally efficient estimate. If the data are in distributional form, and if there is no exact ordinate value for 0.25, 0.5, and 0.75, interpolation error is possible. The ease in computation makes this estimation technique particularly well suited for field use.

2. Kullback-Leibler Information Measure Estimation

The Kullback-Leibler (KL) information measure is a probability density matching method. The KL test minimizes the information measure between observational statistics and a given density function. This estimation method is also a form of the Woolf-G estimation method. [Ref. 27]

Given the experimental density data p, and a theoretical density function model q, the KL test is given by:

$$I_{KL}(p;q) = \sum_{i=1}^{m} p_i \ln\left(\frac{p_i}{q_i}\right) \quad . \tag{3.14}$$

The goal in matching is to select the parameters which minimize the KL test distance value, given as $I_{KL}(p;q)$. Since p and q are probability distributions, $I_{KL}(p;q) \geq 0$.

3. Kolmogoroff-Smirnoff Goodness of Fit Test

The Kolmogoroff-Smirnoff (KS) test determines how well an observed distribution fits a theoretically expected distribution. The KS test is most sensitive of these three estimating techniques to departures from the shape of the distribution function. [Ref. 27]

The goal in the test is to minimize the KS distance measure d_{KS}, which is given by:

$$d_{ks} = \min \left| Pr[p_i] - Pr[q_i] \right| \tag{3.15}$$

where p is the experimental value and q is the theoretical model. The KS test searches for the minimum distance using the variables of the theoretical distribution. Compared to other estimating techniques, "The KS test is more likely to detect deviations from the normal distribution...." [Ref. 27] In a similar form, the KS test can match density functions.

D. MATCHED LOG-NORMAL DISTRIBUTIONS

Most of the published HF signal observations are in distributional form. The KS test is the best of the three methods to estimate the means and variances for matching theoretical distributions. The actual matching is done in the dBm domain. This results in the process of matching a normal distribution to the experimental distributions.

Figure 3.9 is a scatter plot of the means and variances used to match normal distributions to the distributions shown in Figure 3.8. The means cluster around the -100 to -120 dBm (with some higher), but the variance is widely scattered.

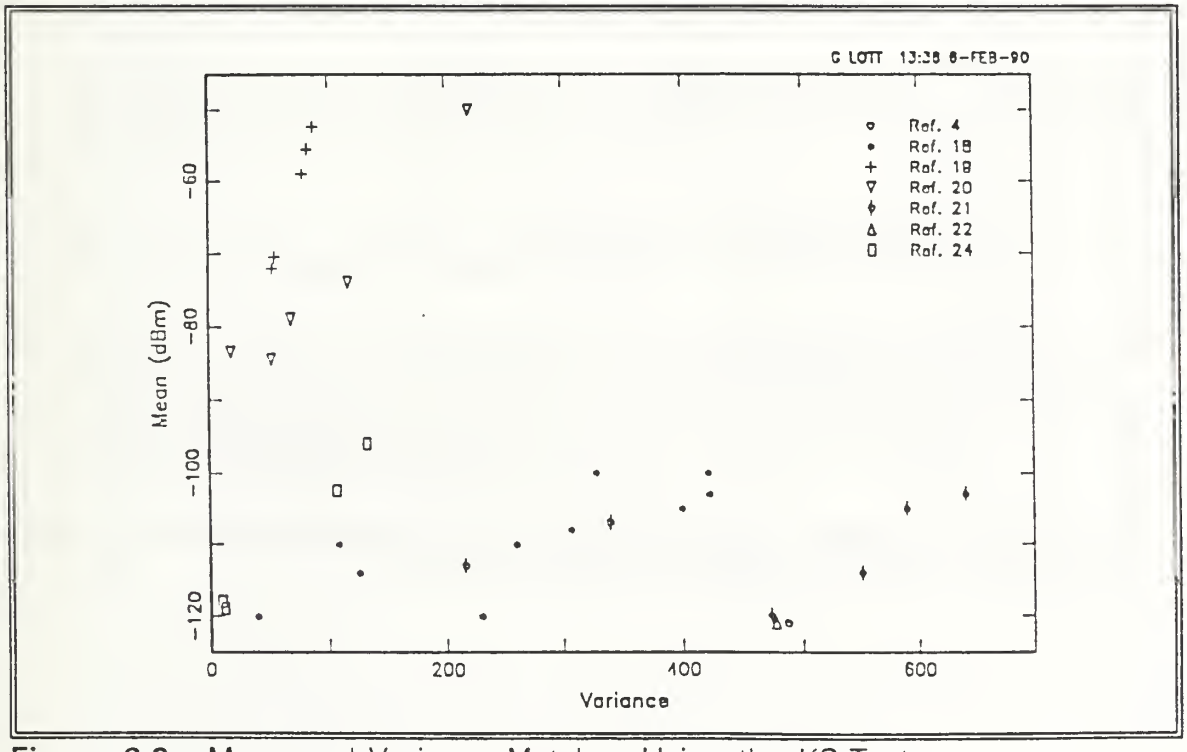


Figure 3.9 - Mean and Variance Matches Using the KS-Test

Most of the observations include day and night measurements. One should expect a smaller daytime mean and a larger nighttime mean and variance.

One can define a dynamic range requirement as the one percent to the 99 percent points on the distribution. Figure 3.10 is an example distribution using a -110 dBm mean and a variance of 100. This distribution leads to a design dynamic range of about 55 dB, and it shows the relatively small dynamic range of the received signals when one considers only signals of military interest.

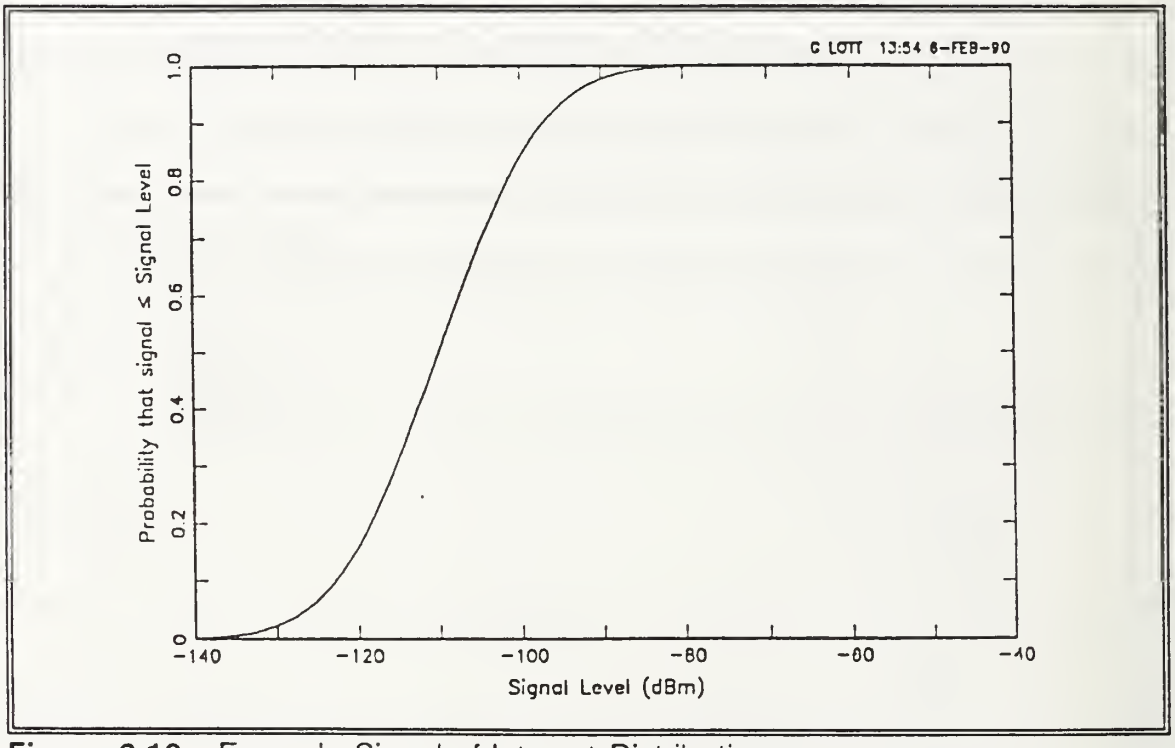


Figure 3.10 - Example Signal-of-Interest Distribution

LIST OF REFERENCES

1. SPAWAR Instruction 0101, 108A; Naval Shore Electronics Criteria, October 1989.

2. Vincent, Wilbur Ray, Jauregui, Stephen, and Adler, Richard W., Training Manual 890110-1, A SNEP Team Training Manual (Draft), May 1989.

3. Lott, Gus K. Jr., High Frequency (HF) Radio Signal Amplitude Characteristics, HF Receiver Site Performance Criteria, and Expanding The Dynamic Range of HF Digital New Energy Receivers By Strong Signal Elimination, Doctoral Dissertation, Naval Postgraduate School, Monterey, California, June 1990.

4. Couch, Leon W., Digital and Analog Communication Systems, Third Edition, Macmillan Publishing Company, New York, 1990.

5. Delfin Systems DN-91-214, Operators Manual for the Advanced PROPHET System, IWG Corporation, San Diego, California, 1991.

6. Vincent, Wilbur Ray, Adler, Richard W., Wadsworth, Donald V.Z., and others, "Quick-Look Report on SNEP Team Visit to NSGA Sabana Seca, PR.," Signal-to-Noise Enhancement Program, December 1991.

7. Cummins, Eugene Joseph Jr., High Frequency Radio Interference, Master's Thesis, Naval Postgraduate School, Monterey, California, March 1979.

8. Harthcock, Clyde T., An Examination of the Radio Frequency Switching Matrix at U.S. Army Field Station Augsburg, U.S. Army Field Station Berlin, and U.S. Naval Security Group Activity Edzell, Master's Thesis, Naval Postgraduate School, Monterey, California, September 1989.

9. 3-D Visions Corporation, GRAFTOOL User's Guide, Torrence, California, 1987-1990.

BIBLIOGRAPHY

Vincent, Wilbur Ray, and Jaurequi, Stephen, Technical Note 881115-1, Description of the Site Performance Problem, Monterey, California, November 1988.

Vincent, Wilbur Ray, Adler, Richard W., Wadsworth, Donald V.Z., and others, "Quick-Look Report on SNEP Team Visit to NSGA Edzell," Signal-to-Noise Enhancement Program, December 1991.

INITIAL DISTRIBUTION LIST

1.	Defense Technical Information Center Cameron Station Alexandria, VA 22304-6145	2
2.	Library, Code 52 Naval Postgraduate School Monterey, CA 93943-5002	2
3.	Chairman, Code EC Department of Electrical and Computer Engineering Naval Postgraduate School Monterey, CA 93943-5000	1
4.	Professor D. V. Wadsworth, Code EC/Ed Department of Electrical and Computer Engineering Naval Postgraduate School Monterey, CA 93943-5000	1
5.	Professor R. Adler, Code EC/Ab Department of Electrical and Computer Engineering Naval Postgraduate School Monterey, CA 93943-5000	1
6.	Professor W. R. Vincent, Code EC/Ja Department of Electrical and Computer Engineering Naval Postgraduate School Monterey, CA 93943-5000	1
7.	Commander Naval Security Group Command Attn: G40 3801 Nebraska Avenue, N.W. Washington, DC 20390	1

8. Commander 1
Naval Security Group Command
Attn: G433
3801 Nebraska Avenue, N.W.
Washington, DC 20390

9. Commander 1
Naval Security Group Command
Attn: G80
3801 Nebraska Avenue, N.W.
Washington, DC 20390

10. Commander 1
Naval Security Group Command
Attn: G81
3801 Nebraska Avenue, N.W.
Washington, DC 20390

11. Commander 1
Naval Electronic Systems Security Engineering Center
Attn: Code 042
3801 Nebraska Avenue, N.W.
Washington, DC 20390

12. Director 1
National Security Agency
Attn: R6
Ft. George G. Meade, MD 20755

545-016

Thesis
S54665 Skimmons
c.1 Automated performance
evaluation technique.

Thesis
S54665 Skimmons
c.1 Automated performance
evaluation technique.

AMERICAN BINDERY

3 2768 00018444 4